# Sparsity Promoting Off-grid Methods with Applications in Direction Finding

A DISSERTATION

SUBMITTED TO THE FACULTY OF THE GRADUATE SCHOOL

OF THE UNIVERSITY OF MINNESOTA

BY

Cheng-Yu Hung

IN PARTIAL FULFILLMENT OF THE REQUIREMENTS

FOR THE DEGREE OF

Doctor of Philosophy

Professor Mostafa Kaveh, Advisor

May, 2017

# Acknowledgements

First, I would like to thank my advisor, Professor Mostafa Kaveh for his support and guidance during my graduate study. He taught me a lot of things including deeply thinking, problem solving, paper writing, and ideas presenting. It is my greatest pleasure to have Mos as my research advisor. He is a considerate gentleman, and I have learned a lot from him. His patience, politeness, knowledge and commitment to excellence always stimulates me to be a better person.

Second, I would like to thank my final defense committee members: Professor Nikos Sidiropoulos, Professor Emad Ebbini, and Professor Shuzhong Zhang. I have benefited from not only interacting with them and learned the knowledge that I need, but also obtaining useful suggestion for my dissertation.

I also would like to thank my former labmates Dr. Jimeng Zheng, and Dr. Amogh Rajanna. It was a great experience working with these smart people. They enriched my PhD career and helped my graduate life in many ways. I will deeply miss our discussions and conversations on campus or on the phone that we made together.

Lastly, I would like to thank my parents, Chi-Ching Hung and Feng-Mei Su, for their love and support for my entire life. I would like to give my special thanks to my lovely wife Ting-Chun Tseng for her company and love throughout these past years.

# Dedication

*Dedicated to*

**My parents, and all my family members.**

## Abstract

In this dissertation, the problem of directions-of-arrival (DoA) estimation is studied by the compressed sensing application of sparsity-promoting regularization techniques. Compressed sensing can recover high-dimensional signals with a sparse representation from very few linear measurements by nonlinear optimization. By exploiting the sparse representation for the multiple measurement vectors or the spatial covariance matrix of correlated or uncorrelated sources, the DoA estimation problem can be formulated in the framework of sparse signal recovery with high resolution. There are three main topics covered in this dissertation. These topics are recovery methods for the sparse model with structured perturbations, continuous sparse recovery methods in the super-resolution framework, and the off-grid DoA estimation with array self-calibration. These topics are summarized below.

For the first topic, structured perturbation in the sparse model is considered. A major limitation of most methods exploiting sparse spectral models for the purpose of estimating directions-of-arrival stems from the fixed model dictionary that is formed by array response vectors over a discrete search grid of possible directions. In general, the array responses to actual DoAs will most likely not be members of such a dictionary. Thus, the sparse spectral signal model with uncertainty of linearized dictionary parameter mismatch is considered, and the dictionary matrix is reformulated into a multiplication of a fixed base dictionary and a sparse matrix. Based on this sparse model, we propose several convex optimization algorithms. However, we are also concerned with the development of a computationally efficient optimization algorithm for off-grid direction finding using a sparse observation model. With an emphasis on designing efficient algorithms, various sparse problem formulations are considered, such as unconstrained formulation, primal-dual formulation, or conic formulation. But, because of the nature of nondifferentiable objective functions, those problems are still challenging

to solve in an efficient way. Thus, the Nesterov smoothing methodology is utilized to reformulate nonsmooth functions into smooth ones, and the accelerated proximal gradient algorithm is adopted to solve the smoothed optimization problem. Convergence analysis is conducted as well. The accuracy and efficiency of smoothed sparse recovery methods are demonstrated for the DoA estimation example.

In the second topic, estimation of directions-of-arrival in the spatial covariance model is studied. Unlike the compressed sensing methods which discretize the search domain into possible directions on a grid, the theory of super resolution is applied to estimate DoAs in the continuous domain. We reformulate the spatial spectral covariance model into a multiple measurement vectors (MMV)-like model, and propose a block total variation norm minimization approach, which is the analog of Group Lasso in the super-resolution framework and that promotes the group-sparsity. The DoAs can be estimated by solving its dual problem via semidefinite programming. This gridless recovery approach is verified by simulation results for both uncorrelated and correlated source signals.

In the last topic, we consider the array calibration issue for DoA estimation, and extend the previously considered single measurement vector model to multiple measurement vectors. By exploiting multiple measurement snapshots, a modified nuclear norm minimization problem is proposed to recover a low-rank matrix with high probability. The definition of linear operator for the MMV model is given, and its corresponding matrix representation is derived so that a reformulated convex optimization problem can be solved numerically. In order to alleviate computational complexity of the method, we use singular value decomposition (SVD) to reduce the problem size. Furthermore, the structured perturbation in the sparse array self-calibration estimation problem is considered as well. The performance and efficiency of the proposed methods are demonstrated by numerical results.

# Contents

# List of Tables

# List of Figures

# Chapter 1

# Introduction

Directions-of-arrival (DoA) estimation is a common problem in array signal processing. The main goal of DoA estimation is to locate closely spaced signals in angle, in the presence of high-variance noise and low number of snapshots. Several methods for high-resolution DoA estimation are well established, and widely used. These include the multiple signal classification (MUSIC) [1], minimum variance distortionless response (MVDR) [2], and the estimatin of signal parameter via rotational invariance techniques (ESPRIT) [3]. The maximum likelihood (ML) [4] estimator of DoA acheives excellent performance, but it suffers from substantial complexity, and sensitivity to initialization. Its computational cost is reduced, for example through the data-supported grid search [5]. In [6], an enhanced matching pursuit (MP) algorithm for DoA estimation is proposed to take advantages of multiple snapshots of received signals to attain better performance over MUSIC and ESPRIT at low signal-to-noise ratios (SNR).

Compressed sensing [7] has motivated the application of the sparse signal representation on overcomplete dictionaries for the design of super-resolution of directions-of-arrival (DoA) estimators. Sparse recovery methods with applications to DoA estimation will be the subject of this dissertation. Since the problem formulation and the sparsity-promoting methods proposed for DoA estimation here have deep connections

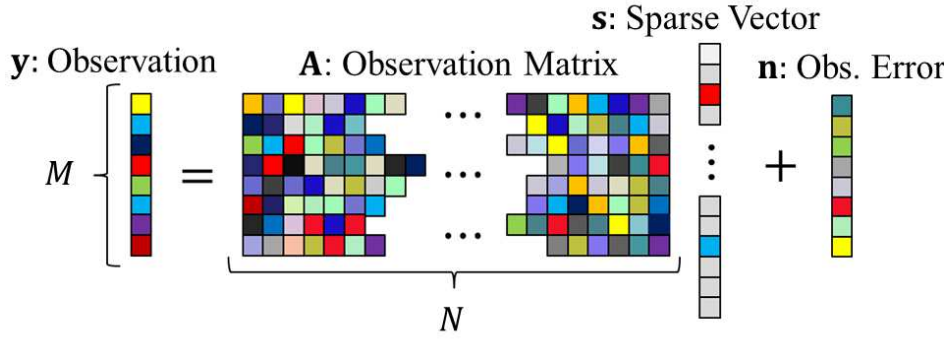


Figure 1.1: Sparse system.

with compressed sensing, a brief introduction of sparse model, and sparsity-encouraging regularization methods are provided in the next section.

## 1.1 Background

### 1.1.1 Sparse System Formulation of Compressed Sensing

In compressed sensing, a linear system as shown in Figure 1.1 is considered

$$\mathbf{y} = \mathbf{A}\mathbf{s} + \mathbf{n}, \tag{1.1}$$

where $\mathbf{y} \in \mathbb{C}^{M\times 1}$ is an observation measurement vector, $\mathbf{A} \in \mathbb{C}^{M\times N}(M \ll N)$ is a known dictionary matrix, $\mathbf{n} \in \mathbb{C}^{M\times 1}$ is a measurement error or additive noise vector, and $\mathbf{s} \in \mathbb{C}^{N\times 1}$ is a $K$-sparse signal vector of interest. There are only $K$ nonzero entries in $\mathbf{s}$, and $K \ll N$. As long as the dictionary matrix $\mathbf{A}$ meets the requirement of the Restricted Isometry Property (RIP) [8, 9, 10], the sparse vector $\mathbf{s}$ can be reconstructed even with a few of measurements by using a Lasso, or basis pursuit denoising solver. However, the dictionary matrix $\mathbf{A}$ may not be known perfectly due to certain noise or modeling perturbations. In [11], the sensitivity of basis mismatch in the dictionary matrix is analyzed.

A commonly-used observation for off-grid effects follows the noisy structured perturbation model given by:

$$\mathbf{y} = (\mathbf{A} + \mathbf{B}\Gamma)\mathbf{s} + \mathbf{n}, \tag{1.2}$$

where $\mathbf{A} \in \mathbb{C}^{M\times N}$ is known, and $\mathbf{B} \in \mathbb{C}^{M\times N}$ is known as part of the off-grid approximation. $\Gamma = diag(\boldsymbol{\beta})$, and $\boldsymbol{\beta} = [\beta_1, \ldots, \beta_N]^T$ is denoted as the unknown coefficient vector for the approximation. $\mathbf{s}$ is the sparse vector associated with grid points nearest the true supports. The above can be solved by formulating a sparsity-promoting constrained nonconvex minimization problem to estimate $\mathbf{s}$ and $\boldsymbol{\beta}$ sequentially by the alternating method [12, 13], but with slow convergence.

Note that instead of adopting the above formulation, the off-grid effect can be avoided by using a continuous sparse signal reconstruction method developed in the super-resolution framework [14].

### 1.1.2 Self-Calibration in Compressed Sensing

A general self-calibration estimation problem in compressed sensing is given by

$$\mathbf{y} = \mathbf{A}(\mathbf{h})\mathbf{x} + \mathbf{n}, \tag{1.3}$$

where $\mathbf{y}$ is a measurement vector, $\mathbf{A}(\mathbf{h})$ is a measurement matrix with unknown calibration parameters $\mathbf{h}$, $\mathbf{x}$ is a sparse signal of interest, and $\mathbf{n}$ is additive noise. The goal is to recover $\mathbf{x}$ and $\mathbf{h}$, given $\mathbf{y}$. $\mathbf{h}$ is used to capture the calibration error, which is common in the sensing devices. The main reason of the calibrating issue in array processing comes from antenna position offsets or environmental changes on the sensors. Therefore, since $\mathbf{x}$ is assumed sparse, we can come up with $L_1$-norm minimization problem

$$(\hat{\mathbf{x}}, \hat{\mathbf{h}}) = \arg\min_{\mathbf{x},\mathbf{h}} \frac{1}{2}||\mathbf{A}(\mathbf{h})\mathbf{x} - \mathbf{y}||_2^2 + \alpha||\mathbf{x}||_1, \quad \alpha > 0. \tag{1.4}$$

However, this is a non-convex optimization problem so that it's challenging to get a global optimal solution.

## 1.2 Dissertation Contributions

There are several topics covered in this dissertation. First, the structured perturbation (off-grid) model of sparse recovery is considered, and efficient algorithms are developed. Then, the off-grid effect is avoided by a gridless sparse recovery method in the super-resolution framework. We then consider the calibration issue in the structured perturbation system, and propose a variant of the nuclear norm minimization problem. The main contributions are summarized as follows.

- **Sparse Recovery Methods with Structured Perturbations and Efficient Algorithm Designs**

  In compressed sensing, the sensing matrix is assumed perfectly known. However, there exists perturbation in the sensing matrix in reality due to sensor offsets or noise disturbance. Directions-of-arrival (DoA) estimation with off-grid effect satisfies this situation, and can be formulated into a (non)convex optimization problem with linear inequalities constraints. There exist many solvers, which can be used to solve this formulation, such as group Lasso [15], basis pursuit denoising (BPDN) [16], or Dantzig selector [17]. The performance analysis and computable performance bounds of those sparse recovery solvers are conducted in [18, 19]. Those solvers can utilize the interior point method (using the CVX tools), but at a large computational cost. In order to design efficient algorithms, we consider various alternative formulations, such as unconstrained formulation, primal-dual formulation, or conic formulation. However, due to the nature of the objective functions, those entail solution of nonsmooth problems. Thus, the Nesterov smoothing is applied and combined with the accelerated gradient descent method to develop efficient algorithms. The convergence rate for the algorithms is analyzed as well. The efficiency and accuracy of smoothed sparse recovery methods are demonstrated in the numerical results of DoA estimation.

- **Gridless Sparse DoA Estimation Recovery Methods**

In this work, the spatial spectral covariance model for the DoA estimation problem is reformulated into a MMV-like model for several reasons, including computational savings, and extrapolating array apertures. Since multiple snapshots of source signals share the same source locations which are sparse in continuous space, this property can be exploited to enhance the estimation of DoAs. Thus, we extend the theory of super-resolution from single measurement vector (SMV) [14, 20] to multiple measurement vector (MMV) by defining a block total variation (BTV) norm for a complex measure with same locations but different amplitudes at multiple snapshots. Then, the minimization problem of BTV norm is proposed. By the parameter mapping of MMV-like system in this extended super-resolution framework, the DoA estimation problem can be solved efficiently via the proposed BTV norm minimization problem. Its dual with infinite constraints can be transformed to semidefinite programming (SDP), which is used to estimate the source locations. The performance of the proposed method is proved through two cases of uncorrelated and correlated source signals.

- **Low Rank Recovery Methods with Structured Perturbations for Array Calibration**

  In this work, the combined calibration and DoA estimation, is approached by extending known SMV approaches [21] to the MMV case. By taking advantage of multiple snapshots, a modified nuclear norm minimization problem is proposed to recover a low-rank matrix with larger matrix dimension. We also give the definition of linear operator for the MMV model, and its corresponding matrix representation so that we can come up with a variant of convex optimization. In order to mitigate the computational complexity, singular value decomposition (SVD) is applied to reduce the problem size. Moreover, the off-grid effect in the sparse array self-calibration problem is considered. The performance of the proposed methods are demonstrated by numerical simulations and compared with

Cramer-Rao Bound (CRB) [22], and the eigenstructure-based method [23].

## 1.3 Outline of this Dissertation

This dissertation covers several different topics about the sparse off-grid recovery. Chapter 2 introduces the off-grid effect in the sparse DoA estimation problem. Nonconvex or convex optimization problems with linear constraints emerge, and several algorithms are proposed to estimate the off-grid parameters and sparse signals by using their sparsity property. Chapter 3 extends to the nonsmooth convex optimization problems with linear constraints, and proposes efficient optimization algorithms by using smoothing techniques. Chapter 4 considers formulation of a continuous sparse recovery problem by the super resolution theory, instead of in the discretized domain. The reconstruction accuracy can be increased by solving a proposed semidefinite programming problem. Chapter 5 introduces the calibration issue from SMV to MMV in sparse array processing. The off-grid effect with calibration is also formulated as a convex optimization problem, and solved by using nuclear norm minimization. The results are summarized in Chapter 6, including conclusions and future directions.

## 1.4 Notations

Vectors and matrices are represented by boldface lowercase and uppercase letters, respectively. $E(\cdot)$ denotes the expectation operator and $(\cdot)^H$ denotes the Hermitian transpose of a matrix. $(\cdot)^T$ denotes the transpose of a matrix. $(\cdot)^*$ denotes the complex conjugate of variables. $diag(\mathbf{x})$ represents a diagonal square matrix with the elements of vector $\mathbf{x}$ on the diagonal, while $diag(\mathbf{X})$ returns a vector with the diagonal elements of matrix $\mathbf{X}$. $[\mathbf{X}]_{ii}$ represents the $i$-th component on the diagonal of matrix $\mathbf{X}$. $\odot$ denotes the Hadamard product. $vec(\cdot)$ is a vectorizing operator, and $\otimes$ denotes the Kronecker product.

# Chapter 2

# Sparse Off-Grid Recovery Methods in the Discretized Domain

In this chapter, a sparse spatial spectral model with off-grid effect is discussed. We proposed several discretized sparse recovery methods. Their performance are demonstrated by conducting simulations in the directions-of-arrival (DoA) estimation scenario.

## 2.1 Introduction

Developments in sparse model recovery and compressed sensing [7] have motivated the use of the sparse signal representation on overcomplete dictionaries for the design of super-resolution of directions-of-arrival (DoA) estimators. In [24], the $L_1$-SVD method was promoted for increased resolution capabilities and robustness to noise without accurate initialization. In [25], the Sparse Spatial Spectral Fitting method (SpSF) was adopted as a similar approach as the $L_1$-SVD, but based on the model of the spatial covariance. The SpSF method achieves similar performance in DoA estimation as

the $L_1$-SVD, and obtains estimates of the source powers at the same time. Another similar approach was also presented in [26]. When the actual DoAs do not belong to the search grid, the performance of the sparsity-exploiting estimators such as the ones mentioned above can be significantly degraded. To accommodate such off-grid situation, Reference [12] proposed the Weighted and Structured Sparse Total Least-squares (WSS-TLS) method. In [27], the Sparse Spectral Fitting with Modeling Uncertainty (SSFMU) estimator was presented, which relaxes a non-covex optimization problem to a convex one. The SSFMU with diagonal loading can effectively ease the sensitivity of selecting improper optimization parameters. In [28], the off-grid frequency estimation problem is solved by an atomic norm minimization. This can then be re-formulated as a semidefinite programming. In [29], a group lasso-based algorithm called Bounded Joint-Sparse (BJS) method is developed to overcome the dictionary mismatch. In [30], a low-complexity iterative alternating descent algorithm (SOMP-LS) is proposed to solve off-grid problems, but its performance appears to be questionable for closely-spaced sources. A number of off-grid model approximations and solutions have been proposed, for example [13, 31, 32, 33, 34, 35].

In this chapter, the covariance-based sparse spatial spectral model with off-grid DoAs is further studied. By linearizing off-grid errors of the discrete array response vectors, a doublely sparse model is derived, which is decomposed into the multiplication of a pre-specified base dictionary, a sparse dictionary, and a sparse signal. The alternating Lasso (ALasso) algorithm is introduced to solve three optimization problems associated with alternately estimating variables, involved in tuning several optimization parameters. In order to overcome the associated computational disadvantage, we consider the same sparsity patterns of variables to develop two lower complexity algorithms: the Lasso-based Least Squares (LLS) and the group-sparsity estimator (GSE). Computer simulations compare the error performance of the proposed methods with SSFMU, SOMP-LS, BJS and multiple signal classification (MUSIC) [36], demonstrating the advantages of ALasso and GSE at low signal-to-noise ratios (SNRs).

## 2.2 Observation Model

### 2.2.1 Multiple Measurement Vector and Spatial Spectral Model

Consider an array of $M$ sensors and suppose that there are $K$ far-field narrowband sources impinging on the array from angles $\theta_1, \ldots, \theta_K$. The observation vector $\mathbf{y}(t) = [y_1(t), \ldots, y_M(t)]^T \in \mathbb{C}^{M\times 1}$ at time $t$ is modeled as

$$\mathbf{y}(t) = \mathbf{G}\mathbf{x}(t) + \mathbf{n}(t), t = 1 \ldots, T, \tag{2.1}$$

where the measurement matrix $\mathbf{G} = [\mathbf{g}(\theta_1), \cdots, \mathbf{g}(\theta_K)] \in \mathbb{C}^{M\times K}$ is composed of the steering vectors $\{\mathbf{g}(\theta_i) = [e^{-j(-(M-1)/2)2\pi\frac{d}{\lambda}sin\theta_i}, \ldots, e^{-j((M-1)/2)2\pi\frac{d}{\lambda}sin\theta_i}]^T\}_{i=1}^K$ with wavelength $\lambda$, and $\mathbf{n}$ is i.i.d. white Gaussian noise with $\mathcal{N}(0, \sigma^2 I)$. The vector $\mathbf{x}(t) = [x_1(t), \ldots, x_K(t)]^T \in \mathbb{R}^{K\times 1}$ or $\mathbb{C}^{K\times 1}$ represents the arriving signal vector with statistical distribution $\mathcal{N}(0, \mathbf{C}_s)$. Denote $\mathcal{T}_\theta = \{sin(\theta_k)\}_{k=1}^K \subset \mathbb{T} = [-1, 1]$ as the support set for the sines of the angles of arrival. If $T > 1$ multiple snapshots are considered, we can define the following MMV system as

$$\mathbf{Y} = \mathbf{G}\mathbf{X} + \mathbf{N}, \tag{2.2}$$

where the obervation matrix $\mathbf{Y} = [\mathbf{y}(1), \ldots, \mathbf{y}(T)] \in \mathbb{C}^{M\times T}$, the source signal matrix $\mathbf{X} = [\mathbf{x}(1), \ldots, \mathbf{x}(T)] \in \mathbb{R}^{K\times T}$ or $\mathbb{C}^{K\times T}$, and the noise matrix $\mathbf{N} = [\mathbf{n}(1), \ldots, \mathbf{n}(T)] \in \mathbb{C}^{M\times T}$. Since multiple snapshots of vectors in $\mathbf{X}$ share the common sparsity pattern of the support set in the domain $\mathbb{T}$, this property can be exploited to jointly estimate the support set $\mathcal{T}_\theta$.

Based on the second-order statistics of the received signals, the spatial spectral model is given by

$$\begin{aligned}\mathbf{R} &= E[\mathbf{y}\mathbf{y}^H] = E[\mathbf{G}\mathbf{x}\mathbf{x}^H\mathbf{G}^H] + \sigma^2\mathbf{I} = \mathbf{G}\tilde{\mathbf{S}}\mathbf{G}^H + \sigma^2\mathbf{I} \\ &= \sum_{i=1}^K E[x_i x_i^*]\mathbf{g}(\theta_i)\mathbf{g}(\theta_i)^H + \sigma^2\mathbf{I} = \sum_{i=1}^K \bar{s}_i\mathbf{g}(\theta_i)\mathbf{g}(\theta_i)^H + \sigma^2\mathbf{I},\end{aligned} \tag{2.3}$$

where $\tilde{\mathbf{S}} = diag([\bar{s}_1, \cdots, \bar{s}_K]) \in \mathbb{R}^{K \times K}$ is the covariance matrix of uncorrelated signals impinging on the array with the signal power $\bar{s}_i = E[x_i x_i^*]$, and $\sigma^2$ is denoted as the power of AWGN. In practice, we use $\bar{\mathbf{R}} = \sum_{t=1}^{T} \mathbf{y}(t)\mathbf{y}(t)^H / T$ as the estimate of the covariance matrix $\mathbf{R}$, where $T$ is denoted the number of snapshots. Thus, the approximation error and AWGN are summed into a new error term $\mathbf{v}$, and the spatial spectral model is expressed as

$$\bar{\mathbf{R}} = \sum_{i=1}^{K} \bar{s}_i \mathbf{g}(\theta_i)\mathbf{g}(\theta_i)^H + \mathbf{v}. \tag{2.4}$$

By vectorizing Equation (2.4), the covariance model is reformulated into

$$\mathbf{r} = \mathbf{P}(\theta)\bar{\mathbf{s}} + \mathbf{v}_v, \tag{2.5}$$

where $\mathbf{r} = vec(\bar{\mathbf{R}}) \in \mathbb{C}^{M^2 \times 1}$, $\mathbf{v}_v = vec(\mathbf{v}) \in \mathbb{C}^{M^2 \times 1}$, $\bar{\mathbf{s}} = [\bar{s}_1, \cdots, \bar{s}_K]^T \in \mathbb{R}^{K \times 1}$, $\mathbf{P}(\theta) = [\mathbf{p}(\theta_1), \cdots, \mathbf{p}(\theta_K)] \in \mathbb{C}^{M^2 \times K}$, and $\mathbf{p}(\theta_i) = vec(\mathbf{g}(\theta_i)\mathbf{g}(\theta_i)^H) \in \mathbb{C}^{M^2 \times 1}$.

Next, two problem formulations in the discrete and continuous domain are introduced in the following sections.

### 2.2.2 Sparse Off-Grid DoA Model

The DoA estimation problem can be treated as a search for the most likely candidates over the discretized grid of directions, which are denoted by $\{\phi_1, \phi_2, \cdots, \phi_L\}$ where $L$ is the number of discrete directions and $L \gg K$. Suppose that the actual DoAs $\{\theta_1, \theta_2, \cdots, \theta_K\}$ belong to the grid of interest represented by $\{\phi_1, \phi_2, \cdots, \phi_L\}$. Then, Equation (2.5) can be transformed into a sparse spatial spectral model as:

$$\mathbf{r} = \mathbf{P}(\phi)\mathbf{s} + \mathbf{v}_v, \tag{2.6}$$

where $\mathbf{P}(\phi) = [\mathbf{p}(\phi_1), \cdots, \mathbf{p}(\phi_L)] \in \mathbb{C}^{M^2 \times L}$ is called measurement matrix and $\mathbf{s} = [s_1, \cdots, s_L]^T \in \mathbb{R}^{L \times 1}$ represents the sparse spatial spectrum, i.e., $\forall i = 1, \cdots, L$, if $\exists j, \ni \phi_i = \theta_j \in \{\theta_1, \theta_2, \cdots, \theta_K\}$ , then $s_i = \bar{s}_j$; otherwise, $s_i = 0$. This problem

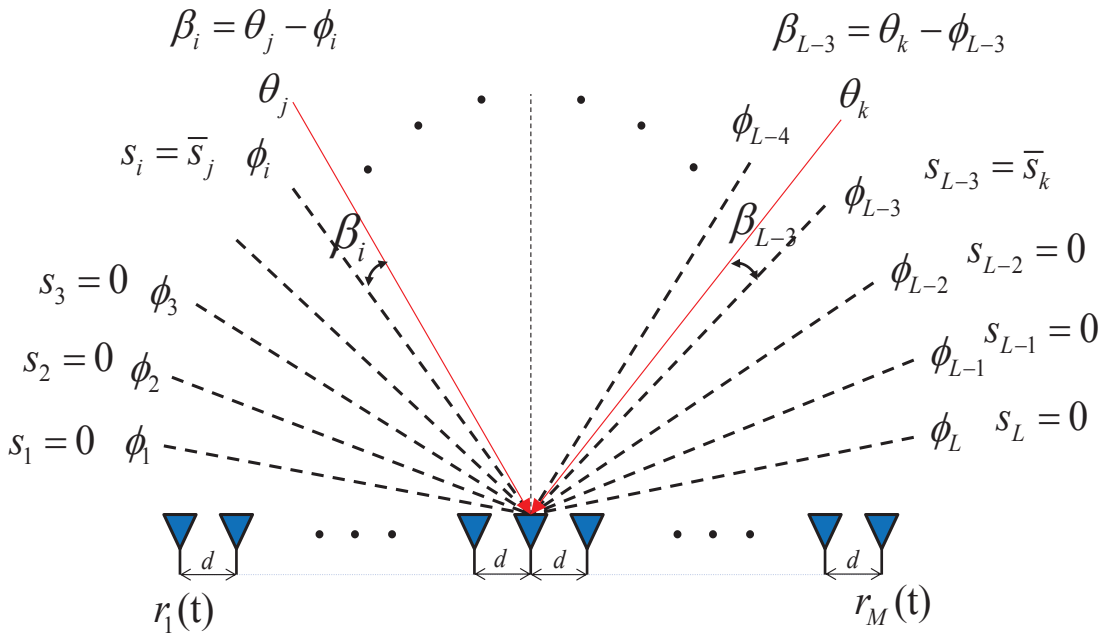


Figure 2.1: Illustration of off-grid error in DoA.

can be solved by $l_1$-norm minimization with proper regularization paprameter $\alpha$ as the following:

$$\arg\min_{\mathbf{s}} ||\mathbf{r} - \mathbf{P}(\phi)\mathbf{s}||_2^2 + \alpha||\mathbf{s}||_1, \tag{2.7}$$

where $||\cdot||_p$ is denoted as $p$-norm, $p = 1$ or 2.

In reality, the actual DoAs most likely will not belong to the discretized grid in the optimization model. Therefore, off-grid errors $\{\beta_i\}_{i=1}^L$ is introduced into the sparse spatial spectral model as shown in Figure 2.1. Such error is defined as $\beta_i = \theta_j - \phi_i$ if there exists $\theta_j$ close to $\phi_i$; otherwise $\beta_i = 0$. It is noted that $\forall i, |\beta_i| \leq r$ for some constant

$r$, which is the bound of error. Using the first order Taylor Series expansion, the array response vector $\mathbf{g}(\theta_j)$ is approxmated as $\mathbf{g}(\theta_j) \cong \mathbf{g}(\phi_i) + \mathbf{g}'(\phi_i)(\theta_j - \phi_i)$, where $\mathbf{g}'(\phi_i)$ is the first order derivative of $\mathbf{g}(\phi_i)$ with respect to $\phi_i$. Then, $\mathbf{p}(\theta_j) = vec(\mathbf{g}(\theta_j)\mathbf{g}(\theta_j)^H) \cong \mathbf{c}_i + (\mathbf{d}_i + \mathbf{e}_i)\beta_i + \mathbf{f}_i\beta_i^2$ where $\mathbf{c}_i = vec(\mathbf{g}(\phi_i)\mathbf{g}(\phi_i)^H)$, $\mathbf{d}_i = vec(\mathbf{g}'(\phi_i)\mathbf{g}(\phi_i)^H)$, $\mathbf{e}_i = vec(\mathbf{g}(\phi_i)\mathbf{g}'(\phi_i)^H)$, and $\mathbf{f}_i = vec(\mathbf{g}'(\phi_i)\mathbf{g}'(\phi_i)^H)$. Equation (2.6) can be rewritten as

$$\mathbf{r} \cong \mathbf{C}\mathbf{s} + (\mathbf{D} + \mathbf{E})diag(\mathbf{b})\mathbf{s} + \mathbf{F}diag(\mathbf{b} \odot \mathbf{b})\mathbf{s} + \mathbf{v}_v \tag{2.8}$$

where $\mathbf{C} = [\mathbf{c}_1, \cdots, \mathbf{c}_L] \in \mathbb{C}^{M^2 \times L}$, $\mathbf{D} = [\mathbf{d}_1, \cdots, \mathbf{d}_L] \in \mathbb{C}^{M^2 \times L}$, $\mathbf{E} = [\mathbf{e}_1, \cdots, \mathbf{e}_L] \in \mathbb{C}^{M^2 \times L}$, $\mathbf{F} = [\mathbf{f}_1, \cdots, \mathbf{f}_L] \in \mathbb{C}^{M^2 \times L}$ , and $\mathbf{b} = [\beta_1, \cdots, \beta_L]^T \in \mathbb{R}^{L \times 1}$ is called the off-grid vector.

We reformulate Equation (2.8) into

$$\mathbf{r} \cong \mathbf{Q}\mathbf{U}\mathbf{s_3} + \mathbf{v}_v \tag{2.9}$$

$$= \mathbf{Q}\mathbf{T}\mathbf{q} + \mathbf{v}_v, \tag{2.10}$$

where $\mathbf{s_3} = [\mathbf{s}^T, \mathbf{s}^T, \mathbf{s}^T]^T \in \mathbb{R}^{3L \times 1}$ is an extended sparse spatial vector , and its corresponding sparse vector $\mathbf{q} = [q_1, \cdots, q_{3L}]^T \in \mathbb{R}^{3L \times 1}$, which is defined as $\forall l \in \{1, \cdots, 3L\}$, if $s_{3_l} \neq 0$, then $q_l = 1$; othewise, $q_l = 0$. $\mathbf{Q} = [\mathbf{C} \;\; (\mathbf{D} + \mathbf{E}) \;\; \mathbf{F}] \in \mathbb{C}^{M^2 \times 3L}$ is called the fixed base dictionary matrix. The sparse dictionary matrices$\mathbf{T}, \mathbf{U}$ are defined as

$$\mathbf{T} = \begin{pmatrix} \mathbf{T_1} & 0 & 0 \\ 0 & \mathbf{T_2} & 0 \\ 0 & 0 & \mathbf{T_3} \end{pmatrix}, \mathbf{U} = \begin{pmatrix} \mathbf{U_1} & 0 & 0 \\ 0 & \mathbf{U_2} & 0 \\ 0 & 0 & \mathbf{U_3} \end{pmatrix}, \tag{2.11}$$

where $\mathbf{T_1} = diag(\mathbf{s})$, $\mathbf{T_2} = diag(\mathbf{s} \odot \mathbf{b})$, $\mathbf{T_3} = diag(\mathbf{s} \odot \mathbf{b} \odot \mathbf{b})$, $\mathbf{U_1} = diag([1, \cdots, 1])$, $\mathbf{U_2} = diag(\mathbf{b})$, and $\mathbf{U_3} = diag(\mathbf{b} \odot \mathbf{b})$. Note that $\mathbf{T}, \mathbf{U}, \mathbf{q}$, and $\mathbf{s_3}$ have the same sparsity pattern. Thus, this system can be viewed as a double-sparsity model [37].

Based on Equation (2.9) or (2.10), the optimization problem can be expressed as the following unconstrained ones:

$$\hat{\mathbf{s}}, \hat{\mathbf{b}} = \arg\min_{\mathbf{s},\mathbf{b}} ||\mathbf{r} - \mathbf{Q}\mathbf{U}\mathbf{s_3}||_2^2 + \alpha_1||\mathbf{s_3}||_1, \tag{2.12}$$

$$\hat{\mathbf{s}}, \hat{\mathbf{b}} = \arg\min_{\mathbf{s},\mathbf{b},\mathbf{q}} ||\mathbf{r} - \mathbf{QTq}||_2^2 + \alpha_2||\mathbf{q}||_1. \tag{2.13}$$

where $\alpha_1, \alpha_2$ are regularization parameters. Both optimization problems are obviously nonconvex ones since the optimization variables, $\mathbf{s}$ and $\mathbf{b}$, multiply each other.

## 2.3 Proposed Methods

In order to solve the above nonconvex problem, we proposes three methods. First, an alternating Lasso (ALasso) algorithm is proposed to solve it by alternately estimating variables $\mathbf{s}$ and $\mathbf{b}$. The convergence of Alasso is guaranteed since it is an application of block coordinate descent [38].

### 2.3.1 Alternating Lasso (ALasso)

There are three main steps to the proposed alternating lasso. First, given the initialized off-grid vector $\mathbf{b}$ and by the use of Equation (2.9), we can find the most likely candidates of DoA by

$$\hat{\mathbf{s}}_\mathbf{3} = \arg\min_{\mathbf{s_3}} ||\mathbf{r} - \mathbf{QUs_3}||_2^2 + \alpha||\mathbf{s_3}||_1, \tag{2.14}$$

where $\hat{\mathbf{s}}_\mathbf{3} = [\hat{\mathbf{s}}^T, \hat{\mathbf{s}}^T, \hat{\mathbf{s}}^T]^T$. Since $\mathbf{r}, \mathbf{Q}$, and $\mathbf{U}$ are given in this convex optimization problem, it can be solved by Lasso. Then, in terms of $\hat{\mathbf{s}}_\mathbf{3}$, $\mathbf{q}$ is determined by the following criteria: Given by a threshold $\xi$, $\forall i \in \{1, \cdots, L\}$, if $\hat{s}_i \geq \xi$, set $q_i = 1, q_{i+L} = 1, q_{i+2L} = 1$; otherwise, $q_i = 0, q_{i+L} = 0, q_{i+2L} = 0$.

Next, by fixing $\mathbf{q}$ and using Equation (2.10), we can update the sparse spatial spectrum $\mathbf{s}$ by solving the following optimization problem

$$\begin{aligned} \hat{\mathbf{T}} = \arg\min_{\mathbf{T}} \; & ||\mathbf{r} - \mathbf{QTq}||_2^2 + \eta||diag(\mathbf{T})||_1 \\ s.t. \; & 0 \leq [\mathbf{T}_1]_{ii}, \forall i \\ & -r[\mathbf{T}_1]_{ii} \leq [\mathbf{T}_2]_{ii} \leq r[\mathbf{T}_1]_{ii}, \forall i \\ & 0 \leq [\mathbf{T}_3]_{ii} \leq r^2[\mathbf{T}_1]_{ii}, \forall i, \end{aligned} \tag{2.15}$$

where $\hat{\mathbf{T}} = diag([\hat{\mathbf{s}},\ \hat{\mathbf{s}} \odot \hat{\mathbf{b}},\ \hat{\mathbf{s}} \odot \hat{\mathbf{b}} \odot \hat{\mathbf{b}}])$, $\hat{\mathbf{T}}_{\mathbf{1}} = diag(\hat{\mathbf{s}})$, $\hat{\mathbf{T}}_{\mathbf{2}} = diag(\hat{\mathbf{s}} \odot \hat{\mathbf{b}})$, and $\hat{\mathbf{T}}_{\mathbf{3}} = diag(\hat{\mathbf{s}} \odot \hat{\mathbf{b}} \odot \hat{\mathbf{b}})$.

Finally, by fixing $\mathbf{s}$, the off-grid vector $\mathbf{b}$ is updated by

$$\begin{aligned} \hat{\mathbf{U}} = \arg\min_{\mathbf{U}} \ & ||\mathbf{r} - \mathbf{Q}\mathbf{U}\mathbf{s}_{\mathbf{3}}||_2^2 + \gamma ||diag(\mathbf{U})||_1 \\ s.t.\ & 0 \leq [\mathbf{U}_1]_{ii} \leq 1, \forall i \\ & -r \leq [\mathbf{U}_2]_{ii} \leq r, \forall i \\ & 0 \leq [\mathbf{U}_3]_{ii} \leq r^2, \forall i, \end{aligned} \tag{2.16}$$

where $\hat{\mathbf{U}}_{\mathbf{2}} = diag(\hat{\mathbf{b}})$.

The drawback of this method is its complexity due to solving three optimization problems, and involving three regularization parameters that have to be tuned. Therefore, we proposed two reduced-accuracy approaches which are of lower complexity, i.e., the group-sparsity estimator (GSE) and Lasso-based Least Squares (LLS) method.

### 2.3.2 Lasso-based Least Squares (LLS)

Consider Equation (2.10) and reformulate it as

$$\mathbf{r} \cong \mathbf{Q}\mathbf{z} + \mathbf{v}_v, \tag{2.17}$$

where $\mathbf{z} = [\mathbf{z}_1^T, \mathbf{z}_2^T, \mathbf{z}_3^T]^T = [\ \mathbf{s}^T,\ (\mathbf{s} \odot \mathbf{b})^T,\ (\mathbf{s} \odot \mathbf{b} \odot \mathbf{b})^T\ ]^T = \mathbf{T}\mathbf{q}$, since $\mathbf{T}$ and $\mathbf{q}$ have the same sparsity pattern. According to the solution of the optimization problem (2.14), the most likely candidate of DoA $\hat{\mathbf{s}}$ is determined. Then, we define the support set $\Omega = \{i, i+L, i+2L : \exists \xi, \hat{\mathbf{s}}_i \geq \xi, \forall i = 1, \ldots, L\}$ with its cardinality $|\Omega| = n$. In terms of the support set $\Omega$, the reduced matrix $\mathbf{Q}_\Omega \in \mathbb{C}^{M^2 \times n}$ is obtained. Since $M^2 \gg n$, the Moore-Penrose pseudo-inverse matrix exists and is given by $(\mathbf{Q}_\Omega^H \mathbf{Q}_\Omega)^{-1}\mathbf{Q}_\Omega^H$. The Least Squares solution is expressed as

$$\hat{\mathbf{z}}^\Omega = (\mathbf{Q}_\Omega^H \mathbf{Q}_\Omega)^{-1}\mathbf{Q}_\Omega^H \mathbf{r}. \tag{2.18}$$

Thus, the estimate of $\mathbf{s}$ and $\mathbf{b}$ is obtained as

$$\hat{\mathbf{s}}^{\Omega} = \hat{\mathbf{z}}_1^{\Omega}, \hat{\mathbf{b}}^{\Omega} = \hat{\mathbf{z}}_2^{\Omega} \oslash \hat{\mathbf{z}}_1^{\Omega}, \tag{2.19}$$

where $\oslash$ denotes element-wise division.

### 2.3.3 Group-Sparsity Estimator (GSE)

By observing the vector $\mathbf{z}$ in Equation (2.17), group sparsity is promoted since $\mathbf{s}$ and $\mathbf{b}$ have the same sparsity pattern. Define $|||[\mathbf{z}_1^T, \mathbf{z}_2^T, \mathbf{z}_3^T]^T||_{2,1} = \sum_{l=1}^{3L} |\delta_k|$, where $\delta_l = |||[\mathbf{z}_{1,l}, \mathbf{z}_{2,l}, \mathbf{z}_{3,l}]||_2, \forall k$. The notion of Group Lasso [15] is used to solve this convex problem

$$\begin{aligned} \hat{\mathbf{z}} = \arg\min_{\mathbf{z}} \; & ||\mathbf{y} - \mathbf{Q}\mathbf{z}||_2^2 + \zeta||\mathbf{z}||_{2,1} \\ & s.t. \; \mathbf{z}_1 \succeq 0, r\mathbf{z}_1 \succeq \mathbf{z}_2 \succeq -r\mathbf{z}_1, r^2\mathbf{z}_1 \succeq \mathbf{z}_3 \succeq 0, \end{aligned} \tag{2.20}$$

where $\succeq$ represents component-wise inequality. Once the estimate of $\mathbf{z}$ is solved, we use the rule of Equation (2.19) to compute the estimates of $\mathbf{s}$ and $\mathbf{b}$.

## 2.4 Numerical Results

In this subsection, Monte Carlo simulation is conducted to evaluate the performance of the proposed methods for problem formulation I in comparison with several existing methods. A ULA of $M = 8$ sensors with $d/\lambda = 0.5$ and $K = 2$ far-field plane waves from the actual DoA of $-5.4°$ and $4.6°$ is considered. Narrowband, zero-mean, and uncorrelated sources for the plane waves are assumed, and the noise is AWGN with zero-mean and unit variance. We use the uniform search grid from $-90°$ to $90°$ with $1°$ separation for all methods except MUSIC with $0.1°$ separation. The number of snapshots is set $T = 3000$. The value of $r$ is set to $0.5°$. The off-grid vector $\mathbf{b}$ is initialized as a zero vector in the ALasso algorithm. The root mean square error (RMSE) of DoAs estimation is defined as $(E[|||[\theta_1 - \hat{\theta}_1, \theta_2 - \hat{\theta}_2]||_2^2])^{1/2}$, and the normalized RMSE of powers estimation is $(E[|||[s_1 - \hat{s}_1, s_2 - \hat{s}_2]||_2^2])^{1/2}/E[|||[s_1, s_2]||_2]$. For each method,

when solving the optimization problem, the regularization parameters are empirically selected to achieve the best performance.

In Figure 2.2, the RMSE of DoA estimation of ALasso, LLS, GSE, SSFMU, SOMP-LS, BJS and MUSIC are presented. One hundred realizations are executed for each SNR. The complexity of SOMP-LS is lower, but its performance is the worst because two sources are close. Although the MUSIC method with finer grid searchs outperforms all the others when SNR is high, its performance degrades rapidly below its large error threshold of approximately SNR=-10dB. We observe that ALasso, LLS, GSE, SSFMU have similar RMSE and better than BJS when the SNR is high, e.g., SNR=0 or 5. Therefore, we are more interested in their performance when SNR is lower, particularly below the MUSIC threshold. Below -5 dB, the ALasso has the best performance. For the RMSE of 0.6, ALasso outperforms SSFMU by about 7.5 dB. The LLS has poor RMSE since the noise effect significantly reduces the accuracy of estimating $\mathbf{z}^{\mathbf{\Omega}}$. The GSE, BJS, and SSFMU have similar RMSE at SNR$=-5$ and $-10$. However, GSE outperforms SSFMU and BJS below $-15$ dB.

## 2.5 Summary

In this chapter, we proposed a sparse spatial spectral estimator that accounts in its model DoAs that are off the search grid. The best solution entails an alternating Lasso approach, which alternately solves for the spatial powers and off-grid DoAs at the expense of significant complexity. Then, by promoting group sparsity, Lasso-based Least Squares and group-sparsity estimator are proposed to reduce the computational complexity. By computer simulations, the performances of the proposed methods are evaluated. Simulation results show that ALasso achieves the best RMSE of DoA estimation. GSE and LLS maintain similar performances as SSFMU at higher SNRs with lower complexity.

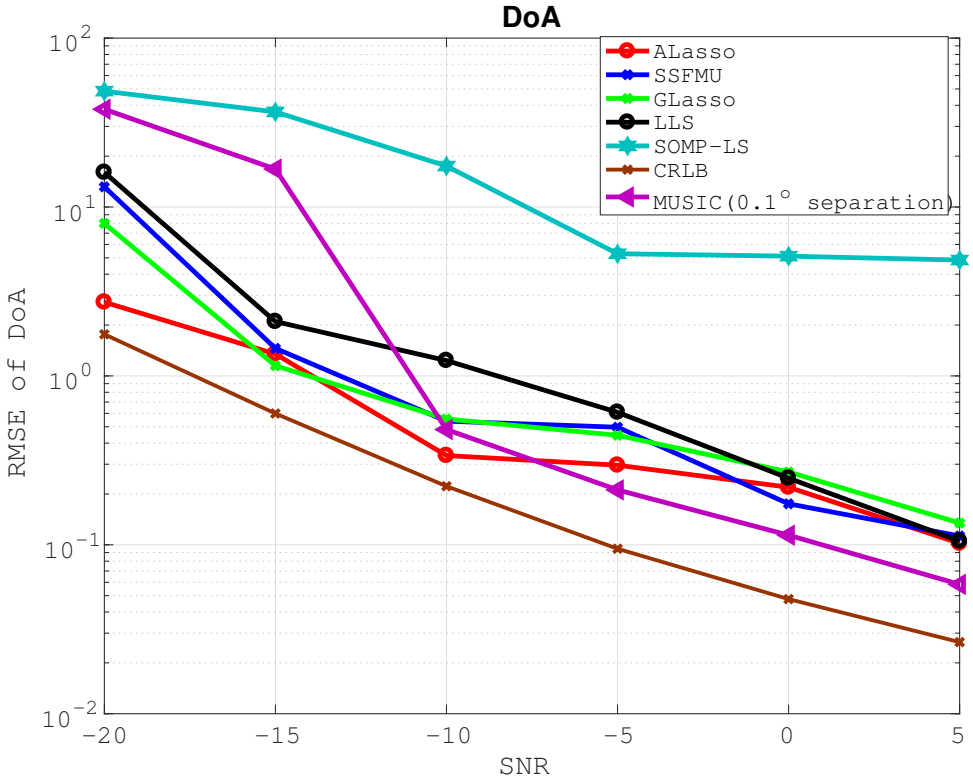


Figure 2.2: RMSE of DoA estimation versus SNR performance of the proposed methods and previous ones.

# Chapter 3

# Smoothed Optimization for DoA Estimation

In this chapter, we solve off-grid estimation problems by the following sparsity promoting formulations: basis pursuit denoising (BPDN), group Lasso (least absolute shrinkage and selection operator), quadratically constrained $l_2$-$l_1$ mixed norm minimization. First, the alternating direction method of multipliers (ADMM)[39] is applied. Then, an iterative algorithm for the BPDN solver are proposed by combining the Nesterov smoothing technique with accelerated proximal gradient method, and the convergence analysis of the method is conducted. We also developed a variant of EGT (Excessive Gap Technique)-based primal-dual method to systematically reduce the smoothing parameter. Finally, we proposed algorithms for quadratically constrained$l_2$-$l_1$ mixed norm minimization by using the smoothed dual conic optimization and continuation technique. All the proposed methods are implemented, and verified in the directions-of-arrival (DoA) problems.

## 3.1 Introduction

Many inverse problems in signal processing, data mining, or statistical machine learning can be cast as a composite optimization problem, which involves the minimization of a sum of differentiable functions and nonsmooth ones, such as solving equation (1.2). Subgradient algorithms [40] are developed to deal with nonsmooth optimization problems but with very slow convergence rate. Instead of using subgradient methods, we attempt to design algorithms for solving nonsmooth optimization (NSO) problems efficiently by using a sequence of approximate smoothing problems to substitute for the original ones. The core of the techniques considered is to make the nondifferentiable functions smooth without introducing substantial approximate errors caused by the smoothing process.

Numerous different smoothing techniques have been proposed to solve NSO problems [41, 42, 43]. A primal-dual symmetric method derived from the excessive gap condition for nonsmooth convex optimization is proposed in [44]. In [32], the nondifferentiable function, which is approximated by the Moreau envelope function [43], is used in the column-wise mismatch problem. In [45], the overlapping group-lasso penalty is smoothed by the Nesterov smoothing technique [41]. A unified framework of smoothing approximation with fast gradient schemes is proposed in [46]. In [47], an adaptive Nesterov-based smoothing method is developed to dynamically choose the smoothing parameter at each iteration of the update.

Instead of solving a constrained nonconvex minimization of (1.2), an unconstrained convex optimization problem, which is composed of one smooth and two nonsmooth functions, can be formulated. In [48], a number of primal-dual iterative approaches for solving large-scale nonsmooth optimization problems, such as the M+LFBF (Monotone+Lipschitz Forward Backward Forward) algorithm, are reviewed. In [49, 50], subgradient methods are proposed, but their complexity can not be better than than $\mathcal{O}(\frac{1}{\sqrt{k}})$ where $k$ is the number of iterations. Alternatively, smoothing as presented in [41] can be applied to mitigate non-smoothness of the objective function. In [51], a proximal

iterative smoothing algorithm was proposed to solve convex nonsmooth optimization problems. In [32], the nondifferentiable function, which is approximated by the Moreau envelope function [43], is used in the column-wise mismatch formulation.

In this chapter, an unconstrained off-grid DoA estimator is studied first. It consists of one differentiable function and two nonsmooth ones, which are a regularized group-sparsity penalty and an indicator function. Inspired by [41, 45], the Nesterov smoothing methodology is used to reformulate the group-sparsity penalty into a "max"-structure function and then add a strongly convex term to smooth it. We propose two reformulations for the group-sparsity penalty since $\ell_2/\ell_1$ mixed norm has a two-layer norm structure. Then, the accelerated proximal gradient (APG) [52] method is used on the smoothed optimization case. Note that our first proposed Nesterov smoothing method is equivalent to the one in [32], as can be deduced from the results of [51]. It's noted that the smoothing parameter has to be chosen empirically in this method. Thus, by the excess gap technique (EGT) [44], we developed a variant of EGT-based primal-dual method in order to select the smoothing parameter systematically. Furthermore, inspired by [53, 54], a variant of algorithm for quadratically constrained $l_2$-$l_1$ mixed norm minimization is proposed by using the smoothed dual conic optimization and continuation technique. The performance and computational efficiency of our second proposed method is demonstrated, and compared with the interior point method (CVX), MUSIC, M+LFBF, and CRLB.

## 3.2 Preliminaries and DoA Model with Structured Perturbations

### 3.2.1 Preliminaries

In this section, some definitions and preliminary results are stated to be referenced later.

**Definition 3.1** (Lipschitz Continuous)**.** *A function $f : \mathbb{R}^n \to \mathbb{R}$ is $\rho$-Lipschitz continuous if there exits $\rho > 0$ such that $|f(\mathbf{x}) - f(\mathbf{y})| \leq \rho\|\mathbf{x} - \mathbf{y}\|$, $\forall \mathbf{x}, \mathbf{y} \in \mathbb{R}^n$.*

**Definition 3.2** (Lipschitz Continuous Gradient)**.** *The gradient of a differentiable convex function $f : \mathbb{R}^n \to \mathbb{R}$ is Lipschitz continuous with parameter $L > 0$ if $\|\nabla f(\mathbf{x}) - \nabla f(\mathbf{y})\| \leq L\|\mathbf{x} - \mathbf{y}\|$, $\forall \mathbf{x}, \mathbf{y} \in \mathbb{R}^n$.*

**Definition 3.3** (Strongly Convex)**.** *The function $f : \mathcal{X} \to \mathbb{R}$ is $\sigma$-strongly convex on a closed convex set $\mathcal{X}$ with parameter $\sigma > 0$ if $f(\mathbf{y}) \geq f(\mathbf{x}) + \nabla f(\mathbf{x})^T(\mathbf{y} - \mathbf{x}) + \frac{\sigma}{2}\|\mathbf{y} - \mathbf{x}\|_2^2$, $\forall \mathbf{x}, \mathbf{y} \in \mathcal{X}$.*

The generic convex composite optimization problem is of the form:

$$\min_{\mathbf{x} \in \mathbb{R}^n} \{f(\mathbf{x}) + h(\mathbf{x}) + i(\mathbf{x})\}, \tag{3.1}$$

that satisfy the following assumptions:

**Assumption 3.1.**

(i) $f : \mathbb{R}^n \to \mathbb{R} \cup \{+\infty\}$ is a proper, closed, convex and continuously differentiable function. Its gradient is Lipschitz continuous with parameter $L_f$.

(ii) $h : \mathbb{R}^n \to \mathbb{R} \cup \{+\infty\}$ is a proper, closed, and convex $\rho_h$-Lipschitz continuous function. It is not necessarily differentiable.

(iii) $i : \mathbb{R}^n \to \mathbb{R} \cup \{+\infty\}$ is a proper, lower semicontinuous, and convex function but possibly nonsmooth. For instance, the indicator function of a closed set is lower semi-continuous.

### 3.2.2 Quick Review of DoA Model with Structured Perturbations

Recap the measurement model in Capter 2 and its covariance is described by

$$\mathbf{v}(t) = \sum_{k=1}^{K} \tilde{s}_k(t)\mathbf{a}(\theta_k) + \mathbf{n}(t) = \tilde{\mathbf{A}}(\boldsymbol{\theta})\tilde{\mathbf{s}}(t) + \mathbf{n}(t), \tag{3.2}$$

$$\mathbf{R}_{\mathbf{v}} = E[\mathbf{v}\mathbf{v}^H] = \sum_{k=1}^{K} \sigma_k^2 \mathbf{a}(\theta_k)\mathbf{a}(\theta_k)^H + \sigma_n^2\mathbf{I}. \tag{3.3}$$

- $\mathbf{v}(t) \in \mathbb{C}^{M\times 1}$ is the measurement vector.
- $\tilde{s}_k(t)$ is the $k$-th received signal with power $\sigma_k^2$.
- $\mathbf{a}(\theta_k)$ denotes the steering vector for direction $\theta_k$ with $m$-th entry $e^{-j2\pi\frac{d_m}{\lambda}sin\theta_k}$, where $\lambda$ is wavelength. $\tilde{\mathbf{A}}(\boldsymbol{\theta}) = [\mathbf{a}(\theta_1), \ldots, \mathbf{a}(\theta_K)]$.

In compressed sensing, $\boldsymbol{\phi} = [\phi_1, \ldots, \phi_N]$ is defined as uniformly discretized grid atoms for the dictionary matrix. The off-grid DoA is denoted by $\beta_i = \theta_k - \phi_i$ if $\phi_i$ is closest to $\theta_k, \forall k$; otherwise, $\beta_i = 0$. We assume that $0 \le |\beta_i| \le r$ and $r = \frac{|\phi_i - \phi_{i+1}|}{2}$.

By using Taylor series, the first-order approximate measurement model [55] is

$$\tilde{\mathbf{v}}(t) = (\tilde{\mathbf{A}}(\boldsymbol{\phi}) + \tilde{\mathbf{B}}\Gamma)\bar{\mathbf{s}}(t) + \mathbf{n}(t), \tag{3.4}$$

where $\tilde{\mathbf{B}} = [\frac{\partial \mathbf{a}(\phi_1)}{\partial \phi_1}, \ldots, \frac{\partial \mathbf{a}(\phi_N)}{\partial \phi_N}] \in \mathbb{C}^{M\times N}$, $\boldsymbol{\beta} = [\beta_1, \ldots, \beta_N]^T$, $\Gamma = diag(\boldsymbol{\beta})$, and $\bar{\mathbf{s}}$ is a $\mathbb{C}^{N\times 1}$ sparse vector. By vectorizing the covariance of (3.4), we have

$$\begin{aligned} \mathbf{y} &= (\mathbf{A}(\boldsymbol{\phi}) + \mathbf{B}\Gamma)\mathbf{s} + \sigma_n\mathbf{1}_n \\ &= (\mathbf{A}(\boldsymbol{\phi})\mathbf{s} + \mathbf{B}\mathbf{p}) + \sigma_n\mathbf{1}_n = [\mathbf{A}(\boldsymbol{\phi}), \mathbf{B}]\mathbf{x} + \sigma_n\mathbf{1}_n. \end{aligned} \tag{3.5}$$

- $\mathbf{y} = vec(\mathbf{R}_{\tilde{\mathbf{v}}})$.
- $\mathbf{A}(\boldsymbol{\phi}) = [\mathbf{a}(\phi_1)^H \otimes \mathbf{a}(\phi_1), \ldots, \mathbf{a}(\phi_N)^H \otimes \mathbf{a}(\phi_N)] \in \mathbb{C}^{M^2\times N}$.
- $\mathbf{B} = [\frac{\partial \mathbf{a}(\phi_1)}{\partial \phi_1} \otimes \frac{\partial \mathbf{a}(\phi_1)}{\partial \phi_1}, \ldots, \frac{\partial \mathbf{a}(\phi_N)}{\partial \phi_N} \otimes \frac{\partial \mathbf{a}(\phi_N)}{\partial \phi_N}] \in \mathbb{C}^{M^2\times N}$.
- $\mathbf{s}$ is a $\mathbb{R}^{N\times 1}$ sparse vector with $K$ nonzero terms $\sigma_k^2$'s.

$\mathbf{1}_n = [e_1^T, \ldots, e_M^T]^T$ where $e_i \in \mathbb{R}^{M\times 1}$ is a all-zero vector except 1 at $i$-th entry. $\mathbf{x} = [\mathbf{s}^T, \mathbf{p}^T]^T \in \mathbb{R}^{2N\times 1}$, and $\mathbf{p} = \boldsymbol{\beta} \odot \mathbf{s}$. Let $\mathbf{G} = [\mathbf{A}(\boldsymbol{\phi}), \mathbf{B}]$ for the following sections. Note that if $r$ is taken small, then $\mathbf{s} \gg \mathbf{p}$ since the value of $\beta_k$ is much smaller than $\sigma_k^2$ at mild SNRs.

Since $\mathbf{s}, \mathbf{p}$ have the same sparsity pattern, we can solve (3.5) over a closed convex set $\mathcal{X}$ by group Lasso :

$$\begin{aligned} &\arg\min_{\mathbf{x}\in\mathcal{X}} \ \frac{1}{2}||\mathbf{y} - \mathbf{G}\mathbf{x}||_2^2 + \eta||\mathbf{x}||_{2,1}, \\ &\text{s.t.} \ \ \mathcal{X} = \{\mathbf{x} = [\mathbf{s}^T, \mathbf{p}^T]^T : \mathbf{s} \geq 0, -r\mathbf{s} \leq \mathbf{p} \leq r\mathbf{s}\}. \end{aligned} \tag{3.6}$$

where $\eta > 0$ is a regularization parameter, and $r$ is defined previously. Because the constraint set $\mathcal{X}$ is simple, we can transform it into an unconstrained one by using an indicator function:

$$\arg\min_{\mathbf{x}\in\mathbb{R}^{2N\times 1}} F(\mathbf{x}) = \{\frac{1}{2}||\mathbf{y} - \mathbf{G}\mathbf{x}||_2^2 + \eta||\mathbf{x}||_{2,1} + \iota_{\mathcal{X}}(\mathbf{x})\}, \tag{3.7}$$

where $\iota_{\mathcal{X}}(\mathbf{x}) = \mathbf{0}$ if $\mathbf{x} \in \mathcal{X}$; otherwise, $\infty$. Let $f(\mathbf{x}) := \frac{1}{2}||\mathbf{y}-\mathbf{G}\mathbf{x}||_2^2$, $h(\mathbf{x}) := \eta||\mathbf{x}||_{2,1}$, and $g(\mathbf{x}) := \iota_{\mathcal{X}}(\mathbf{x})$. However, two nonsmooth functions in the objective makes this problem difficult to solve efficiently.

## 3.3 Alternating Direction Method of Multipliers (ADMM)

Let us consider the unconstrained problem first.

$$\arg\min_{\mathbf{x}\in\mathbb{R}^{2N\times 1}} F(\mathbf{x}) = \{f(\mathbf{x}) + h(\mathbf{x}) + \iota_{\mathcal{X}}(\mathbf{x})\}, \tag{3.8}$$

$f(\mathbf{x}) := \frac{1}{2}||\mathbf{y} - \mathbf{G}\mathbf{x}||_2^2$, $h(\mathbf{x}) := \eta||\mathbf{x}||_{2,1}$, $\iota_{\mathcal{X}}(\mathbf{x})$ is an indicator function. This problem can be solved by consensus ADMM (C-ADMM), which uses a consensus global variable $\mathbf{x}$ and local variables $\mathbf{z}_i$:

$$\begin{aligned} &\arg\min_{\mathbf{x},\mathbf{z}_i} \frac{1}{2}||\mathbf{y} - \mathbf{G}\mathbf{z}_1||_2^2 + \eta||\mathbf{z}_2||_{2,1} + \iota_{\mathcal{X}}(\mathbf{z}_3). \\ &s.t. \quad \mathbf{z}_1 = \mathbf{x}, \ \mathbf{z}_2 = \mathbf{x}, \ \mathbf{z}_3 = \mathbf{x} \end{aligned} \tag{3.9}$$

We call this a "consensus problem" since the constraint forces all the local variables to be equal.

ADMM of this problem can be derived from the augmented Lagrangian

$$L_\rho(\mathbf{z},\mathbf{x},\mathbf{u}) = \sum_{i=1}^{3}(f_i(\mathbf{z}_i) + \mathbf{u}_i^T(\mathbf{z}_i - \mathbf{x}) + \frac{\rho}{2}\|\mathbf{z}_i - \mathbf{x}\|_2^2), \tag{3.10}$$

where $f_1(\mathbf{z}_1) = \frac{1}{2}||\mathbf{y} - \mathbf{G}\mathbf{z}_1||_2^2$, $f_2(\mathbf{z}_2) = \eta||\mathbf{z}_2||_{2,1}$, $f_3(\mathbf{z}_2) = \iota_{\mathcal{X}}(\mathbf{z}_3)$, and $\rho$ is a penalty parameter. The resulting consensus ADMM is summarized in Algorithm 3.1.

**Algorithm 3.1** Consensus Alternating Direction Method of Multipliers (ADMM)

**Input:** $\mathbf{x}^0 = \mathbf{0}$, $\mathbf{z}_i^0 = \mathbf{0}, \forall i$, $\mathbf{u}^0 = [\mathbf{u}_1^0, \mathbf{u}_2^0, \mathbf{u}_3^0] = \mathbf{0}$, $\rho = 1$

**Step k:** $(k \geq 0)$

1: $\mathbf{z}_1^{k+1} = \arg\min_{\mathbf{z}_1} L_\rho(\mathbf{z}_1, \mathbf{x}^k, \mathbf{u}^k)$
$\Rightarrow \mathbf{z}_1^{k+1} = (\mathbf{G}^H\mathbf{G} + \rho\mathbf{I})^{-1}(\mathbf{G}^H\mathbf{y} + \rho\mathbf{x}^k - \mathbf{u}_1^k)$
$\mathbf{z}_2^{k+1} = \arg\min_{\mathbf{z}_2} L_\rho(\mathbf{z}_2, \mathbf{x}^k, \mathbf{u}^k)$
$\Rightarrow \mathbf{z}_2^{k+1} = \frac{\mathbf{x}^k + \mathbf{u}_2^k/\rho}{\|\mathbf{x}^k + \mathbf{u}_2^k/\rho\|_2}\max(\|\mathbf{x}^k + \mathbf{u}_2^k/\rho\|_2 - \eta/\rho, 0)$
$\mathbf{z}_3^{k+1} = \arg\min_{\mathbf{z}_3} L_\rho(\mathbf{z}_3, \mathbf{x}^k, \mathbf{u}^k) = Proj_{\mathcal{X}}(\mathbf{x}^k - \frac{\mathbf{u}_3^k}{\rho})$

2: $\mathbf{x}^{k+1} = \arg\min_{\mathbf{x}} L_\rho(\mathbf{z}^{k+1}, \mathbf{x}, \mathbf{u}^k) = \frac{\rho(\sum_i \mathbf{z}_i + \sum_i \mathbf{u}_i)}{3\rho}$

3: $\mathbf{u}_1^{k+1} = \mathbf{u}_1^k + \rho(\mathbf{z}_1^{k+1} - \mathbf{x}^{k+1})$
$\mathbf{u}_2^{k+1} = \mathbf{u}_2^k + \rho(\mathbf{z}_2^{k+1} - \mathbf{x}^{k+1})$
$\mathbf{u}_3^{k+1} = \mathbf{u}_3^k + \rho(\mathbf{z}_3^{k+1} - \mathbf{x}^{k+1})$

The convergence of ADMM is in terms of the following two assumptions:

**Assumption 3.2.** *The extended-real-valued function* $f_i(\mathbf{z}_i) : \mathbb{R}^n \to \mathbb{R} \cup \{+\infty\}$ *are closed, proper, and convex.*

**Assumption 3.3.** *The unaugmented Lagragian* $L_0$ *has a saddle point. Namely, there exists a not necessarily unique solution* $(\mathbf{z}^*, \mathbf{x}^*, \mathbf{u}^*)$ *such that*

$$L_0(\mathbf{z}^*, \mathbf{x}^*, \mathbf{u}) \leq L_0(\mathbf{z}^*, \mathbf{x}^*, \mathbf{u}^*) \leq L_0(\mathbf{z}, \mathbf{x}, \mathbf{u}^*) \tag{3.11}$$

In [39], under assumptions 2 and 3, ADMM is shown to have its iterations satisfy residual convergence, objective convergence, and dual variable convergence. The following summarizes the algorithm.

Although ADMM converges to modest accuracy within a few tens of iterations for many applications, some examples show that ADMM has very slow convergence to high accuracy. This motivates us to think if there exist other techniques which have better convergence than ADMM.

## 3.4 Smoothing Techniques

In the following sections, we will show how to deal with problem (3.7) by combining the accelerated proximal gradient algorithm with the Nesterov smoothing technique. We aim to smooth the group-sparsity penalty $h(\mathbf{x}) = \eta||\mathbf{x}||_{2,1}$ so that the APG method can be used. A variant of EGT-based primal-dual method and smoothed dual conic optimization method are described as well. In order to present the idea more clearly, we introduce the notation $||\mathbf{x}||_{2,1} = \sum_{g_i \in \Omega} \|\mathbf{x}_{g_i}\|_2$, where $\mathbf{x}_{g_i} \in \mathbb{R}^{|g_i|}$ denotes the subvector of $\mathbf{x}$ having the same sparse pattern in group $g_i$, where $|\cdot|$ is the cardinality of a set. Each group $g_i$ represents a subset of index set $\{1, \cdots, 2N\}$ and is disjoint from the others. Denote $\Omega = \{g_1, \ldots, g_{|\Omega|}\}$ as the set of groups, and $2N = \sum_{i=1}^{|\Omega|} |g_i|$. In our case, $|\Omega| = N$, $|g_i| = 2, g_i = \{i, i+N\}, \forall i = 1, \cdots, N$, $\mathbf{x}_{g_i} = [x_i, x_{i+N}]^T \in \mathbb{R}^2$ where $x_i = s_i$ and $x_{i+N} = p_i$. Denote $x_i$, $s_i$, and $p_i$ as the $i$-th entry of $\mathbf{x}, \mathbf{s}$, and $\mathbf{p}$, respectively.

## 3.5 The Nesterov Smoothing

### 3.5.1 Reformulation of Group-sparsity Penalty

Since $h(\mathbf{x})$ is an $\ell_2$-$\ell_1$ mixed norm with two layers, i.e., the inner is $\ell_2$ norm and the outer is $\ell_1$ norm, we can utilize the dual norm property to reformulate it as a maximization of a linear function over an auxiliary variable with "simple" constraints in two different ways.

First, inspired by [45], by using the convex conjugate function and the fact that the dual norm of $\ell_2$ norm is $\ell_2$ norm, $\|\mathbf{x}_{g_i}\|_2$ has the max-structure as $\max_{\|\mathbf{u}_{g_i}\|_2 \leq 1} \mathbf{u}_{g_i}^T \mathbf{x}_{g_i}$

where $\mathbf{u}_{g_i} \in \mathbb{R}^{|g_i|}$ denotes an auxiliary vector. Then, $h(\mathbf{x})$ can be written as

$$\begin{aligned} h(\mathbf{x}) &= \eta \sum_{g_i \in \Omega} \|\mathbf{x}_{g_i}\|_2 = \sum_{g_i \in \Omega} \max_{\|\mathbf{u}_{g_i}\|_2 \leq 1} \{\eta \langle \mathbf{x}_{g_i}, \mathbf{u}_{g_i} \rangle\} \\ &= \max_{\mathbf{u} \in \mathcal{U}_{l_2}} \sum_{g_i \in \Omega} \{\eta \langle \mathbf{x}_{g_i}, \mathbf{u}_{g_i} \rangle\} = \max_{\mathbf{u} \in \mathcal{U}_{l_2}} \{\eta \langle \mathbf{x}, \mathbf{u} \rangle\}, \end{aligned} \tag{3.12}$$

where $\mathcal{U}_{l_2} = \{\mathbf{u} \in \mathbb{R}^{2N \times 1} : \|\mathbf{u}_{g_i}\|_2 \leq 1, \forall g_i \in \Omega\}$ is the set of vectors in the space of the Cartesian product of $\ell_2$ norm unit ball. In the Nesterov smoothing technique, if a nonsmooth convex function has the max-structure, then we have its corresponding smoothed function

$$h_\mu^{l_2}(\mathbf{x}) := \max_{\mathbf{u} \in \mathcal{U}_{l_2}} \{\eta \langle \mathbf{x}, \mathbf{u} \rangle - \mu d_{l_2}(\mathbf{u})\} \tag{3.13}$$

with a smoothing parameter $\mu > 0$. We suppose that a *prox-function* $d_{l_2}(\mathbf{u})$ [41] is continuous and strongly convex on $\mathcal{U}_{l_2}$ with a strong convexity parameter $\sigma$. Its *prox-center* of $d(\mathbf{u})$ is denoted by $\mathbf{u}_0 = \arg\min_{\mathbf{u} \in \mathcal{U}_{l_2}} \{d_{l_2}(\mathbf{u})\}$. By the definition of strongly convex, $d_{l_2}(\mathbf{u}) \geq \frac{\sigma}{2}\|\mathbf{u} - \mathbf{u}_0\|_2^2$. Since $d_{l_2}(\mathbf{u})$ is strongly convex, $h_\mu^{l_2}(\mathbf{x})$ is a smooth and convex function so that its solution is unique and its gradient can be computed easily.

Second, inspired by by the fact that the dual norm of $\ell_1$ norm is $\ell_\infty$ norm, $\|\mathbf{x}\|_1$ has the max-structure as $\max_{\|\mathbf{u}\|_\infty \leq 1} \mathbf{u}^T\mathbf{x}$, where $\mathbf{u}$ denotes an auxiliary vector. Therefore, we propose a second reformulation. Let us define $\nu_i := \|\mathbf{x}_{g_i}\|_2$ and $\boldsymbol{\nu} = [\nu_1, \ldots, \nu_{|\Omega|}]^T \in \mathbb{R}^{N \times 1}$, and then $h(\mathbf{x})$ can be rewritten as

$$h(\mathbf{x}) = \eta \sum_{g_i \in \Omega} \|\mathbf{x}_{g_i}\|_2 = \eta \sum_{i=1}^{|\Omega|} \nu_i = \eta \|\nu\|_1. \tag{3.14}$$

We define a new function $h(\boldsymbol{\nu})$ as

$$h(\boldsymbol{\nu}) = \eta \|\nu\|_1 = \max_{\mathbf{u} \in \mathcal{U}_{l_1}} \{\eta \langle \boldsymbol{\nu}, \mathbf{u} \rangle\}, \tag{3.15}$$

where $\mathcal{U}_{l_1} = \{\mathbf{u} \in \mathbb{R}^{N \times 1} : \|\mathbf{u}\|_\infty \leq 1\}$ is the set of vectors in the space of $\ell_\infty$ norm unit ball. Since it has the max-structure, we have its corresponding smoothed function

$$h_\mu^{l_1}(\boldsymbol{\nu}) := \max_{\mathbf{u} \in \mathcal{U}_{l_1}} \{\eta \langle \boldsymbol{\nu}, \mathbf{u} \rangle - \mu d_{l_1}(\mathbf{u})\} \tag{3.16}$$

with a smoothing parameter $\mu > 0$. Then, $h_\mu^{l_1}(\boldsymbol{\nu})$ is also a smooth and convex function if a strongly convex function $d_{l_1}(\mathbf{u})$ is chosen. Note that the dimension of $\mathbf{x}$ is twice as many as $\boldsymbol{\nu}$.

Since both $h_\mu^{l_2}(\mathbf{x})$ and $h_\mu^{l_1}(\boldsymbol{\nu})$ are smooth and convex, their gradients can be formed by the following modified theorem [41]

**Theorem 3.1.** *For any $\mu > 0$, the functions $h_\mu^{l_2}(\mathbf{x})$ and $h_\mu^{l_1}(\boldsymbol{\nu})$ are well-defined and continuously differentiable in $\mathbf{x}$ and $\boldsymbol{\nu}$, respectively. Moreover, both functions are convex and their gradients:*

$$\nabla h_\mu^{l_2}(\mathbf{x}) = \eta \mathbf{u}^{l_2}, \qquad \nabla h_\mu^{l_1}(\boldsymbol{\nu}) = \eta \mathbf{u}^{l_1} \tag{3.17}$$

*are Lipschitz continuous with the same constant $L_\mu = \frac{1}{\mu\sigma}$, where $\mathbf{u}^{l_2}$ and $\mathbf{u}^{l_1}$ are the optimal solutions to (3.13) and (3.16), respectively.*

Suppose that $\forall \mathbf{u} \in \mathcal{U}_{l_2}$; we choose $d_{l_2}(\mathbf{u}) = \frac{1}{2}\|\mathbf{u}\|_2^2$ with a strong convexity parameter $\sigma = 1$. Then $\forall g_i$, $\mathbf{u}_{g_i}^{l_2}$, which is a subvector of $\mathbf{u}^{l_2}$, can be calculated as $\mathbf{u}_{g_i}^{l_2} = \mathcal{S}_2(\frac{\eta}{\mu}\mathbf{x}_{g_i})$ where $\mathcal{S}_2(\cdot)$ denotes the projection operator of projecting a vector $\mathbf{a}$ to a $\ell_2$ unit ball

$$\mathcal{S}_2(\mathbf{a}) = \begin{cases} \frac{\mathbf{a}}{\|\mathbf{a}\|_2}, & \text{if } \|\mathbf{a}\|_2 > 1 \\ \mathbf{a}, & \text{if } \|\mathbf{a}\|_2 \leq 1. \end{cases} \tag{3.18}$$

Similarly, $\forall \mathbf{u} \in \mathcal{U}_{l_1}$, if we choose $d_{l_1}(\mathbf{u}) = \frac{1}{2}\|\mathbf{u}\|_2^2$, then $\mathbf{u}^{l_1}$ can be computed as $\mathbf{u}^{l_1} = \mathcal{S}_1(\frac{\eta}{\mu}\boldsymbol{\nu})$ where $\mathcal{S}_1(\cdot)$ denotes the projection operator of projecting a vector $\mathbf{a}$ to an $\ell_\infty$ unit ball

$$\mathcal{S}_1(\mathbf{a}) = \begin{cases} 1, & \text{if } a_i > 1, \forall i \\ a_i, & \text{if } |a_i| \leq 1, \forall i \\ -1, & \text{if } a_i < -1, , \forall i \end{cases} \tag{3.19}$$

where $a_i$ is the $i$-th entry of $\mathbf{a}$.

Note that the dimension of $\boldsymbol{\nu}$ is a half of the one of $\mathbf{x}$. Therefore, for the case of $\nabla h_\mu^{l_1}(\boldsymbol{\nu})$, zero-padding is performed such that $\nabla h_\mu^{l_1}(\mathbf{x}) := [\nabla h_\mu^{l_1}(\boldsymbol{\nu})^T, \mathbf{0}^T]^T \in \mathbb{R}^{2N \times 1}$,

where $\mathbf{0}$ is a $\mathbb{R}^{N\times 1}$ zero vector, so that a new gradient $\nabla h_{\mu}^{l_1}(\mathbf{x})$ can be used in the accelerated proximal gradient. This is acceptable only when parameter $r$ is taken small enough. Since $\mathbf{p} \ll \mathbf{s}$ holds in this case, the value of $\nu_i$ mainly comes from the contribution of $\mathbf{s}$, so that zero vector can be assigned as the partial derivative of $\mathbf{p}$.

### 3.5.2 Accelerated Smoothing Proximal Gradient (ASPG)

Now, we solve two "smoothed" versions of problem (3.7)

$$\arg\min_{\mathbf{x}\in\mathbb{R}^n}\{H_i(\mathbf{x})+\iota_{\mathcal{X}}(\mathbf{x})\}, i=1 \text{ or } 2. \tag{3.20}$$

where $H_i(\mathbf{x}) := f(\mathbf{x})+h_{\mu}^{l_i}(\mathbf{x})$, $i=1$ or 2, and then its gradient is computed as $\nabla H_i(\mathbf{x}) = \nabla f(\mathbf{x}) + \eta\mathbf{u}^{l_i}$.

Problem (3.20) is suggested to be solved by the accelerated proximal gradient method [52] in which a proximal operator is used:

$$\text{prox}_{\iota}(\mathbf{y}) = \arg\min_{\mathbf{x}\in\mathbb{R}^n}\{\frac{1}{2}\|\mathbf{y}-\mathbf{x}\|^2+\iota(\mathbf{x})\}. \tag{3.21}$$

In fact, the proximal operator $\text{prox}_{\iota_{\mathcal{X}}}(\mathbf{y})$ of indicator function $\iota_{\mathcal{X}}(\mathbf{x})$ is the projection operator onto the set $\mathcal{X}$, $\Pi_{\mathcal{X}}(\mathbf{x})$. The ASPG method is summarized in the Algorithm 3.2.

### 3.5.3 Convergence Analysis

We now show the convergence rate of the algorithm by the following theorem:

**Theorem 3.2.** *Suppose $\mathbf{x}^k$ is the k-th iterative solution in Algorithm 3.2, and $\mathbf{x}^*$ is the optimal solution of problem (3.7). Assume that $\epsilon$-approximation is required, i.e., $F(\mathbf{x}^k)-F(\mathbf{x}^*)\le\epsilon$. If we set $\mu=\frac{\epsilon}{2D_i}$, where $D_i=\max_{\mathbf{u}\in\mathcal{U}_{l_i}} d_{l_i}(\mathbf{u})$, then*

$$F(\mathbf{x}^k)-F(\mathbf{x}^*)\le\frac{\epsilon}{2}+\frac{2(L_f+2\frac{D_i}{\epsilon\sigma})\|\mathbf{x}^0-\mathbf{x}^*\|^2}{(k+1)^2}, \tag{3.22}$$

**Algorithm 3.2** Accelerated Smoothing Proximal Gradient

**Input:** $\mathbf{x}^0 = \mathbf{x}^1 = \mathbf{0}$; $\gamma = 0.5$; $\mu = 10^{-8}$; step-size $\alpha^0 = 1$;
**Step k:** ($k \geq 1$) Let $\alpha := \alpha^{k-1}$. Compute
$\mathbf{w}^{k+1} = \mathbf{x}^k + \frac{k}{k+3}(\mathbf{x}^k - \mathbf{x}^{k-1})$

1: **repeat**
2: Compute $\nabla f(\mathbf{w}^{k+1}) = \mathbf{G}^H(\mathbf{G}\mathbf{w}^{k+1} - \mathbf{y})$,
3: Compute $\nabla h_\mu^{l_i}(\mathbf{w}^{k+1}) = \eta \mathbf{u}^{l_2}$ if $i = 2$,
4: Compute $\nabla h_\mu^{l_i}(\mathbf{w}^{k+1}) = \eta \mathbf{u}^{l_1}$ if $i = 1$,
5: $\mathbf{z} = \Pi_{\mathcal{X}}(\mathbf{w}^{k+1} - \alpha \nabla f(\mathbf{w}^{k+1}) - \alpha \nabla h_\mu^{l_i}(\mathbf{w}^{k+1}))$,
6: Break if $F_i(\mathbf{z}) \leq \hat{F}_i^{\alpha}(\mathbf{z}, \mathbf{w}^{k+1}) = F_i(\mathbf{w}^{k+1}) + (\nabla F_i(\mathbf{w}^{k+1}))^T(\mathbf{z} - \mathbf{w}^{k+1}) + \frac{1}{2\alpha}\|\mathbf{z} - \mathbf{w}^{k+1}\|_2^2$,
7: Update $\alpha := \gamma\alpha$,
8: **return** $\alpha^k := \alpha$, $\mathbf{x}^{k+1} := \mathbf{z}$

Note 1: $\mathbf{u}^{l_2}$ is composed of $\mathbf{u}_{g_i}^{l_2} = \mathcal{S}_2(\frac{\eta}{\mu}\mathbf{w}_{g_i}^{k+1}), \forall g_i$.
Note 2: $\mathbf{u}^{l_1} = [\mathcal{S}_1(\frac{\eta}{\mu}\boldsymbol{\nu})^T, \mathbf{0}^T]^T$ where $\nu_i = \|\mathbf{w}_{g_i}^{k+1}\|_2$, $\nu_i$ : $i$-th entry of $\boldsymbol{\nu}$

*where $L_f$ is Lipschitz continuous gradient parameter of $f(\mathbf{x})$. The number of iteration $k$ has an upper bound by*

$$\sqrt{\frac{4\|\mathbf{x}^0 - \mathbf{x}^*\|^2}{\epsilon}(L_f + \frac{2D_i}{\epsilon\sigma})} - 1 \tag{3.23}$$

*Proof.* Denote the smoothed version of the objective function $F(\mathbf{x})$ as

$$\min_{\mathbf{x}\in\mathbb{R}^n} F^{l_i}(\mathbf{x}) = \{f(\mathbf{x}) + h_\mu^{l_i}(\mathbf{x}) + \iota_{\mathcal{X}}(\mathbf{x})\}, i = 1 \text{ or } 2 \tag{3.24}$$

with the Lipschitz continuous gradient constant $L = L_f + \frac{1}{\mu\sigma}$. By using similar proof schemes in [56], we decompose

$$F(\mathbf{x}^k) - F(\mathbf{x}^*) = (F(\mathbf{x}^k) - F^{l_i}(\mathbf{x}^k)) + (F^{l_i}(\mathbf{x}^k) - F^{l_i}(\mathbf{x}^*)) + (F^{l_i}(\mathbf{x}^*) - F(\mathbf{x}^*)). \tag{3.25}$$

Then, based on the theorem from [57], we have the following bound for an optimal solution $\mathbf{x}^*$:

$$F(\mathbf{x}^k) - F(\mathbf{x}^*) \leq \frac{2L_f\|\mathbf{x}^0 - \mathbf{x}^*\|^2}{(k+1)^2}. \tag{3.26}$$

Also, by the definition of $h_\mu^{l_i}(\mathbf{x})$, we have

$$F^{l_i}(\mathbf{x}^k) \leq F(\mathbf{x}^k) \leq F^{l_i}(\mathbf{x}^k) + \mu D_i. \tag{3.27}$$

This implies that

$$F(\mathbf{x}^k) - F^{l_i}(\mathbf{x}^k) \leq \mu D_i. \tag{3.28}$$

$$F^{l_i}(\mathbf{x}^*) - F(\mathbf{x}^*) \leq 0. \tag{3.29}$$

Thus,

$$F(\mathbf{x}^k) - F(\mathbf{x}^*) \leq \mu D_i + \frac{2L\|\mathbf{x}^0 - \mathbf{x}^*\|^2}{(k+1)^2} = \mu D_i + \frac{2(L_f + \frac{1}{\mu\sigma})\|\mathbf{x}^0 - \mathbf{x}^*\|^2}{(k+1)^2}. \tag{3.30}$$

Let $\mu = \frac{\epsilon}{2D_i}$, then

$$F(\mathbf{x}^k) - F(\mathbf{x}^*) \leq \frac{\epsilon}{2} + \frac{2(L_f + \frac{2D_i}{\epsilon\sigma})\|\mathbf{x}^0 - \mathbf{x}^*\|^2}{(k+1)^2}. \tag{3.31}$$

If we let $\frac{\epsilon}{2} + \frac{2(L_f + \frac{2D_i}{\epsilon\sigma})\|\mathbf{x}^0 - \mathbf{x}^*\|^2}{(k+1)^2} = \epsilon$, then we have the upper bound in (3.23). □

This theorem implies its convergence rate is $\mathcal{O}(\frac{1}{k})$. We cannot achieve convergence rate $\mathcal{O}(\frac{1}{k^2})$ of accelerated proximal gradient method due to the smoothing process, but better than the subgradient methods with $\mathcal{O}(\frac{1}{\sqrt{k}})$ [40, 49].

## 3.6 Excessive Gap Technique

The smoothing papramter $\mu$ is chosen empirically in ASPG. Thus, inspired by [44], we choose $\mu$ systematically by the excessive gap technique with primal-dual gradient methods.

### 3.6.1 Preliminaries

In [44], we solve

$$\arg\min_{\mathbf{x}\in Q_1} F(\mathbf{x}), \tag{3.32}$$

where $f$ is continuous convex, but not neccesarily differentiable. $Q_1$ is a bounded closed convex set in a finite-dimensional real vector space $E_1$. The author considers the objective function $F(\mathbf{x})$ with the following structure

$$F(\mathbf{x}) = f(\mathbf{x}) + \max_{\mathbf{u}\in Q_2}\{\langle A\mathbf{x}, \mathbf{u}\rangle - \phi(\mathbf{u})\} \tag{3.33}$$

where $F(\mathbf{x})$ is continuous and convex on $Q_1$. $Q_2$ is a bounded closed convex set in a finite-dimensional real vector space $E_2$, A is a linear operator, and $\phi(\mathbf{u})$ is continuous and convex on $Q_2$. The function $f(\mathbf{x})$ and $\phi(\mathbf{u})$ are assumed to have Lipschitz-continuous gradient with Lipschitz constants $L_1(f)$ and $L_2(\phi)$. Its dual form can be derived as

$$\arg\max_{\mathbf{u}\in Q_2} \Phi(\mathbf{u}), \tag{3.34}$$

where $\Phi(\mathbf{u}) = -\phi(\mathbf{u}) + \min_{\mathbf{x}\in Q_1}\{\langle A\mathbf{x}, \mathbf{u}\rangle + f(\mathbf{x})\}$. Note that the structures of $f(\mathbf{x})$ and $\phi(\mathbf{u})$, $Q_1$, and $Q_2$ are assumed simple enough such that the optimization problem can be solved in a closed form. Remember that function $F(\mathbf{x})$ and $\Phi(\mathbf{u})$ are assumed nondifferentiable, so we are going to construct a smooth approximation of them.

Let us consider a *prox-function* $d_2(\mathbf{u})$ of the set $Q_2$. Namely, $d_2(\mathbf{u})$ is continuous and strongly convex on $Q_2$ with parameter $\sigma_2 > 0$. The *prox-center* of $d_2(\mathbf{u})$ is denoted by

$$\mathbf{u}_0 = \arg\max_{\mathbf{u}\in Q_2} d_2(\mathbf{u}). \tag{3.35}$$

Without loss of generality, we suppose that $d_2(\mathbf{u}_0) = 0$, so we have the following property:

$$d_2(\mathbf{u}) \geq d_2(\mathbf{u}_0) + \frac{1}{2}\sigma_2\|\mathbf{u} - \mathbf{u}_0\|^2 = \frac{1}{2}\sigma_2\|\mathbf{u} - \mathbf{u}_0\|^2. \tag{3.36}$$

Now, we can construct a smooth approximation function $F_{\mu_2}(\mathbf{x})$

$$F_{\mu_2}(\mathbf{x}) = f(\mathbf{x}) + \max_{\mathbf{u}\in Q_2}\{\langle A\mathbf{x}, \mathbf{u}\rangle - \phi(\mathbf{u}) - \mu_2 d_2(\mathbf{u})\} \tag{3.37}$$

where $\mu_2$ is a positive smoothing parameter. We define $\mathbf{u}_{\mu_2}(\mathbf{x})$ as the optimal solution of the above problem. And $\mathbf{u}_{\mu_2}(\mathbf{x})$ is unique because $d_2(\mathbf{u})$ is strongly convex. In terms of Danskin's theorem, the gradient of $F_{\mu_2}(\mathbf{x})$ can be computed as

$$\nabla F_{\mu_2}(\mathbf{x}) = \nabla f(\mathbf{x}) + A^H \mathbf{u}_{\mu_2}(\mathbf{x}) \tag{3.38}$$

with Lipschitz-continuous constant $L_1(F) = L_1(f) + \frac{1}{\sigma_2 \mu_2}\|A\|^2$.

By the same way, let us consider a *prox-function* $d_1(\mathbf{x})$ of the set $Q_1$. Namely, $d_2(\mathbf{x})$ is continuous and strongly convex on $Q_1$ with parameter $\sigma_1 > 0$. The *prox-center* of $d_1(\mathbf{x})$ is denoted by

$$\mathbf{x}_0 = \arg\max_{\mathbf{u}\in Q_1} d_1(\mathbf{x}). \tag{3.39}$$

Without loss of generality, we suppose that $d_1(\mathbf{x}_0) = 0$, so we have the following property:

$$d_1(\mathbf{x}) \geq d_1(\mathbf{x}_0) + \frac{1}{2}\sigma_1\|\mathbf{x} - \mathbf{x}_0\|^2 = \frac{1}{2}\sigma_1\|\mathbf{x} - \mathbf{x}_0\|^2. \tag{3.40}$$

Thus, a smooth approximation function $\Phi_{\mu_1}(\mathbf{u})$ is

$$\Phi_{\mu_1}(\mathbf{u}) = -\phi(\mathbf{u}) + \min_{\mathbf{x}\in Q_1}\{\langle A\mathbf{x}, \mathbf{u}\rangle + f(\mathbf{x}) + \mu_1 d_1(\mathbf{x})\} \tag{3.41}$$

where $\mu_1$ is a positive smoothing parameter. We define $\mathbf{x}_{\mu_1}(\mathbf{u})$ as the optimal solution of the above problem. And $\mathbf{x}_{\mu_1}(\mathbf{u})$ is unique because $d_1(\mathbf{x})$ is strongly convex. In terms of Danskin's theorem, the gradient of $\Phi_{\mu_1}(\mathbf{u})$ can be computed as

$$\nabla \Phi_{\mu_1}(\mathbf{u}) = -\nabla\phi(\mathbf{u}) + A^H \mathbf{x}_{\mu_1}(\mathbf{u}) \tag{3.42}$$

with Lipschitz-continuous constant $L_2(\Phi) = L_2(\phi) + \frac{1}{\sigma_1 \mu_1}\|A\|^2$.

We know, for any $\mathbf{x} \in Q_1$ and $\mathbf{u} \in Q_2$,

$$\Phi(\mathbf{u}) \leq F(\mathbf{x}) \tag{3.43}$$

always holds. However, we also have

$$F_{\mu_2}(\mathbf{x}) \leq F(\mathbf{x}) \tag{3.44}$$

$$\Phi(\mathbf{u}) \leq \Phi_{\mu_1}(\mathbf{u}) \tag{3.45}$$

, so that there exists a probability to have the following *excessive gap condition (EGC)*:

$$F_{\mu_2}(\bar{\mathbf{x}}) \leq \Phi_{\mu_1}(\bar{\mathbf{u}}) \tag{3.46}$$

for certain $\bar{\mathbf{x}} \in Q_1$ and $\bar{\mathbf{u}} \in Q_2$. Then, an upper bound for the primal-dual pair $(\bar{\mathbf{x}}, \bar{\mathbf{u}})$ is derived by the following lemma:

**Lemma 3.1.** *Let $\bar{\mathbf{x}} \in Q_1$ and $\bar{\mathbf{u}} \in Q_2$ satisfy EGC. Then,*

$$\begin{aligned} 0 &\leq \max\{F(\bar{\mathbf{x}}) - F^*, F^* - \Phi(\bar{\mathbf{u}})\} \\ &\leq F(\bar{\mathbf{x}}) - \Phi(\bar{\mathbf{u}}) \leq \mu_1 D_1 + \mu_2 D_2 \end{aligned}$$

*where $D_1 = \max_{\mathbf{x} \in Q_1} d_1(\mathbf{x})$, $D_2 = \max_{\mathbf{u}_1 \in Q_2} d_2(\mathbf{u})$.*

We also need to justify that some starting primal-dual pair can satisfy the EGC by defining the *primal gradient mapping*

$$T_{\mu_2}(\mathbf{x}) = \arg\min_{\mathbf{z} \in Q_1} \{\langle \nabla F_{\mu_2}(\mathbf{x}), \mathbf{z} - \mathbf{x} \rangle + \frac{1}{2} L_1(F_{\mu_2}(\mathbf{x})) \|\mathbf{z} - \mathbf{x}\|^2\} \tag{3.47}$$

and the following lemma:

**Lemma 3.2** (Choose initial points)**.** *Choose an arbitrary $\mu_2 > 0$. For a starting point $\mathbf{x}_0$, define*

$$\bar{\mathbf{x}} = T_{\mu_2}(\mathbf{x}_0), \bar{\mathbf{u}} = \mathbf{u}_{\mu_2}(\mathbf{x}_0).$$

*Then the EGC (3.57) is satisfied for any $\mu_1 \geq \frac{1}{\sigma_1} L_1(F_{\mu_2})$.*

Thus, if EGC is satisfied for some certain primal-dual pair, then the primal-dual pair can be updated iteratively when keeping satisfy the EGC as $\mu_1$ and $\mu_2$ go to zero.

In other words, we can try to decrease $\mu_1$ with fixed $\mu_2$ for the primal problem; decrease $\mu_2$ with fixed $\mu_1$ for the dual problem. The following theorem gives a description for solving the primal problem:

**Theorem 3.3.** *Let $\bar{\mathbf{x}} \in Q_1$ and $\bar{\mathbf{u}} \in Q_2$ satisfy EGC (3.57) for $\mu_1, \mu_2 > 0$. Fix $\tau \in (0,1)$ and choose $\mu_1^+ = (1-\tau)\mu_1$,*

$$\begin{aligned}
\hat{\mathbf{x}} &= (1-\tau)\bar{\mathbf{x}} + \tau \mathbf{x}_{\mu_1}(\bar{\mathbf{u}}), \\
\bar{\mathbf{u}}_+ &= (1-\tau)\bar{\mathbf{u}} + \tau \mathbf{u}_{\mu_2}(\hat{\mathbf{x}}), \\
\bar{\mathbf{x}}_+ &= T_{\mu_2}(\hat{\mathbf{x}}).
\end{aligned}$$

*Then $(\bar{\mathbf{x}}_+, \bar{\mathbf{u}}_+)$ satisfies EGC with smoothness parameter $\mu_1^+, \mu_2^+$ provided that $\tau$ is chosen by $\frac{\tau^2}{1-\tau} \leq \frac{\mu_1 \sigma_1}{L_1(F_{\mu_2})}$.*

### 3.6.2 Proposed Methods

Now, let us consider the optimization problem (3.6) we want to solve

$$\begin{aligned}
&\arg\min_{\mathbf{x}\in\mathcal{X}} \;\; F(\mathbf{x}) = \{f(\mathbf{x}) + h(\mathbf{x})\}, \\
&\text{s.t.} \;\; \mathcal{X} = \{\mathbf{x} = [\mathbf{s}^T, \mathbf{p}^T]^T : \mathbf{s} \geq 0, -r\mathbf{s} \leq \mathbf{p} \leq r\mathbf{s}\}.
\end{aligned} \tag{3.48}$$

where $f(\mathbf{x}) := \frac{1}{2}||\mathbf{y} - \mathbf{G}\mathbf{x}||_2^2$, $h(\mathbf{x}) := \eta||\mathbf{x}||_{2,1} = \max_{\mathbf{u}_2 \in \mathcal{U}_{l_2}} \{\eta \langle \mathbf{x}, \mathbf{u}_2 \rangle\}$.
Since $\mathbf{G}$ is a fat matrix, the error fitting function $f(\mathbf{x})$ is not strongly convex. Thus, we replace $f(\mathbf{x})$ by $f_r(\mathbf{x}) = ||\mathbf{y} - \mathbf{G}\mathbf{x}||_2$. Although $f_r(\mathbf{x})$ is nondifferentiable, it can be expressed in a *max*-structure form, and smoothed by using a strongly convex function. Instead of solving (3.6), we propose

$$\begin{aligned}
&\arg\min_{\mathbf{x}\in\mathcal{X}} \;\; F(\mathbf{x}) = \{f_r(\mathbf{x}) + h(\mathbf{x})\}, \\
&\text{s.t.} \;\; \mathcal{X} = \{\mathbf{x} = [\mathbf{s}^T, \mathbf{p}^T]^T : \mathbf{s} \geq 0, -r\mathbf{s} \leq \mathbf{p} \leq r\mathbf{s}\}.
\end{aligned} \tag{3.49}$$

Thus, we will smoothe not only regularization term $h(\mathbf{x})$, but also the new error fitting function $f_r(\mathbf{x})$. This way can help in solving problems in closed form. We can rewrite

(3.49) into the following primal problem by using the dual norm definition:

$$\arg\min_{\mathbf{x}\in\mathcal{X}} F(\mathbf{x}) = \{\max_{\mathbf{u}=[\mathbf{u}_1^T,\mathbf{u}_2^T]^T,\mathbf{u}_1\in\mathcal{U}_2,\mathbf{u}_2\in\mathcal{U}_{l_2}} \langle\mathbf{G}\mathbf{x},\mathbf{u}_1\rangle - \langle\mathbf{y},\mathbf{u}_1\rangle + \eta\langle\mathbf{x},\mathbf{u}_2\rangle\}, \tag{3.50}$$

And its dual problem is

$$\max_{\mathbf{u}=[\mathbf{u}_1^T,\mathbf{u}_2^T]^T,\mathbf{u}_1\in\mathcal{U}_2,\mathbf{u}_2\in\mathcal{U}_{l_2}} \Phi(\mathbf{u}) := \{-\langle\mathbf{y},\mathbf{u}_1\rangle + \min_{\mathbf{x}\in\mathcal{X}}\langle\mathbf{G}\mathbf{x},\mathbf{u}_1\rangle + \eta\langle\mathbf{x},\mathbf{u}_2\rangle\} \tag{3.51}$$

where $\mathbf{u}$ is a dual variable vector composed of $\mathbf{u}_1$ and $\mathbf{u}_2$, $\mathcal{U}_{l_2} = \{\mathbf{u} \in \mathbb{R}^{2N\times 1} : \|\mathbf{u}_{g_i}\|_2 \leq 1, \forall g_i \in \Omega\}$, and $\mathcal{U}_2 = \{\mathbf{u} \in \mathbb{R}^{M\times 1} : \|\mathbf{u}\|_2 \leq 1\}$.

Since both $F(\mathbf{x})$ and $\Phi(\mathbf{u})$ are nondifferentiable, we can construct a smoothing approximation of primal-dual problem

$$\min_{\mathbf{x}\in\mathcal{X}} F_{\mu_2}(\mathbf{x}) := \{\max_{\mathbf{u}=[\mathbf{u}_1^T,\mathbf{u}_2^T]^T} \langle\mathbf{G}\mathbf{x}-\mathbf{y},\mathbf{u}_1\rangle + \eta\langle\mathbf{x},\mathbf{u}_2\rangle - \frac{\mu_2}{2}\|\mathbf{u}\|_2^2\}, \tag{3.52}$$

$$\max_{\mathbf{u}=[\mathbf{u}_1^T,\mathbf{u}_2^T]^T} \Phi_{\mu_1}(\mathbf{u}) := \{-\langle\mathbf{y},\mathbf{u}_1\rangle + \min_{\mathbf{x}\in\mathcal{X}}\langle\mathbf{G}\mathbf{x},\mathbf{u}_1\rangle + \eta\langle\mathbf{x},\mathbf{u}_2\rangle + \frac{\mu_1}{2}\|\mathbf{x}\|_2^2\} \tag{3.53}$$

by using two strongly convex functions $d_1(\mathbf{x}) = \frac{1}{2}\|\mathbf{x}\|_2^2$, and $d_2(\mathbf{u}) = \frac{1}{2}\|\mathbf{u}\|_2^2$ with two smoothing parameters $\mu_1$, and $\mu_2$.

For the primal problem, denote $\mathbf{u}_{1,\mu_2}, \mathbf{u}_{2,\mu_2}$ as the unique optimal solution of $F_{\mu_2}(\mathbf{x})$, which can be derived in closed form solutions:

$$\mathbf{u}_{1,\mu_2}(\mathbf{x}) = \mathbf{Proj}_{\mathcal{U}_2}(\frac{\mathbf{G}\mathbf{x}-\mathbf{y}}{\mu_2}) \tag{3.54}$$

$$\mathbf{u}_{2,\mu_2}(\mathbf{x}) = \mathbf{Proj}_{\mathcal{U}_{l_2}}(\frac{\eta\mathbf{x}}{\mu_2}) \tag{3.55}$$

. By Danskin's theorem, the gradient of $F_{\mu_2}(\mathbf{x})$ is computed as $\nabla F_{\mu_2}(\mathbf{x}) = \mathbf{G}^H\mathbf{u}_{1,\mu_2}(\mathbf{x}) + \eta\mathbf{u}_{2,\mu_2}(\mathbf{x})$ with Lipschitz-continuous constant $L_1(F_{\mu_2}(\mathbf{x})) = \frac{1}{\mu_2}\|[\mathbf{G},\eta\mathbf{I}]^H\|^2$.

Similarly, for the dual problem, denote $\mathbf{x}_{\mu_1}$ as the unique optimal solution of $\Phi_{\mu_1}(\mathbf{u})$, which can be derived in a closed form solution:

$$\mathbf{x}_{\mu_1}(\mathbf{u}) = \mathbf{Proj}_{\mathcal{X}}(-\frac{\mathbf{G}^H\mathbf{u}_1 + \eta\mathbf{u}_2}{\mu_1}) \tag{3.56}$$

. By Danskin's theorem, the gradient of $\Phi_{\mu_1}(\mathbf{u})$ is $\nabla\Phi_{\mu_1}(\mathbf{u}) = \begin{bmatrix} -\mathbf{y} \\ \mathbf{0} \end{bmatrix} + \begin{bmatrix} \mathbf{G}\mathbf{x}_{\mu_1}(\mathbf{u}) \\ \eta\mathbf{x}_{\mu_1}(\mathbf{u}) \end{bmatrix}$ wth Lipschitz-continuous constant $L_2(\Phi_{\mu_1}(\mathbf{u})) = \frac{1}{\mu_1}\|[\mathbf{G}^H, \eta\mathbf{I}]^H\|^2$.

Since we know that

- $\Phi(\mathbf{u}) \leq F(\mathbf{x})$
- By definition, $F_{\mu_2}(\mathbf{x}) \leq F(\mathbf{x})$, $\Phi(\mathbf{u}) \leq \Phi_{\mu_1}(\mathbf{u})$
- Excessive gap condition (EGC) holds when, for certain $\mathbf{x}$ and $\mathbf{u}$ with sufficiently large $\mu_1, \mu_2$, this inequality occurs

$$F_{\mu_2}(\mathbf{x}) \leq \Phi_{\mu_1}(\mathbf{u}) \tag{3.57}$$

Then, we have the following modified lemma:

**Lemma 3.3.** *Let $\mathbf{x} \in \mathcal{X}$ and $\mathbf{u} = [\mathbf{u}_1^T, \mathbf{u}_2^T]^T, \mathbf{u}_1 \in \mathcal{U}_2, \mathbf{u}_2 \in \mathcal{U}_{l_2}$ satisfy EGC. Then,*

$$\begin{aligned} 0 &\leq \max\{F(\mathbf{x}) - F^*, F^* - \Phi(\mathbf{u})\} \\ &\leq \Phi(\mathbf{u}) - F(\mathbf{x}) \leq \mu_1 D_1 + \mu_2 D_2 + \mu_2 D_3 \end{aligned}$$

*where $D_1 = \max_{\mathbf{x}\in\mathcal{X}} \|\mathbf{x}\|^2$, $D_2 = \max_{\mathbf{u}_1\in\mathcal{U}_2} \|\mathbf{u}_1\|^2$, $D_3 = \max_{\mathbf{u}_2\in\mathcal{U}_{l_2}} \|\mathbf{u}_2\|^2$*

.

By this lemma, EGC provides an upper bound of primal-dual pair $(\mathbf{x}, \mathbf{u})$ so that we can update iteratively the primal-dual pair $(\mathbf{x}, \mathbf{u})$ and keep satisfying EGC as $\mu_1, \mu_2 \to 0$. We also apply the primal gradient mapping:

$$T_{\mu_2}(\mathbf{x}) = \arg\min_{\mathbf{z}\in\mathcal{X}}\{\langle\nabla F_{\mu_2}(\mathbf{x}), \mathbf{z} - \mathbf{x}\rangle + \frac{1}{2}L_1(F_{\mu_2}(\mathbf{x}))\|\mathbf{z} - \mathbf{x}\|^2\}$$

and the dual gradient mapping:

$$T_{\mu_1}(\mathbf{u}) = \arg\min_{\mathbf{v}\in\mathcal{U}_2}\{\langle\nabla\Phi_{\mu_1}(\mathbf{x}), \mathbf{v} - \mathbf{u}\rangle + \frac{1}{2}L_2(\Phi_{\mu_1}(\mathbf{x}))\|\mathbf{v} - \mathbf{u}\|^2\}$$

to choose some starting point when satisfyling the EGC. In our case, they can be simplied in closed forms:

$$T_{\mu_2}(\hat{\mathbf{x}}) = Proj_{\mathcal{X}}(\mathbf{x} - \frac{1}{L_1(F_{\mu_2})}\nabla F_{\mu_2}(\mathbf{x})) \tag{3.58}$$

$$T_{\mu_1}(\hat{\mathbf{u}}) = Proj_{\mathcal{U}_2}(\mathbf{u} - \frac{1}{L_2(F_{\mu_1})}\nabla \Phi_{\mu_1}(\mathbf{u})) \tag{3.59}$$

The lemma for choosing initial points is:

**Lemma 3.4** (Choose initial points)**.** *Choose an arbitrary $\mu_2 > 0$. For a starting point $\mathbf{x}_0$, define*

$$\bar{\mathbf{x}} = T_{\mu_2}(\mathbf{x}_0), \bar{\mathbf{u}} = \mathbf{u}^*_{\mu_2}(\mathbf{x}_0) = \begin{bmatrix} \mathbf{u}^*_{1,\mu_2}(\mathbf{x}_0) \\ \mathbf{u}^*_{2,\mu_2}(\mathbf{x}_0) \end{bmatrix}.$$

*Then the EGC (3.57) is satisfied for any $\mu_1 \geq L_1(F_{\mu_2})$.*

We also give the theorem for the primal part of iterative algoritms:

**Theorem 3.4.** *Let $\bar{\mathbf{x}} \in \mathcal{X}$ and $\bar{\mathbf{u}} \in \mathcal{U} := \mathcal{U}_2 \cup \mathcal{U}_{l_2}$ satisfy EGC (3.57) for $\mu_1, \mu_2 > 0$. Fix $\tau \in (0,1)$ and choose $\mu_1^+ = (1-\tau)\mu_1$,*

$$\begin{aligned} \hat{\mathbf{x}} &= (1-\tau)\bar{\mathbf{x}} + \tau \mathbf{x}_{\mu_1}(\bar{\mathbf{u}}), \\ \bar{\mathbf{u}}_+ &= (1-\tau)\bar{\mathbf{u}} + \tau \mathbf{u}_{\mu_2}(\hat{\mathbf{x}}), \\ \bar{\mathbf{x}}_+ &= T_{\mu_2}(\hat{\mathbf{x}}) = Proj_{\mathcal{X}}(\hat{\mathbf{x}} - \frac{1}{L_1(F_{\mu_2})}\nabla F_{\mu_2}(\hat{\mathbf{x}})). \end{aligned}$$

*Then $(\bar{\mathbf{x}}_+, \bar{\mathbf{u}}_+)$ satisfies EGC with smoothness parameter $\mu_1^+, \mu_2^+$ provided that $\tau$ is chosen by $\frac{\tau^2}{1-\tau} \leq \frac{\mu_1}{L_1(F_{\mu_2})}$.*

The updates for primal-dual pair is summaried in Algorithm 3.3.

## 3.7 Smoothed Dual Conic Optimization

### 3.7.1 Preliminaries

In [53], a general framework is established to construct optimal first-order methods for dealing with certain type of convex optimization problems. Namely, the following conic

**Algorithm 3.3** Excessive Gap Technique (EGT)-based Primal-Dual Method

**Input:** $\mu_1 = \|[\mathbf{G}^T, \eta\mathbf{I}]^T\|\sqrt{\frac{D_2+D_3}{D_1}}, \mu_2 = \|[\mathbf{G}^T, \eta\mathbf{I}]^T\|\sqrt{\frac{D1}{D_2+D_3}}$,
$\bar{\mathbf{x}}_0 = T_{\mu_2}(\mathbf{x}_0), \bar{\mathbf{u}}_0 = \mathbf{u}_{\mu_2}(\mathbf{x}_0)$

**Step k:** $(k \geq 0)$

1: $\tau = \frac{2}{k+3}$

2: If $k$: even, then
$\hat{\mathbf{x}} = (1-\tau)\bar{\mathbf{x}} + \tau\mathbf{x}_{\mu_1}(\bar{\mathbf{u}})$
$\bar{\mathbf{u}}_+ = (1-\tau)\bar{\mathbf{u}} + \tau\mathbf{u}_{\mu_2}(\hat{\mathbf{x}})$
$\bar{\mathbf{x}}_+ = T_{\mu_2}(\hat{\mathbf{x}}) = Proj_{\mathcal{X}}(\hat{\mathbf{x}} - \frac{1}{L_1(F_{\mu_2})}\nabla F_{\mu_2}(\hat{\mathbf{x}}))$
$\mu_1^+ = (1-\tau)\mu_1, \mu_2^+ = \mu_2$

3: If $k$: odd, then
$\hat{\mathbf{u}} = (1-\tau)\bar{\mathbf{u}} + \tau\mathbf{u}_{\mu_2}(\bar{\mathbf{x}})$
$\bar{\mathbf{x}}_+ = (1-\tau)\bar{\mathbf{x}} + \tau\mathbf{x}_{\mu_1}(\hat{\mathbf{u}})$
$\bar{\mathbf{u}}_+ = T_{\mu_1}(\hat{\mathbf{u}}) = Proj_{\mathcal{U}}(\hat{\mathbf{u}} - \frac{1}{L_2(F_{\mu_1})}\nabla\Phi_{\mu_1}(\hat{\mathbf{u}}))$
$\mu_2^+ = (1-\tau)\mu_2, \mu_1^+ = \mu_1$

formulation is considered:

$$\arg\min_{\mathbf{x}} f(\mathbf{x})$$
$$\text{s.t.} \quad \mathcal{A}(\mathbf{x}) + \mathbf{b} \in \mathcal{K}$$

where $\mathbf{x} \in \mathbb{R}^n$ is a vector of optimization variables, function $f$ is convex but not necessarily smooth. $\mathcal{K} \in \mathbb{R}^m$ is a closed, convex cone, $\mathcal{A}$ is a linear operator: $\mathbb{R}^n \to \mathbb{R}^m$, and $\mathbf{b}$ is a constant vector.

Since the objective function $f$ might not be smooth and obtaining a feasible point on the constraint set might be expensive, resolving these issues using first-order methods in the dual problem or its approximation might be more preferable than in the primal problem. Thus, the dual of conic formulation is given as

$$\arg\max_{\mathbf{z}} g(\mathbf{z})$$
$$\text{s.t.} \quad \mathbf{z} \in \mathcal{K}^*,$$

where $g(\mathbf{z})$ denotes the Lagrage dual function

$$g(\mathbf{z}) \triangleq \inf_{\mathbf{x}} \mathcal{L}(\mathbf{x}, \mathbf{z}) = \inf_{\mathbf{x}} f(\mathbf{x}) - \langle \mathbf{z}, \mathcal{A}(\mathbf{x}) + \mathbf{b} \rangle, \tag{3.60}$$

and $\mathcal{K}^*$ is defined as the dual cone

$$\mathcal{K}^* \triangleq \{\mathbf{z} \in \mathbb{R}^m : \langle \mathbf{z}, \mathbf{x} \rangle \geq 0, \forall \mathbf{x} \in \mathcal{K}\}. \tag{3.61}$$

We have benefits from the dual problem, since it's usually efficient for projections onto the dual cone.

However, the dual function is usually not differentiable since the nature of the primal problem. Subgradient methods can serve as a solution, but suffers from slow convergence. Thus, the Nesterov smoothing technique is applied on the primal problem:

$$\begin{aligned} &\arg\min_{\mathbf{x}} f_\mu(\mathbf{x}) \triangleq f_\mu(\mathbf{x}) + \mu d(\mathbf{x}) \\ &\text{s.t.} \;\; \mathcal{A}(\mathbf{x}) + \mathbf{b} \in \mathcal{K}, \end{aligned}$$

where $d(\mathbf{x})$ is a strongly convex function with a smoothing positive parameter $\mu$. Then, the smoothed dual problem is the following

$$\begin{aligned} &\arg\max_{\mathbf{z}} g_\mu(\mathbf{z}) \\ &\text{s.t.} \;\; \mathbf{z} \in \mathcal{K}^*, \end{aligned}$$

where $g_\mu(\mathbf{z})$ is a smoothed surrogate of function $g$. In some applications, the smoothed dual problem can be reformulated to an unconstrained problem

$$\arg\max_{\mathbf{z}} -g_{sm}(\mathbf{z}) - h(\mathbf{z}),$$

where $g_{sm}(\mathbf{z})$ is smooth and convex, and $h$ is convex, but nonsmooth. This kind of composite problems can be solved efficiently by using optimal first-order methods. For example, the generalized projected gradient algorithm can be applied for the composite problem, and the corresponding iteration is the following

$$\mathbf{z}_{k+1} \leftarrow \arg\min_{\mathbf{z}} g_{sm}(\mathbf{z}_k) + \langle \nabla g_{sm}(\mathbf{z}_k), \mathbf{z} - \mathbf{z}_k \rangle + \frac{1}{2t_k} \|\mathbf{z} - \mathbf{z}_k\|^2 + h(\mathbf{z}),$$

where $t_k$ is the step size. [50] shows that $\epsilon$-optimality can be achieved in $\mathcal{O}(1/\epsilon)$ iterations if $t_k$ is selected properly. Furthermore, in [58, 59, 60, 61, 62], the iteration complexity can be improved to $\mathcal{O}(1/\sqrt{\epsilon})$ by using the following iterations:

$$\begin{aligned} \mathbf{z}_{k+1} &\leftarrow \arg\min_{\mathbf{z}\in\mathcal{K}^*} \|\nu_k + t_k \nabla g_{sm}(\nu_k) - \mathbf{z}\|_2 \\ \nu_{k+1} &\leftarrow \mathbf{z}_{k+1} + \alpha_k(\mathbf{z}_{k+1} - \mathbf{z}_k) \end{aligned} \tag{3.62}$$

where $\nu_0 = \mathbf{z}_0$ and the sequence $\{\alpha_k\}$ need to be designed specifically.

### 3.7.2 Proposed Methods

Instead of solving linear inequalities constrained BPDN problem

$$\arg\min_{\mathbf{x}\in\mathcal{X}} f(\mathbf{x}) + h(\mathbf{x}), \tag{3.63}$$

where $f(\mathbf{x}) := \frac{1}{2}||\mathbf{y}-\mathbf{G}\mathbf{x}||_2^2$, $h(\mathbf{x}) := \eta||\mathbf{x}||_{2,1}$, $\mathcal{X} = \{\mathbf{x} = [\mathbf{s}^T, \mathbf{p}^T]^T : \mathbf{s} \geq 0, -r\mathbf{s} \leq \mathbf{p} \leq r\mathbf{s}\}$
Inspired by [53], a quadratically constrained with linear inequalities constraints problem is considered

$$\begin{aligned} &\arg\min_{\mathbf{x}} ||\mathbf{x}||_{2,1} \\ &s.t. \quad \|\mathbf{y} - \mathbf{G}\mathbf{x}\|_2 \leq \epsilon, \mathbf{x} \in \mathcal{X}, \end{aligned} \tag{3.64}$$

since it's more natural to decide an appropriate $\epsilon$ rather than an appropriate regularization parameter $\eta$.
Note that $\mathcal{X}$ is a set of elements satisfying linear inequalities, so it can be replaced by a matrix form representation $\mathbf{A}\mathbf{x} \leq \mathbf{0}$.
Then, let's consider conic form of the primal problem

$$\begin{aligned} &\arg\min_{\mathbf{x}\in\mathbb{R}^{2N\times 1}} ||\mathbf{x}||_{2,1} \\ &s.t.\ (\mathbf{y} - \mathbf{G}\mathbf{x}, \epsilon) \in \mathcal{K}_2^M := \{(\mathbf{a}, b) \in \mathbb{C}^M \times \mathbb{R} : \|\mathbf{a}\|_2 \leq b\}, \\ &\quad \mathbf{A}\mathbf{x} \leq \mathbf{0}, \end{aligned} \tag{3.65}$$

and derive its dual by Lagrange multipliers

$$\arg \max_{\mathbf{z}\in\mathbb{C}^{M\times 1},\mathbf{w}\geq\mathbf{0}} g(\mathbf{z},\mathbf{w}) \tag{3.66}$$

where $g(\mathbf{z},\mathbf{w}) = \inf_{\mathbf{x}} ||\mathbf{x}||_{2,1} - \langle \mathbf{z}, \mathbf{y} - \mathbf{G}\mathbf{x}\rangle - \epsilon\|\mathbf{z}\|_2 + \langle \mathbf{w}, \mathbf{A}\mathbf{x}\rangle$.

Note that both objectives are nonsmooth in the primal and dual formulation. So, we smoothe $||\mathbf{x}||_{2,1}$ by adding the strongly convex *prox-function* $d(\mathbf{x}) = \frac{\sigma\mu}{2}\|\mathbf{x} - \mathbf{x}_0\|_2^2$ with a smoothing paramter $\mu$ and a strong convexity parameter $\sigma = 1$. $\mathbf{x}_0$ is denoted as the *prox-center* of $d(\mathbf{x})$

$$\mathbf{x}_0 = \arg\min_{\mathbf{x}\in\mathcal{X}} d(\mathbf{x}).$$

Without loss of generality, $d(\mathbf{x}_0) = 0$ is assumed.

In this way, the smoothed dual problem is given by

$$\arg \max_{\mathbf{z}\in\mathbb{C}^{M\times 1},\mathbf{w}\geq\mathbf{0}} g_\mu(\mathbf{z},\mathbf{w})$$

where

$$g_\mu(\mathbf{z},\mathbf{w}) = \inf_{\mathbf{x}} ||\mathbf{x}||_{2,1} + \frac{\mu}{2}\|\mathbf{x} - \mathbf{x}_0\|_2^2 - \langle \mathbf{z}, \mathbf{y} - \mathbf{G}\mathbf{x}\rangle - \epsilon\|\mathbf{z}\|_2 + \langle \mathbf{w}, \mathbf{A}\mathbf{x}\rangle$$

is a smooth function over $\mathbf{x}$. The optimal solution of $g_\mu(\mathbf{z},\mathbf{w})$ is unique because of the strong convexity of $d(\mathbf{x})$. Define $\mathbf{x}(\mathbf{z},\mathbf{w})$ as the optimal solution of $g_\mu(\mathbf{z},\mathbf{w})$ which is computed as

$$\mathbf{x}(\mathbf{z},\mathbf{w}) = GroupSoftThreshold(\mathbf{x}_0 - \frac{1}{\mu}(\mathbf{G}^H\mathbf{z} + \mathbf{A}^H\mathbf{w}), \frac{1}{\mu}),$$

where an group-thresholding operator $GroupSoftThreshold(\mathbf{x}, t)$ of $\mathbf{x} = [\mathbf{s}^T, \mathbf{p}^T]^T \in \mathbb{R}^{2N}$ is defined as

$$GroupSoftThreshold(\mathbf{x}, t) \triangleq \frac{[x_i, x_{i+N}]}{\sqrt{x_i^2 + x_{i+N}^2}} \max\{\sqrt{x_i^2 + x_{i+N}^2} - t, 0\}, 1 \leq i \leq N. \tag{3.67}$$

Let's rewrite the smoothed dual problem as

$$\arg \min_{\mathbf{z}\in\mathbb{C}^{M\times 1},\mathbf{w}\geq\mathbf{0}} -\bar{g}_\mu(\mathbf{z},\mathbf{w}) = g_{sm}(\mathbf{z},\mathbf{w}) + h(\mathbf{z}) \tag{3.68}$$

where

$$g_{sm}(\mathbf{z},\mathbf{w}) = -||\mathbf{x}(\mathbf{z},\mathbf{w})||_{2,1} - \frac{\mu}{2}\|\mathbf{x}(\mathbf{z},\mathbf{w}) - \mathbf{x}_0\|_2^2 + \langle \mathbf{z}, \mathbf{y} - \mathbf{G}\mathbf{x}(\mathbf{z},\mathbf{w})\rangle - \langle \mathbf{w}, \mathbf{A}\mathbf{x}(\mathbf{z},\mathbf{w})\rangle,$$

$$h(\mathbf{z}) = \epsilon\|\mathbf{z}\|_2.$$

The problem (3.68) we try to solve is in a composite form with smooth part $g_{sm}$ and nonsmooth part $h$. The smoothed part $g_{sm}(\mathbf{z},\mathbf{w})$ is differentiable and its gradient is computed as $\nabla g_{sm}(\mathbf{z},\mathbf{w}) = \begin{bmatrix} \mathbf{y} - \mathbf{G}\mathbf{x}(\mathbf{z},\mathbf{w}) \\ -\mathbf{A}\mathbf{x}(\mathbf{z},\mathbf{w}) \end{bmatrix}$ in accordance with Danskin's theorem.

Then, the generalized gradient projection method [63, 62] is applied to solve (3.68) by updating

$$(\mathbf{z}_{k+1},\mathbf{w}_{k+1}) = \arg \min_{\mathbf{z}\in\mathbb{C}^{M\times 1},\mathbf{w}\geq\mathbf{0}} g_{sm}(\mathbf{z}_k,\mathbf{w}_k) + \tag{3.69}$$

$$\langle \nabla g_{sm}(\mathbf{z}_k,\mathbf{w}_k), (\mathbf{z}-\mathbf{z}_k, \mathbf{w}-\mathbf{w}_k)\rangle + \frac{L_k}{2}\|(\mathbf{z}-\mathbf{z}_k, \mathbf{w}-\mathbf{w}_k)\|^2 \tag{3.70}$$

$$+ \epsilon\|\mathbf{z}\|_2, \tag{3.71}$$

where $L_k$ is the inverse of step size $t_k$. Actually, closed form solution for $(\mathbf{z}_{k+1},\mathbf{w}_{k+1})$ can be derived as

$$\begin{aligned} \mathbf{z}_{k+1} &= \arg\min_{\mathbf{z}} \ \langle \mathbf{y} - \mathbf{G}\mathbf{x}(\mathbf{z},\mathbf{w}), \mathbf{z}-\mathbf{z}_k\rangle + \frac{L_k}{2}\|\mathbf{z}-\mathbf{z}_k\|^2 + \epsilon\|\mathbf{z}\|_2 \\ &= Shrink(\mathbf{z}_k - \frac{1}{L_k}(\mathbf{y} - \mathbf{G}\mathbf{x}(\mathbf{z},\mathbf{w})), \frac{2\epsilon}{L_k}), \end{aligned} \tag{3.72}$$

$$\begin{aligned} \mathbf{w}_{k+1} &= \arg\min_{\mathbf{w}\geq 0} \ \frac{2}{L_k}\langle -\mathbf{A}\mathbf{x}(\mathbf{z},\mathbf{w}), \mathbf{w}-\mathbf{w}_k\rangle + \frac{L_k}{2}\|\mathbf{w}-\mathbf{w}_k\|^2 \\ &= \mathbf{w}_k + \frac{1}{L_k}\mathbf{A}\mathbf{x}(\mathbf{z},\mathbf{w}), \end{aligned} \tag{3.73}$$

where an $l_2$-shrinkage operation $Shrink(\mathbf{x},t)$ is defined as

$$Shrink(\mathbf{x},t) \triangleq \max\{1 - \frac{t}{\|\mathbf{x}\|_2}, 0\}\cdot\mathbf{x} = \begin{cases} 0, & \|\mathbf{x}\|_2 \leq t \\ (1 - t/\|\mathbf{x}\|_2)\cdot\mathbf{x}, & \|\mathbf{x}\|_2 > t \end{cases}. \tag{3.74}$$

The right-hand side first-order approximation of (3.69) satisfies an upper bound property

$$-\bar{g}_\mu(\mathbf{z}_{k+1}, \mathbf{w}_{k+1}) \leq \langle \nabla g_{sm}(\mathbf{z}_k, \mathbf{w}_k), (\mathbf{z}_{k+1} - \mathbf{z}_k, \mathbf{w}_{k+1} - \mathbf{w}_k) \rangle + \frac{L_k}{2} \|(\mathbf{z}_{k+1} - \mathbf{z}_k, \mathbf{w}_{k+1} - \mathbf{w}_k)\|^2 + \epsilon \|\mathbf{z}_{k+1}\|_2 \tag{3.75}$$

which holds for sufficiently large $L_k$. Typically, if $L_k \geq L, \forall k$, then the upper bound (3.75) holds, where $L$ is Lipschitz constant. Under those assumptions, $\epsilon$-optimality can be acheived in $\mathcal{O}(L/\epsilon)$ iterations by performing (3.69). A variation of the generalized gradient projection method proposed by Nesterov, which is an optimal first-order method with $\mathcal{O}(L/\sqrt{\epsilon})$ iterations, is used instead of (3.69). The approach is summaried in Algorithm 3.4.

**Algorithm 3.4** Smoothed Dual Conic Optimization

**Input:** $\mathbf{x}_0 = \mathbf{0}$, $\mathbf{z}_0 = \mathbf{0}$, $\mathbf{w}_0 = \mathbf{0}$, $\mu = 1$, $L_k = 1$, $c_0 = 1$,$\gamma = 0.5$
$\mathbf{s}_0 = [\mathbf{z}_0^T, \mathbf{w}_0^T]^T$

**Step k:** ($k \geq 0$) Let $L := L_k$,

1: $[\mathbf{z}_k^T, \mathbf{w}_k^T]^T = (1 - c_k)\mathbf{s}_k + c_k[\mathbf{z}_k^T, \mathbf{w}_k^T]^T$
2: $\mathbf{x}(\mathbf{z}_k, \mathbf{w}_k) = \inf_{\mathbf{x}} ||\mathbf{x}||_{2,1} + \frac{\mu}{2}\|\mathbf{x} - \mathbf{x}_0\|_2^2 - \langle \mathbf{z}_k, \mathbf{y} - \mathbf{G}\mathbf{x} \rangle - \epsilon\|\mathbf{z}\|_2 + \langle \mathbf{w}_k, \mathbf{A}\mathbf{x} \rangle$
3: **repeat**
4: $(\mathbf{z}_{k+1}, \mathbf{w}_{k+1}) = \arg\min_{\mathbf{z},\mathbf{w} \geq \mathbf{0}} \langle \nabla g_{sm}(\mathbf{z}_k, \mathbf{w}_k), (\mathbf{z} - \mathbf{z}_k, \mathbf{w} - \mathbf{w}_k) \rangle + \frac{L}{2}\|(\mathbf{z} - \mathbf{z}_k, \mathbf{w} - \mathbf{w}_k)\|^2 + \epsilon\|\mathbf{z}\|_2$
5: Break if $g_{sm}(\mathbf{z}_{k+1}, \mathbf{w}_{k+1}) \leq g_{sm}(\mathbf{z}_k, \mathbf{w}_k) +$ $\langle \nabla g_{sm}(\mathbf{z}_k, \mathbf{w}_k), (\mathbf{z} - \mathbf{z}_k, \mathbf{w} - \mathbf{w}_k) \rangle + \frac{L}{2}\|(\mathbf{z} - \mathbf{z}_k, \mathbf{w} - \mathbf{w}_k)\|^2$,
6: Update $L := L/\gamma$,
7: **return** $L_k := L$
8: $\mathbf{s}_k = (1 - c_k)\mathbf{s}_k + c_k[\mathbf{z}_{k+1}^T, \mathbf{w}_{k+1}^T]^T$, $c_{k+1} = \frac{2}{1 + \sqrt{1 + 4/c_k^2}}$

It is noted that the smaller smoothing parameter $\mu$, the better accuracy performance. On the other hand, the continuation shceme, which was proposed in NESTA [54], improves the convergence rate. The idea is that a sequence of subproblems is solved by Algorithm 3.4 with decreasing smoothing parameters $\mu_k$. Each result of subproblems will be feed into the next round. The standard continuation scheme combined with Algorithm 3.4 is listed below:

***Standard Continuation*** [54]

**Input:** $X_0$: the set of variables in Algorithm 3.4, $\mu_0 = 1$, $\alpha = 0.5$

**Step j:** $(j \geq 0)$

1: $X_{j+1} \leftarrow$ *Algorithm 3.4*

2: $\mu_{j+1} = \alpha\mu_j$

## 3.8 Numerical Results

In the following numerical example of the off-grid DoA estimation, the proposed two accelerated smoothing proximal gradient methods are designated as ASPG-L2 (using $h_\mu^{l_2}(\mathbf{x})$) and ASPG-L1 (using $\nabla h_\mu^{l_1}(\boldsymbol{\nu})$), the consensus ADMM method is designated as ADMM. the variant of excess-gap technique method is called EGT-based, and the variant of smoothed dual conic optimization method is called SDCO. We also solve problem (3.6) by using CVX packages. The CVX method can be viewed as a benchmark, which is used to evaluate the estimation performance degradation caused by smoothing in the proposed methods. The estimation errors of these methods are compared with the same for the MUSIC estimator, M+LFBF and the CRLB. Consider $K = 2$ source signals from DoAs $\boldsymbol{\theta} = [13.2220, 28.6022]$ degree impinging on a uniform linear array of $M = 8$ sensors with half-wavelength interelement spacing. The two sources are randomly generated with normal distribution of zero mean and variance $\sigma_s^2$. The noise term is i.i.d. AWGN with zero mean and variance $\sigma_n^2$. We use one hundred snapshots to estimate the covariance matrix. The size $N$ of search grid is set to 360 with $r = 0.25$ degree, which is used for all methods. In the ASPG method, $d_{l_i}(\mathbf{u}) = \frac{1}{2}\|\mathbf{u}\|_2^2, \forall i$, the decreasing factor is $\gamma = 0.5$, and smoothing parameter is chosen as $\mu = 10^{-8}$. The root-mean-square-error (RMSE) of DoA estimation is $(E[\frac{1}{K}\|\hat{\boldsymbol{\theta}} - \boldsymbol{\theta}\|_2^2])^{\frac{1}{2}}$. One hundred realizations are performed at each SNR.

In Figure 3.2, the RMSE of CVX, ADMM, ASPG-L1, ASPG-L2, EGT-based, SDCO are almost the same and better than MUSIC and M+LFBF at low SNRs. At high

SNRs, the performance of ASPG-L1, CVX, ADMM, EGT-based, SDCO, and MUSIC approach CRLB, but not ASPG-L2. The reason is that the sparse property of group-sparsity penalty $\|\mathbf{x}_{g_i}\|_2$ is lost during the smoothing process by only using the property that the dual norm of $\ell_2$ norm is also $\ell_2$ norm so that sparsity is not promoted in this way. In Figure 3.1, the estimated power spectrum of ASPG methods is presented at SNR = 0 dB. Due to the smoothing process, both have lost their sparsity. However, the two peaks of ASPG-L1 are more separated than ASPG-L2. In other words, ASPG-L1 estimator owns higher DoA resolution.

We also have verified that the computational efficiencies of the proposed methods are better than the CVX method. At SNR = 0 dB, the running time at each realization of SDCO, ASPG-L2, and ASPG-L1 are 12.93s, 4.43s, 7.05s 2.54s and 2.74s, which are faster than the CVX method with 22.51s, and M+LFBF with 5.59s. The ADMM method needs almost 7s to get an optimal solution, which is slower than expected.The cpu time consumption of EGT-based method is almost 13s, which is too slower than ASPG-L1, and ASPG-L2, although the smoothing parameter is chosen in a systematic way.

Table 3.1: CPU Time (Seconds) of Methods at SNR=0 dB

| Alg. | CVX | MUSIC | ASPG-L2 | ASPG-L1 | EGT | SDCO | M+LFBF | ADMM |
|---|---|---|---|---|---|---|---|---|
| M=8 | 22.52s | 0.0061s | 2.54s | 2.74s | 12.93s | 4.43s | 5.59s | 7.05s |

## 3.9 Summary

In this chapter, two ASPG methods were proposed for the estimation of off-grid DoAs using a sparse model for the observation first. The group-sparsity penalty is reformulated and smoothed by the Nesterov smoothing technique so that its gradient can be calculated easily. Then, the accelerated proximal gradient is used to solve the unconstrained optimization problem with the smoothed objective functions plus only one nonsmooth function. The smoothing parameter is selected empirically. So, the variant

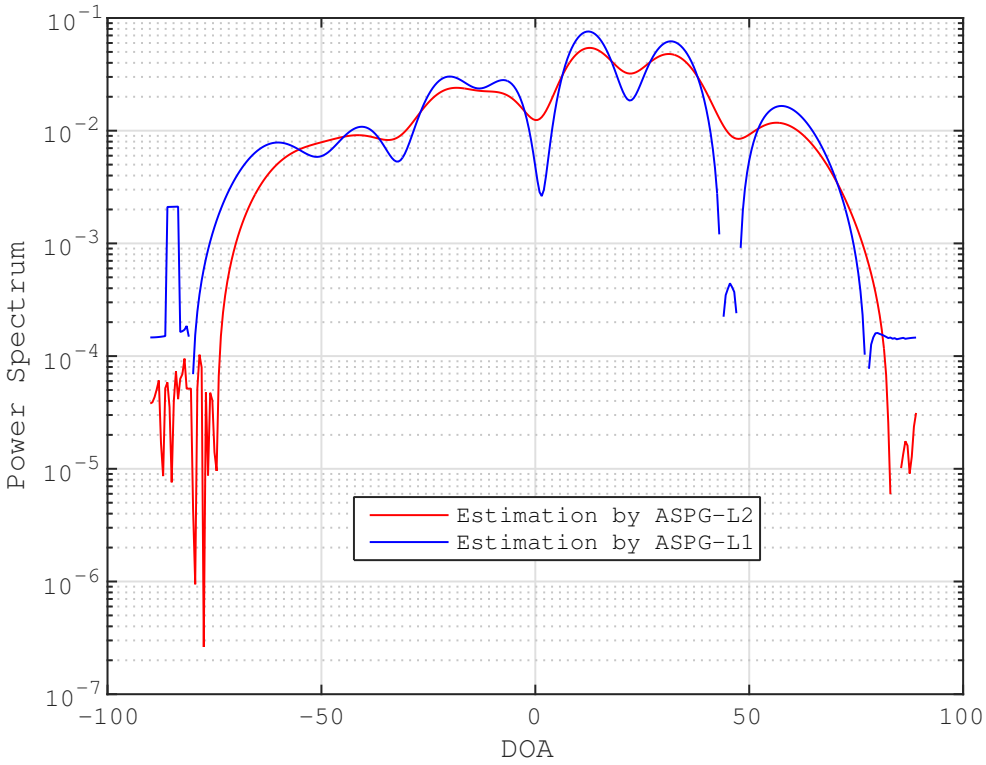


Figure 3.1: Power Spectrum versus DoA.

of EGT-based mehtod is employed since the smoothing parameter can be chosen systematically. Instead of using BPDN solver, the variant od SDCO method is proposed, and its smoothing parameter can be decided by using the continuation technique. The performance and computational efficiencies of the proposed methods were verified by a numerical example of DoA estimation.

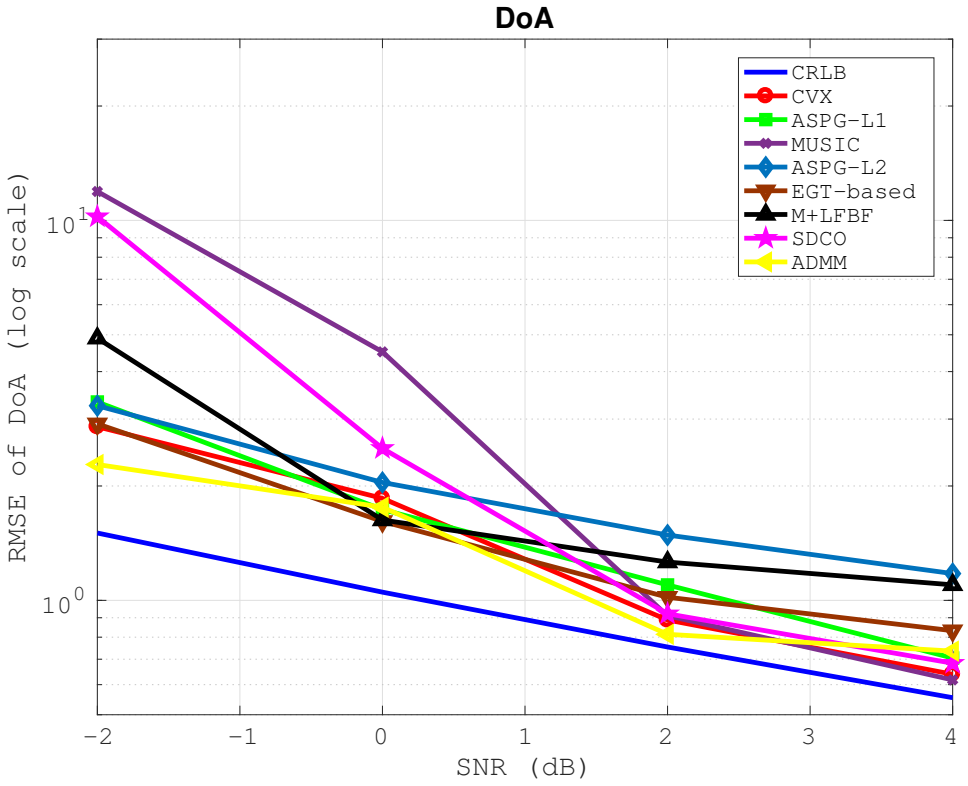


Figure 3.2: RMSE of DoA estimation versus SNR.

# Chapter 4

# Gridless Sparse Recovery Methods in the Continuous Domain

In this chapter, instead of the off-grid model in the previous chapter, a super-resolution framework is used for gridless DoA estimation.

## 4.1 Introduction

The super-resolution (SR) approach presented by Candès and Fernandes-Granda [14, 20] aims to provide continuous parameter recovery by solving a total variation (TV) norm minimization of a complex measure, which is not the TV norm [64] used in image processing. In [33], atomic norm minimization (ANM) is proposed to estimate continuous frequency spectrum with a subset of sensors. However, the above SR methods have only been developed for the single-measurement-vector (SMV) model. In [65], an exact joint sparse frequency recovery method is proposed by using ANM in multiple-measurement-vector (MMV) system, and a theoretical analysis in the continuous dictionary setting is

provided. In [66], the TV norm minimization employed in MMV is studied to improve performance of DoA estimation, but the source signals are assumed to be zero-mean positive-valued random variables, which is not a general case. In [67], a sublinear time randomized algorithm is designed to recover sparse Fourier sampling signals with continuous-valued frequencies.

In this work, we formulate the DoA estimation problem in the spatial covariance model, and reformulate it into a MMV-like model. Use of the covariance model in the formulation of a DoA estimator is desirable for a number of reasons, including computational savings for large number of snapshots, and exploitation of the methods that extrapolate array appertures through their co-arrays, such as for the case of minimum-redundancey [68] or co-prime arrays [69]. We extend the theory of super-resolution from SMV to MMV by defining a block total variation (BTV) norm for a complex measure with same locations but different amplitudes at multiple snapshots. Then, we propose a BTV norm minimization approach for the MMV-like model. The performance of the proposed method is demonstrated by simulations for cases of uncorrelated and correlated source signals and compared with MUSIC, ANM-MMV [65], and the Cramer-Rao Lower Bound (CRLB).

## 4.2 Problem Formulation and Preliminaries

### 4.2.1 The DoA Estimation Problem

Based on the DoA model considered in Chapter 2, the SMV, MMV, and covariance model are as follows

$$\mathbf{y}(t) = \mathbf{G}\mathbf{x}(t) + \mathbf{n}(t), t = 1, \ldots, T, \tag{4.1}$$

$$\mathbf{Y} = [\mathbf{y}(1), \ldots, \mathbf{y}(T)] = \mathbf{G}\mathbf{X} + \mathbf{N}, \tag{4.2}$$

$$\tilde{\mathbf{R}} = E[\mathbf{y}\mathbf{y}^H] = \mathbf{G}\mathbf{C}_\mathbf{x}\mathbf{G}^H + \sigma^2\mathbf{I}. \tag{4.3}$$

In practice, the estimate of covariance matrix is calculated as $\mathbf{R} = \sum_{t=1}^{T} \mathbf{y}(t)\mathbf{y}(t)^H/T$. If $K$ sources are uncorrelated, i.e., $\mathbf{C_x}$ is a diagonal matrix with diagonal entries $[\sigma_1^2, \cdots, \sigma_1^K]$ , then the spatial covariancel model can be rewritten as

$$\mathbf{R} = \sum_{k=1}^{K} \sigma_k^2 \mathbf{g}(\theta_k)\mathbf{g}(\theta_k)^H + \mathbf{V}, \tag{4.4}$$

where $\mathbf{V}$ represents the contributions of AWGN and the approximation error due to the sample averaging.

Based on the above models, the goal of DoA estimation problem is to estimate the support set $\mathcal{T}_\theta$. In the next subsection, the super-resolution theory is introduced to fit the DoA estimation problem in the SMV scenario.

### 4.2.2 Preliminary Method of Continuous Signal Recovery

Following the theory of super-resolution [14], consider a continuous signal $s(\tau)$ which has sparse representations in the domain $[-1, 1]$ as a weighted linear combinations of spikes:

$$s(\tau) = \sum_{k=1}^{K} a_k \delta_{\tau_k}, \tag{4.5}$$

where $a_k$ may be real or complex valued, $\tau_k \in [-1, 1], \forall k$ and $\delta_{\tau_k}$ is a Dirac measure at location $\tau_k$. Denote $\mathbf{s} = [a_1, \ldots, a_K]^T$ as the data vector. The Fourier transform of $s(\tau)$ is written as

$$r(n) = \int_{-1}^{1} e^{-j2\pi n\tau} s(d\tau) = \sum_{k=1}^{K} a_k e^{-j2\pi n\tau_k}, n = -f_c, \ldots, f_c$$

where $f_c$ is an integer and $2f_c + 1$ is the number of Fourier transform frequency coefficients. With arbitrary noise $\mathbf{e}$ cosidered in this model, we simplify the above equation as

$$\mathbf{r} = \mathcal{F}s + \mathbf{e}, \tag{4.6}$$

where $\mathbf{r} = [r(-f_c), \ldots, r(f_c)]^T \in \mathbb{C}^{M\times 1}$, and $\mathcal{F}$ denotes the linear operator to measure the $2f_c + 1$ lowest frequency coefficients.

In order to estimate $\tau_k$, the total variation (TV) norm for a complex meaure [70] on a Borel set $B \in$ Borel $\sigma$-algebra $\mathcal{B}(\mathbb{T})$ is introduced and defined as $\|s\|_{TV} = \sup \sum_{k=1}^{\infty} |s(B_k)|$, where the supremum is taken over all partitions of $B$ into countable and disjoint measurable subsets $B_k$. The minimization of $\|s\|_{TV}$ in the continuous domain is used to promote the sparsity of continuous signal $s$, which is the analog of the $l_1$-norm minimization of $\|\mathbf{s}\|_1 = \sum_k |a_k|$ in the discrete domain. In [20], convex optimization problem is suggested as

$$\min_s \|s\|_{TV} \quad \text{s.t. } \|\mathcal{F}s - \mathbf{r}\|_2 \leq \epsilon. \tag{4.7}$$

When the signal-measurement-vector system (4.1) is considered, by letting $\tau_k = sin(\theta_k), \forall k$ and $f_c = (M-1)/2$, the DoA estimation problem can be cast in the super-resolution framework as follows

$$\mathbf{r} = \mathcal{F}s + \mathbf{e} = \mathbf{G}\mathbf{x}(t) + \mathbf{n}(t) = \mathbf{y}(t), \tag{4.8}$$

and then solved by the TV norm minimization (4.7). For the spatial covariance model (4.4), we can also vectorize the covariance matrix into a SMV system, and solved by TV norm minimization [71].

## 4.3 Reformulation of the Spatial Covariance Model

Instead of vectorizing the spatial covariance model (4.4), we recast it into a MMV-like model by the following:

$$\begin{aligned}\mathbf{R} = [\mathbf{r}_0, \mathbf{r}_1, \ldots, \mathbf{r}_{M-1}] &= \sum_{k=1}^{K} \sigma_k^2 \mathbf{g}(\theta_k)\mathbf{g}(\theta_k)^H + \mathbf{V}, \\ &= \sigma_1^2 \bar{\mathbf{G}}(\theta_1) + \cdots + \sigma_K^2 \bar{\mathbf{G}}(\theta_K) + \mathbf{V},\end{aligned} \tag{4.9}$$

where $\mathbf{g}(\theta_k)\mathbf{g}(\theta_k)^H = \bar{\mathbf{G}}(\theta_k)$ is a Toeplitz matrix expressed by $\bar{\mathbf{G}}(\theta_k) = [\mathbf{a}_0(\theta_k), \mathbf{a}_1(\theta_k), \ldots, \mathbf{a}_{M-1}(\theta_k)] \in \mathbb{C}^{M\times M}$. For ULA, the $l$th column of $\bar{\mathbf{G}}(\theta_k)$ is represented as $\mathbf{a}_l(\theta_k)= [e^{-j(-l)\xi_k}, \ldots, e^{-j(M-1-l)\xi_k}]^T \in \mathbb{C}^{M\times 1}$, $\forall l = 0, \ldots, M-1$, in which $\xi_k = \frac{d}{\lambda} 2\pi sin\theta_k$. Then, the $l$th column $\mathbf{r}_l \in \mathbb{C}^{M\times 1}$ can be expressed as

$$\begin{aligned}\mathbf{r}_l &= \sigma_1^2\mathbf{a}_l(\theta_1) + \cdots + \sigma_K^2\mathbf{a}_l(\theta_K) + \mathbf{v}_l = \sum_k \sigma_k^2\mathbf{a}_l(\theta_k) + \mathbf{v}_l, \\ &= \mathbf{A}_l\mathbf{p} + \mathbf{v}_l, \forall l = 0, \ldots, M-1 \end{aligned} \tag{4.10}$$

where $\mathbf{A}_l = [\mathbf{a}_l(\theta_1), \ldots, \mathbf{a}_l(\theta_K)] \in \mathbb{C}^{M\times K}$, $\mathbf{p} = [\sigma_1^2, \ldots, \sigma_K^2]^T \in \mathbb{R}^{K\times 1}$, and $\mathbf{v}_l$ is the $l$th column of $\mathbf{V}$. The matrix $\mathbf{A}_l$ is composed of every $l$th column from matrices $\bar{\mathbf{G}}(\theta_1), \ldots, \bar{\mathbf{G}}(\theta_K)$. Therefore, $\mathbf{R}$ can be rewritten as

$$\begin{aligned}\mathbf{R} &= [\mathbf{r}_0, \mathbf{r}_1, \ldots, \mathbf{r}_{M-1}] \\ &= [\mathbf{A}_0\mathbf{p}, \mathbf{A}_1\mathbf{p}, \ldots, \mathbf{A}_{M-1}\mathbf{p}] + \mathbf{V}, \end{aligned} \tag{4.11}$$

which is a similar form to an MMV system in Equation (4.2). In Equation (4.11), we have $M$ vectors, $\mathbf{r}_0, \ldots, \mathbf{r}_{M-1}$ with the same power vector $\mathbf{p}$. Unlike the MMV system, each matrix $\mathbf{A}_l$ is different, and each column of $\mathbf{A}_i$ is a rotational steering vector to the corresponding column of $\mathbf{A}_j$, i.e., $\mathbf{a}_i(\theta_k) = \mathbf{a}_{i+1}(\theta_k)e^{j\xi_k}$. Equation (4.11) will be used to estimate the DoA support set by the proposed method in the next sections. We will show how to extend the SR theory from SRV to MMV-like system before introducing the proposed method.

## 4.4 Continuous Group Sparsity Recovery Methods

Based on the theory of super-resolution, we extend a continuous signal into the MMV space by defining $s(\tau; t), \tau \in [-1, 1], t = 1, \ldots, T$ as

$$s(\tau; t) = \sum_{k=1}^{K} b_{kt}\delta_{\tau_k}, \tag{4.12}$$

where $b_{kt}$ is a real or complex-valued amplitude of measurement at time $t$, and $\tau_k \in [-1, 1], \forall k$ is a location of $k$th spike. Denote $\mathcal{T} = \{\tau_k\}_{k=1}^K$ as the support set and $\mathbf{S} = [\mathbf{s}_1, \ldots, \mathbf{s}_T]$ as the data matrix where $\mathbf{s}_t = [b_{1t}, \ldots, b_{Kt}]^T$. Similarly in [14], the Fourier transform of $s(\tau; t)$ with respect to $\tau$ is

$$r(n; t) = \int_{-1}^{1} e^{-j2\pi n\tau} s(d\tau) = \sum_{k=1}^{K} b_{k,t} e^{-j2\pi n\tau_k}, \tag{4.13}$$
$$n = -f_c, \ldots, f_c, \quad t = 1, \ldots, T.$$

When Gaussian noise is considered in this model, Equation (4.13) can be simplified as

$$\mathbf{r}_{sr}^t = \mathcal{F}_t s(\tau; t) + \mathbf{e}^t, \forall t = 1, \ldots, T \tag{4.14}$$

where $\mathbf{r}_{sr}^t = [r(-f_c; t), \ldots, r(f_c; t)]^T \in \mathbb{C}^{M\times 1}$, and $\mathbf{e}^t$ denotes i.i.d. Gaussian noise vector with $\mathbb{C}\mathcal{N}(0, \sigma^2\mathbf{I})$. $\mathcal{F}_t$ denotes the linear operator at time $t$. Let $\mathbf{R}_{sr} = [\mathbf{r}_{sr}^1, \ldots, \mathbf{r}_{sr}^T]$.

By using multiple measurements to estimate $\tau_k$, a block total variation ($BTV$) norm for a complex meaure with multiple measurements on a set $B \in \mathcal{B}(\mathbb{T})$ is defined as

$$\|s\|_{TV,p} = \sup \sum_{k=1}^{\infty} \|s(B_k; :)\|_p, \tag{4.15}$$

where $\|s(B_k; :)\|_p = (\sum_{t=1}^T |s(B_k; t)|^p)^{1/p}$ and $s(B_k; t) = b_{k,t}$ if the supremum is taken over all partitions $\{B_k\}$ of $B$ belonging to Borel $\sigma$-algebra [70] to optimally have a finite and disjoint measurable subsets $\{B_k\}$ at time $t$. Since at different time $t$, multiple continuous signals $s(\tau; t)$ share the same spike locations, the group sparsity of $s(\tau; t)$ can be promoted by using the minimization of $\|s\|_{TV,p}$. This is equivalent to the minimization of $\|\mathbf{S}\|_{1,p} = \sum_k \|\mathbf{S}_{k,:}\|_p$ where $\mathbf{S}_{k,:}$ is the $k$th row of data matrix $\mathbf{S}$ by the notion of Group Lasso [15]. Similarly in [20], based on Equation (4.12) and (4.14), the block total variation ($BTV$) minimization problem is proposed as

$$\min_s \|s\|_{TV,p} \quad \text{s.t.} \ \sum_{t=1}^{T} \|\mathcal{F}_t s - \mathbf{r}_{sr}^t\|_2 \leq \epsilon, \tag{4.16}$$

where $1 \leq p \leq +\infty$.

When considering the MMV-like model (4.11) and letting $\tau_k = sin(\theta_k)$, $t = l$, $T = M-1$, $\mathbf{R}_{sr} = \mathbf{R}$ and $f_c = (M-1)/2$, the DoA estimation problem can be formulated in the new super-resolution framework as the following

$$\mathbf{r}_{sr}^{l} = \mathcal{F}_l s(\tau; l) + \mathbf{e}^l = \mathbf{A}_l \mathbf{p} + \mathbf{v}_l = \mathbf{r}_l,\ l = 0, \ldots, M-1,$$

and then solved by the proposed $BTV$ norm minimization

$$\min_{s} \|s\|_{TV,1} \quad \text{s.t.} \quad \sum_{l=0}^{M-1} \|\mathcal{F}_l s - \mathbf{r}_l\|_2 \leq \epsilon. \tag{4.17}$$

Note that the minimization of $\|s\|_{TV,1}$ is analog to $\|\mathbf{S}\|_{1,1}$ in this case. A theorem about DoA resolution for MMV system can be claimed similarly by using Theorem 1.2 in [14].

**Theorem 4.1.** *Let $\mathcal{T} = \{\tau_k\}_{k=1}^{K}$ as the support set. If the minimum distance $\Delta(\boldsymbol{\theta})$ obeys*

$$\Delta(\boldsymbol{\theta}) = \inf_{\tau_i, \tau_j \in \mathbb{T}} |\tau_i - \tau_j| \geq \frac{4}{f_c} \frac{\lambda}{d},$$

*then the high resolution detail of continuous signal $s$ can be recovered with high probability by solving block total variation norm minimization problem (4.17).*

In order to estimate the support set, the dual form of (4.17) is derived as

$$\begin{aligned} &\max_{\mathbf{U}} \ \mathrm{Re}\{\langle \mathbf{R}, \mathbf{U} \rangle\} - \frac{\epsilon}{M} \|\mathbf{U}\|_F \\ &\text{s.t. } \|\mathcal{F}_l^* \mathbf{u}_l(\tau)\|_\infty \leq 1, \forall l = 0, \ldots, M-1, \end{aligned} \tag{4.18}$$

where $\mathbf{U} = [\mathbf{u}_0, \ldots, \mathbf{u}_{M-1}] \in \mathbb{C}^{M \times M}$ and $\mathcal{F}_l^* \mathbf{u}_l(\tau) = \sum_{|k| \leq f_c} u_{l,k} e^{j \frac{d}{\lambda} 2\pi (k-l)\tau}$ where $\mathbf{u}_l = [u_{l,-f_c}, \ldots, u_{l,f_c}]^T \in \mathbb{C}^{M \times 1}$. $\mathrm{Re}\{\langle \mathbf{R}, \mathbf{U} \rangle\}$ takes the real part of $tr(\mathbf{U}^H \mathbf{R})$ where $tr(\cdot)$ takes the sum of diagonal entries of matrix. By a generalized Slater condition [72], strong duality holds since $\mathbf{u}_l = \mathbf{0}, \forall l$, which satisfies the constraint, is contained in the feasible set. Although this problem is still with infinite constraints, it can be reformulated as a

semidefinite matrix and an affine hyperplane. Thus, the dual problem is rewritten as

$$\begin{aligned} &\max_{\mathbf{U}} \ \mathrm{Re}\{< \mathbf{R}, \mathbf{U} >\} - \frac{\epsilon}{M}\|\mathbf{U}\|_F \\ &\text{s.t.} \ \begin{bmatrix} \mathbf{Q}^l & \mathbf{u}_l \\ \mathbf{u}_l^H & 1 \end{bmatrix} \succeq 0, \forall l = 0, \ldots, M-1 \\ &\quad \sum_{i=1}^{M-j} \mathbf{Q}^l_{i,i+j} = \begin{cases} 1, & j = 0, \\ 0, & j = 1, 2, \ldots, M-1 \end{cases}, \end{aligned} \tag{4.19}$$

where $\mathbf{Q}^l \in \mathbb{C}^{M \times M}$ is a Hermitian matrix, $\forall l$. The derivation of (4.19) is in Appendix A.

The following lemma is modified from [14] and used to estimate the support set by linking a primal solution with a dual solution.

**Lemma 4.1.** *Let $s_{est}$ and $\mathbf{u}_{l,est}$ be a pair of primal-dual solutions to (4.16) and (4.19). Then*

$$(\mathcal{F}_l^* \mathbf{u}_{l,est})(\tau) = sign(s_{est}(\tau; l)), \forall \tau \in \mathbb{T} \ s.t. \ s_{est}(\tau; l) \neq 0,$$

*where $sign(\cdot)$ takes the sign of any number.*

By performing the root finding procedure on the $|(\mathcal{F}_l^* \mathbf{u}_{l,est})(\tau)|^2 = 1, \ \forall l$, we can obtain the estimated support sets $\mathcal{T}_{est}^l = \{\tau_{k,est}^l\}_{k=1}^K$ and its union set $\mathcal{T}_{est} = \bigcup_l \mathcal{T}_{est}^l$. Then, the measurement matrix $\mathbf{G}_{est}$ is reconstructed based on $\mathcal{T}_{est}$. Finally in terms of Equation (4.2), Group Lasso [15] can be used to determine the true source locations as the following

$$\hat{\mathbf{X}} = \arg\min_{\mathbf{X}} \frac{1}{2}||\mathbf{Y} - \mathbf{G}_{est}\mathbf{X}||_F^2 + \gamma||\mathbf{X}||_{2,1}, \tag{4.20}$$

where $||\mathbf{X}||_{2,1} = \sum_{k=1}^{|\mathcal{T}_{est}|} \|\mathbf{X}_{k,:}\|_2$, and $\mathbf{X}_{k,:}$ denotes the $k^{th}$ row of $\mathbf{X}$ and $|\mathcal{T}_{est}|$ is the cardinality of $\mathcal{T}_{est}$.

## 4.5 Numerical Results

The proposed method (SR-BTV) is applied to the DoA estimation problem and compared with MUSIC, ANM-MMV [65] and the CRLB. An uniform linear array (ULA) of $M = 9$ sensors with half-wavelength interelement spacing is considered. The minimum distance $\Delta(\boldsymbol{\theta})$ is set to 1. Suppose $K = 2$ narrowband plane waves impinging on ULA from DoAs with $sin(\boldsymbol{\theta}) = [0.2165251, 0.4665251]$. The distance of two sources is 0.25, which is $\frac{\Delta(\boldsymbol{\theta})}{4}$. Two cases of uncorrelated and correlated sources are considered. In the uncorrelated case, two source signals are zero-mean complex-valued Gaussian random variables with equal power. In the correlated case, the correlation coefficient of two sources is set to 0.9. For MUSIC, the search grid of $[-1, 1]$ is uniformly separated with step size 0.0001. We performed one hundred realizations for each SNR. The number of snapshots is $T = 100$.

The RMSE of DoA estimation for the case of uncorrelated source signals is presented in Figure 4.1. At high SNR, the performance of SR-BTV and MUSIC are almost the same and approach the CRLB. However, at low SNR, the SR-BTV method shows a lower resolution threshold than MUSIC. For instance, when RMSE $\approx 10^{-1}$, the SR-BTV method outperforms MUSIC about 2 dB. ANM-MMV has slight improvement over MUSIC at low SNR, but does not have good performance at high SNR. In Figure 4.2, the performance for the correlated case is presented. Since the covariance matrix of source signals is not diagonal anymore, the performance of SR-BTV, ANM-MMV and MUSIC degrade and all are more far away from the CRLB compared with the uncorrelated case. However, the SR-BTV and ANM-MMV are more robust to source correlations and achieves better performance than MUSIC at low SNR. At SNR$= -10$ dB, the RMSE of SR-BTV is approxmately 0.0464 while the RMSE of MUSIC is about 0.4318.

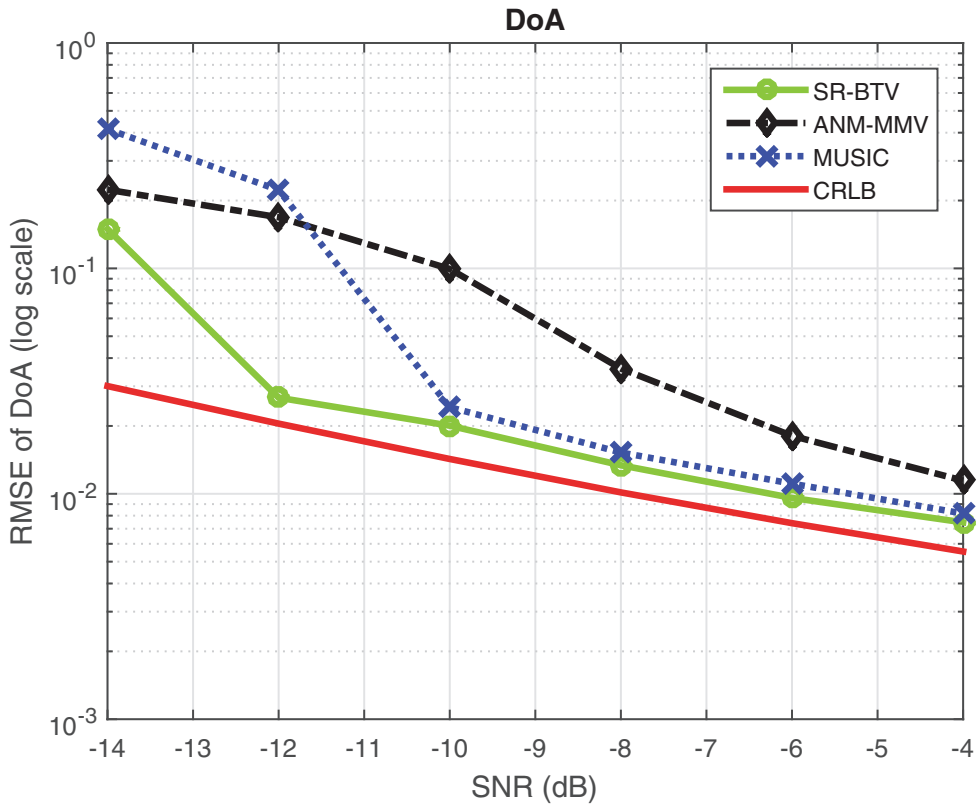


Figure 4.1: RMSE of DoA estimation versus SNR for the case of uncorrelated sources.

## 4.6 Summary

By reformulating the spatial covariance model into an MMV-like system, group sparsity is exploited in the super-resolution framework. A BTV norm minimization approach is proposed for the reformulated model. The DoAs are estimated by solving its dual. Numerical results demonstrate the robust performance of SR-BTV compared wtih MUSIC and ANM-MMV in cases of uncorrelated and correlated sources.

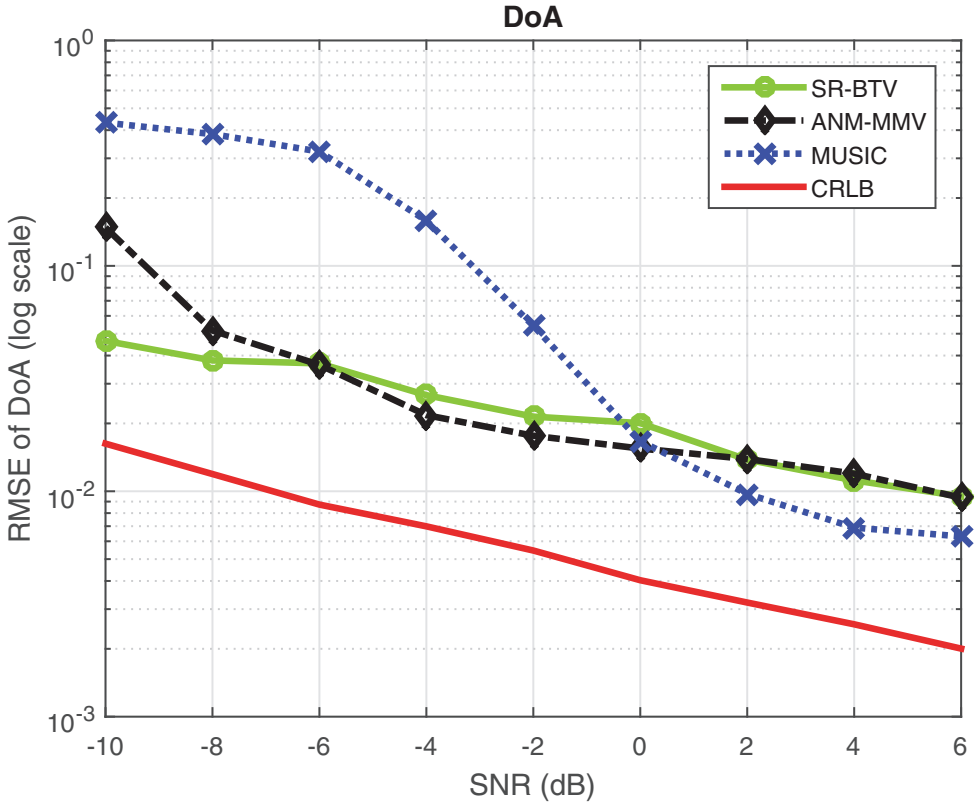


Figure 4.2: RMSE of DoA estimation versus SNR for the case of correlated sources.

# Chapter 5

# Array Self-Calibration and Sparsity Promoting DoA Estimation

## 5.1 Introduction

DoA estimation algorithms assume perfect knowledge the array responses for all directions of interest. Such knowledge necessitates perfectly calibrated sensors in both phase and gain. Maintenance of such calibration under varying physical conditions, and in time is difficult, and in many cases expensive. Accordingly, algorithms that can provide calibration algorithmically and automatically are of great interest. This chapter is concerned with the development of a self-calibration method in the context of sparsity promoting DoA estimation.

To design an efficient self-calibration algorithm is a challenging problem. Among the self-calibration algorithms, the maximum likelihood estimation is the most powerful one to jointly estimate the signals of interest and the calibration parameters. But this approach suffers from excessive computational complexity such that it is not suitable

to real-time applications. Some self-calibration algorithms were developed based on the eigendecomposition of a covariance matrix to estimate the phase and gain of the calibration error. Examples of this lower computational complexity approach, which is called eigenstructure-based (ES) methods, can be found in [23, 73, 74]. In [75], the blind calibration formulation and methods were developed, and the necessary and sufficient condition for estimating the calibration offsets is characterized. In [76], $l_1$ norm minimization is used to formulate the blind calibration problem, which is highly non-convex. In [77], the approximate message passing algorithm combined with the blind calibration problem is considered, and solved by a convex relaxation algorithm. In [78], several convex optimization methods were proposed for solving the blind calibration of sparse inverse problems. In [21], a self-calibration problem is introduced and solved in the framework of biconvex compressed sensing via a SparseLift method, which is inspired by PhaseLift [79, 80, 81] that is about the "Lifting" technique. The notion of "Lifting" is used for blind deconvolution [82, 83], which attempts to recover two unknown signals from their convolution. In [11], uncertainties of measuring the sensing matrix is investigated, especially the sensitivity of compressed sensing to mismatch between the assumed basis and the actual basis.

In this work, we extend the Ling's work [21] from single measurement vector (SMV) system to multiple measurement vector (MMV) system. By taking advantage of multiple snapshots of measurement in the self-calibration problem, a new problem is formulated and a low-rank matrix is generated, but with larger dimension. We also give the definition of linear operator for the MMV model, and its corresponding matrix representation so that we can generate a variant of convex optimization problem. In order to mitigate the computational complexity of the method, singular value decomposition (SVD) is applied to reduce the problem size. Our proposed method is verified in the array self-calibration and direction-of-arrival (DoA) estimation. Moreover, the off-grid effect in the sparse array self-calibration problem is considered as well. The performance of the proposed methods are demonstrated by numerical simulations and compared with

Cramer-Rao Bound (CRB) [22], and the eigenstructure-based method [23].

## 5.2 Self-Calibration Preliminaries

Based on the equation (1.3) mentioned in Chapter 1, a generic self-calibration problem in compressed sensing is given by

$$\mathbf{y} = \mathbf{G}(\mathbf{h})\mathbf{x} + \mathbf{n}. \tag{5.1}$$

Therefore, if $\mathbf{x}$ is assumed sparse, an $l_1$-norm minimization problem is proposed

$$(\hat{\mathbf{x}}, \hat{\mathbf{h}}) = \arg\min_{\mathbf{x},\mathbf{h}} \frac{1}{2}||\mathbf{G}(\mathbf{h})\mathbf{x} - \mathbf{y}||_2^2 + \alpha||\mathbf{x}||_1, \quad \alpha > 0. \tag{5.2}$$

This optimization problem is non-convex with associated difficulties for its solution. The most common approach is to use the alternating method, i.e., solve $\mathbf{x}$ for fixed $\mathbf{h}$, and solve $\mathbf{h}$ for fixed $\mathbf{x}$. However, (5.2) is too general to solve in an efficient numerical framework. Thus, an important special case of (5.1) is considered

$$\mathbf{y} = \mathbf{D}\mathbf{G}\mathbf{x} + \mathbf{n}, \quad \mathbf{D} = \mathrm{diag}(\mathbf{B}\mathbf{h}) \tag{5.3}$$

where $\mathbf{y} \in \mathbb{C}^{M\times 1}$ is the observation vector, $\mathbf{G} \in \mathbb{C}^{M\times N}$ $(M \ll N)$ is a known fat matrix, $\mathbf{x} \in \mathbb{C}^{N\times 1}$ is a $K$-sparse signal of interest, and $\mathbf{n} \in \mathbb{C}^{M\times 1}$ is additive white Gaussian noise vector. $\mathbf{D} \in \mathbb{C}^{M\times M}$ is a diagonal matrix that depends on unknown parameter $\mathbf{h} \in \mathbb{C}^{m\times 1}$, and $\mathbf{B} \in \mathbb{C}^{M\times m}$ $(M > m)$ is known. This case is based on the fact that the unknown calibration parameters $\mathbf{h}$ lie in the subspace (column space or range) of $\mathbf{B}$ . This type of model can be applied in many applications, such as directions-of-arrival estimation.

### 5.2.1 Array Self-Calibration for DoA Estimation

Consider the direction-of-arrivals estimation problem with an array of $M$ sensors. Suppose that there are $K$ far-field narrowband sources impinge on the array from angles

$\theta_1, \ldots, \theta_K$. The observation vector $\mathbf{y}(t) = [y_1(t), \ldots, y_M(t)]^T \in \mathbb{C}^{M\times 1}$ at time $t$ is modeled as

$$\mathbf{y}(t) = \mathbf{D}(\mathbf{h})\mathbf{A}\mathbf{s}(t) + \mathbf{n}(t), \tag{5.4}$$

where the measurement matrix $\mathbf{A} = [\mathbf{a}(\theta_1), \cdots, \mathbf{a}(\theta_K)] \in \mathbb{C}^{M\times K}$ is composed of the steering vectors $\{\mathbf{a}(\theta_i) = [e^{-j(-(M-1)/2)2\pi\frac{d}{\lambda}sin\theta_i}, \ldots, e^{-j((M-1)/2)2\pi\frac{d}{\lambda}sin\theta_i}]^T\}_{i=1}^K$ with wavelength $\lambda$, and $\mathbf{n}$ is i.i.d. white Gaussian noise with $\mathcal{N}(0, \sigma^2 I)$. The vector $\mathbf{s}(t) = [s_1(t), \ldots, s_K(t)]^T \in \mathbb{C}^{K\times 1}$ represents the arriving stochastic signal vector with covariance matrix $\mathbf{C}_s$. $\mathbf{D}$ is parameterized by unknown parameters $\mathbf{h}$, which captures the unknown calibration of the sensors. The calibration case of interest is when $\mathbf{D}(\mathbf{h}) = \text{diag}(\mathbf{Bh})$ is a diagonal matrix in which its diagonal entries represent unknown complex gains for each antennas. $\mathbf{B}$ is assumed to be a known matrix, which is used to model the situation when the diagonal elements of $\mathbf{D}$ change slowly entry-wise. This calibrating effect captures the condition of gain discrepancies due to the environmental temperature or humidity changes, or position displacement of antenna arrays.

As we have done earlier, we discretized the angle space into grid of directions, which are denoted by $\{\phi_1, \phi_2, \cdots, \phi_N\}$ where $N$ is the number of discrete directions and $N \gg K$. Suppose that the actual DoAs $\{\theta_1, \theta_2, \cdots, \theta_K\}$ belong to the grid of interest represented by $\{\phi_1, \phi_2, \cdots, \phi_N\}$. Then, Equation (5.4) can be transformed into a sparse model as:

$$\mathbf{y}(t) = \mathbf{D}\mathbf{G}\mathbf{x}(t) + \mathbf{n}(t), \quad \mathbf{D} = \text{diag}(\mathbf{Bh}), \tag{5.5}$$

where the measurement matrix $\mathbf{G} = [\mathbf{g}(\phi_1), \cdots, \mathbf{g}(\phi_N)] \in \mathbb{C}^{M\times N}$ is composed of the steering vectors $\{\mathbf{g}(\phi_i) = [e^{-j(-(M-1)/2)2\pi\frac{d}{\lambda}sin\phi_i}, \ldots, e^{-j((M-1)/2)2\pi\frac{d}{\lambda}sin\phi_i}]^T\}_{i=1}^N$. $\mathbf{x} \in \mathbb{C}^m$ is a $K$-sparse signal of interest. A known $\mathbf{B}$ is composed of the first $m$ columns of the Discrete Fourier Transform (DFT) matrix, which models slow changes on calibrations of the sensors.

Then, a sparsity-promoting optimization problem to recover $\mathbf{x}$ and $\mathbf{h}$ is

$$\arg\min_{\mathbf{x},\mathbf{h}} \frac{1}{2}||\text{diag}(\mathbf{Bh})\mathbf{Gx} - \mathbf{y}||_2^2 + \alpha||\mathbf{x}||_1, \tag{5.6}$$

where $\alpha > 0$ is a regularization parameter. This is still challenging to solve it efficiently, since the objective function is non-convex. Thus, a novel method is proposed by [] to solve it efficiently and analytically, which is called SparseLift.

### 5.2.2 SparseLift

In order to cope with the bilinearity of the function $||\text{diag}(\mathbf{Bh})\mathbf{x} - \mathbf{y}||_2^2$, a "lifting" technique [83] is applied to lift a vector-valued quadratic function to a matrix-valued linear function. In other words, instead of estimating two vectors $\mathbf{x}, \mathbf{h}$, a low rank matrix recovery problem is proposed to recover a rank-one matrix $\mathbf{hx}^T$. Let us consider the $i$-th entry of $\mathbf{y}$:

$$y_i = (\mathbf{Bh})_i \mathbf{g}_i^T \mathbf{x} + n_i = \mathbf{b}_i^H \mathbf{h}\mathbf{x}^T \mathbf{g}_i + n_i = \mathbf{b}_i^H \tilde{\boldsymbol{X}} \mathbf{g}_i + n_i \tag{5.7}$$

where $\mathbf{b}_i$ is the $i$-th column of $\mathbf{B}^H$, $\mathbf{g}_i^T$ is the $i$-th row of $\mathbf{G}$, and $\tilde{\boldsymbol{X}} \triangleq \mathbf{hx}^T \in \mathbb{C}^{m\times N}$ is a rank-one matrix. Define a linear operator $\mathcal{A} : \mathbb{C}^{m\times N} \to \mathbb{C}^M$

$$\mathcal{A}(\tilde{\boldsymbol{X}}) \triangleq \{\mathbf{b}_i^H \tilde{\boldsymbol{X}} \mathbf{g}_i\}_{i=1}^M, \tag{5.8}$$

such that

$$\mathbf{y} = \mathcal{A}(\tilde{\boldsymbol{X}}) + \mathbf{n}. \tag{5.9}$$

The adjont operator $\mathcal{A}^*(\mathbf{u}) : \mathbb{C}^M \to \mathbb{C}^{m\times N}$ of $\mathcal{A}(\tilde{\boldsymbol{X}})$, and $\mathcal{A}^*\mathcal{A}(\tilde{\boldsymbol{X}})$ are also given by

$$\mathcal{A}^*(\mathbf{u}) \triangleq \sum_{i=1}^M u_i \mathbf{b}_i \mathbf{g}_i^H \tag{5.10}$$

$$\mathcal{A}^*\mathcal{A}(\tilde{\boldsymbol{X}}) = \sum_{i=1}^M \mathbf{b}_i \mathbf{b}_i^H \tilde{\boldsymbol{X}} \mathbf{g}_i \mathbf{g}_i^H. \tag{5.11}$$

Then, the low rank matrix recovery optimization problem is proposed by

$$\begin{aligned} &\arg\min_{\boldsymbol{X}} \quad rank(\boldsymbol{X}) \\ &\text{subject to } ||\mathcal{A}(\boldsymbol{X}) - \mathbf{y}||_2 \leq \eta, \end{aligned} \tag{5.12}$$

Generally, the above problem is $NP$-hard, so that it is replaced by formulating a nuclear norm minimization problem, which is more tracktable as follows

$$\begin{aligned} &\arg\min_{\boldsymbol{X}} \quad ||\boldsymbol{X}||_* \\ &\text{subject to } ||\mathcal{A}(\boldsymbol{X}) - \mathbf{y}||_2 \leq \eta, \end{aligned} \tag{5.13}$$

In order to solve the above problem numerically, we need matrix form $\Phi \in \mathbb{C}^{M \times mN}$ of $\mathcal{A}(\boldsymbol{X})$ such that

$$\Phi \text{vec}(\boldsymbol{X}) = \text{vec}(\mathcal{A}(\boldsymbol{X})). \tag{5.14}$$

By using the Kronecker product property, i.e., for any matrix $\mathbf{A}, \mathbf{B}, \mathbf{C}$, $(\mathbf{B}^T \otimes \mathbf{A})\text{vec}(\mathbf{C}) = \text{vec}(\mathbf{ACB})$, we can derive the block form of $\Phi$, and $\Phi^H$ as the following

$$\Phi^H = [\varphi_1, \cdots, \varphi_i, \cdots, \varphi_M] \in \mathbb{C}^{mN \times M}, \quad \varphi_i = \mathbf{g}_i^* \otimes \mathbf{b}_i \in \mathbb{C}^{mN \times 1}, \tag{5.15}$$

$$\Phi = [\tilde{\varphi}_{1,1}, \cdots, \tilde{\varphi}_{m,1}, \cdots, \tilde{\varphi}_{1,N}, \cdots, \tilde{\varphi}_{m,N}] \in \mathbb{C}^{M \times mN}, \tag{5.16}$$

where $\tilde{\varphi}_{i,j} = \text{diag}(\tilde{\mathbf{b}}_i)\tilde{\mathbf{g}}_j \in \mathbb{C}^{M \times 1}, \forall i = 1, \cdots, m$, and $j = 1, \cdots, N$, $\tilde{\mathbf{b}}_i$ is the $i$-th column of $\mathbf{B}$, and $\tilde{\mathbf{g}}_j$ is the $j$-th column of $\mathbf{G}$.

Then, we can solve the following convex problem

$$\begin{aligned} &\arg\min_{\boldsymbol{X}} \ ||\boldsymbol{X}||_* \\ &\text{subject to } ||\Phi\text{vec}(\boldsymbol{X}) - \mathbf{y}||_2 \leq \eta, \end{aligned} \tag{5.17}$$

Note that $\mathbf{x}$ is a sparse signal. Thus, $\tilde{\boldsymbol{X}} = \mathbf{h}\mathbf{x}^T \in \mathbb{C}^{m \times N}$ is not only of rank-one, but also sparse. So, low rank and sparsity property of $\tilde{\boldsymbol{X}}$ are promoted by

$$\begin{aligned} &\arg\min_{\tilde{\boldsymbol{X}}} \ ||\tilde{\boldsymbol{X}}||_* + \lambda||\tilde{\boldsymbol{X}}||_1 \\ &\text{subject to } ||\Phi\text{vec}(\tilde{\boldsymbol{X}}) - \mathbf{y}||_2 \leq \eta. \end{aligned}$$

Since finding a proper $\lambda$ might be hard, minimizing nuclear norm needs high computations, and $||\tilde{\boldsymbol{X}}||_1 \geq ||\tilde{\boldsymbol{X}}||_*$ always holds, [84] shows that it suffices to use

$$\begin{aligned} &\arg\min_{\tilde{\boldsymbol{X}}} \ ||\tilde{\boldsymbol{X}}||_1 \\ &\text{subject to } ||\Phi \text{vec}(\tilde{\boldsymbol{X}}) - \mathbf{y}||_2 \leq \eta. \end{aligned} \tag{5.18}$$

In the end, a low rank matrix can be recovered by solving the above constrained $L_1$-norm minimization problem. In [21], the following theorem is provided to show that the estimation error for rank-one matrix is upper bounded under certain assumptions. This also implies that there exists high probability of success to have upper bounded estimation errors.

**Theorem 5.1.** *Suppose* $X_0 = \mathbf{h}_0\mathbf{x}_0^T$ *is the true matrix. Considering* $\mathbf{y} = diag(\mathbf{Bh})\mathbf{Gx} + \mathbf{n} = \mathcal{A}(X) + \mathbf{n}$ *with* $\|\mathbf{n}\| \leq \eta$*, the solution* $\hat{X}$ *given by (5.13) has the following error bound if* $\mathbf{G}$ *is a random Fourier matrix and* $\mathbf{B}$ *is a tall DFT matrix.*

$$\|\hat{X} - X_0\|_F \leq (C_0 + C_1\sqrt{P}\sqrt{mK})\eta \tag{5.19}$$

*with probability of success at least* $1 - \mathcal{O}(M^{-\alpha+1})$ *for fixed* $\alpha > 1$*. Both* $C_0$ *and* $C_1$ *are constant.* $M$ *and* $P$ *satisfy* $M = PQ$*,* $P \geq log(4\sqrt{2mK}\gamma)/log2$*,* $Q \geq C_\alpha \mu_{max}^2 mK(log(M) + log(mN))$*, where* $\gamma = \sqrt{2N(log(2mN)+1)+1}$ *and* $\mu_{max} = max_{i,j}\sqrt{M}|\mathbf{B}_{ij}|$*.*

## 5.3 Self-calibration DoA Estimation in MMV System

Instead of only considering the self-calibration in single measurement vector (SMV) system in [21], a self-calibration DoA estimation in multiple measurement vectors (MMV) system is investigated. Suppose that we have $L$ snapshots of measurement vectors in (5.5). Then, the MMV model is the following

$$\mathbf{Y} = \mathbf{DGX} + \mathbf{N}, \quad \mathbf{D} = \text{diag}(\mathbf{Bh}) \tag{5.20}$$

where $\mathbf{Y} = [\mathbf{y}_1, \cdots, \mathbf{y}_L] \in \mathbb{C}^{M\times L}$ is measurement matrix, $\mathbf{D} \in \mathbb{C}^{M\times M}$ is a diagonal matrix that depends on unknown parameter $\mathbf{h} \in \mathbb{C}^{m\times 1}$, $\mathbf{G} \in \mathbb{C}^{M\times N}$ $(M \ll N)$ is a known fat matrix, $\mathbf{X} = [\mathbf{x}_1, \cdots, \mathbf{x}_L] \in \mathbb{C}^{N\times L}$ is a sparse matrix of interest whose columns are all $K$-sparse signals and have the same sparse pattern, and $\mathbf{N} \in \mathbb{C}^{M\times L}$ is additive white Gaussian noise matrix whose entry is with zero-mean and $\sigma^2$-variance, and $\mathbf{B} \in \mathbb{C}^{M\times m}(m < M)$ is composed of the first $m$ columns of the Discrete Fourier Transform (DFT) matrix, which models slow changes on calibrations of the sensors. This is a generalization of a SMV system. The question is that can we get improvement by using the MMV model? The answer is Yes. The MMV structure of (5.20) and the group sparsity property of $\mathbf{X}$ will be exploited to enhance the performance of DoA estimation.

### 5.3.1 Proposed Methods

In order to express our idea explicitly, the case of $L = 2$ snapshots for MMV system is assumed in this section, i.e., $\mathbf{Y} = [\mathbf{y}_1, \mathbf{y}_2]$, $\mathbf{X} = [\mathbf{x}_1, \mathbf{x}_2]$. It is easy to extend our work to any case of $L > 2$. Consider $\mathbf{Y}_{i,:} \triangleq [y_{i,1}, y_{i,2}]$, the $i$-th row of the measurement matrix $\mathbf{Y}$ without noise first. Then,

$$\mathbf{Y}_{i,1} = y_{i,1} = (\mathbf{Bh})_i \mathbf{g}_i^T \mathbf{x}_1 = \mathbf{b}_i^H \mathbf{h} \mathbf{x}_1^T \mathbf{g}_i = \mathbf{b}_i^H \tilde{\boldsymbol{X}}_1 \mathbf{g}_i \tag{5.21}$$

$$\mathbf{Y}_{i,2} = y_{i,2} = (\mathbf{Bh})_i \mathbf{g}_i^T \mathbf{x}_2 = \mathbf{b}_i^H \mathbf{h} \mathbf{x}_2^T \mathbf{g}_i = \mathbf{b}_i^H \tilde{\boldsymbol{X}}_2 \mathbf{g}_i \tag{5.22}$$

where where $\mathbf{b}_i$ is the $i$-th column of $\mathbf{B}^H$, $\mathbf{g}_i^T$ is the $i$-th row of $\mathbf{G}$, and $\tilde{\boldsymbol{X}}_1 = \mathbf{h}\mathbf{x}_1^T$, $\tilde{\boldsymbol{X}}_2 = \mathbf{h}\mathbf{x}_2^T \in \mathbb{C}^{m\times N}$ are rank-one matrix. Thus, we reformulate $\mathbf{Y}_{i,:}$ as

$$\mathbf{Y}_{i,:} = [y_{i,1}, y_{i,2}] = \mathbf{b}_i^H [\mathbf{h}\mathbf{x}_1^T, \mathbf{h}\mathbf{x}_2^T] \begin{bmatrix} \mathbf{g}_i & \mathbf{0} \\ \mathbf{0} & \mathbf{g}_i \end{bmatrix} = \mathbf{b}_i^H \tilde{\boldsymbol{X}} \tilde{\mathbf{G}}_i \tag{5.23}$$

where

$$\tilde{\mathbf{G}}_i = \begin{bmatrix} \mathbf{g}_i & \mathbf{0} \\ \mathbf{0} & \mathbf{g}_i \end{bmatrix} \in \mathbb{C}^{LN\times L} \tag{5.24}$$

and

$$\tilde{\boldsymbol{X}} := [\tilde{\boldsymbol{X}}_1, \tilde{\boldsymbol{X}}_2] = \mathbf{h}[\mathbf{x}_1^T, \mathbf{x}_2^T] = \mathbf{h} \begin{bmatrix} \mathbf{x}_1 \\ \mathbf{x}_2 \end{bmatrix}^T \in \mathbb{C}^{m \times LN} \tag{5.25}$$

is also a rank-one matrix by concatenating two rank-one matrices.

Define the linear operator $\mathcal{A}(\tilde{\boldsymbol{X}}) : \mathbb{C}^{m \times LN} \to \mathbb{C}^{M \times L}$ s.t.

$$\mathcal{A}(\tilde{\boldsymbol{X}}) \triangleq \{\mathbf{b}_i^H \tilde{\boldsymbol{X}} \tilde{\mathbf{G}}_i\}_{i=1}^M \tag{5.26}$$

The adjoint operator $\mathcal{A}^*(\mathbf{U}) : \mathbb{C}^{M \times L} \to \mathbb{C}^{m \times LN}$ of $\mathcal{A}(\tilde{\boldsymbol{X}})$, and $\mathcal{A}^*\mathcal{A}(\tilde{\boldsymbol{X}})$ are also given by

$$\mathcal{A}^*(\mathbf{U}) \triangleq \sum_{i=1}^M \mathbf{b}_i \mathbf{u}_i \tilde{\mathbf{G}}_i^H \tag{5.27}$$

$$\mathcal{A}^*\mathcal{A}(\tilde{\boldsymbol{X}}) = \sum_{i=1}^M \mathbf{b}_i \mathbf{b}_i^H \tilde{\boldsymbol{X}} \tilde{\mathbf{G}}_i \tilde{\mathbf{G}}_i^H, \tag{5.28}$$

where $\mathbf{U} = [\mathbf{u}_1^T, \cdots, \mathbf{u}_M^T]^T \in \mathbb{C}^{M \times L}, \mathbf{u}_i \in \mathbb{C}^{1 \times L}, \forall i$.

Then, we can solve 5.20 by a nuclear norm minimization problem

$$\begin{aligned} &\arg\min_{\tilde{\boldsymbol{X}}} \ ||\tilde{\boldsymbol{X}}||_* \\ &\text{subject to } ||\mathcal{A}(\tilde{\boldsymbol{X}}) - \mathbf{Y}||_2 \leq \eta. \end{aligned} \tag{5.29}$$

But, we still need the matrix representation $\Phi : ML \times mNL$ of $\mathcal{A}$ such that

$$\Phi \text{vec}(\tilde{\boldsymbol{X}}) = \text{vec}(\mathcal{A}(\tilde{\boldsymbol{X}})) = \text{vec}(\mathbf{Y}^T). \tag{5.30}$$

We can derive the block form of $\Phi^H$ as the following

$$\Phi^H = [\varphi_1, \cdots, \varphi_i, \cdots, \varphi_M] \in \mathbb{C}^{mLN \times ML}, \quad \varphi_i = \tilde{\mathbf{G}}_i^* \otimes \mathbf{b}_i \in \mathbb{C}^{mLN \times L}, \tag{5.31}$$

where $\otimes$: Kronecker product. And the block form of $\Phi$ is

$$\Phi = [\breve{\varphi}_{1,1}, \cdots, \breve{\varphi}_{m,1}, \breve{\varphi}_{1,2}, \cdots, \breve{\varphi}_{m,2}, \cdots, \cdots, \breve{\varphi}_{1,N}, \cdots, \breve{\varphi}_{m,N}, \tag{5.32}$$
$$\bar{\varphi}_{1,1}, \cdots, \bar{\varphi}_{m,1}, \bar{\varphi}_{1,2}, \cdots, \bar{\varphi}_{m,2}, \cdots, \cdots, \bar{\varphi}_{1,N}, \cdots, \bar{\varphi}_{m,N}] \in \mathbb{C}^{ML \times mLN},$$
$$\breve{\varphi}_{i,j} = \begin{bmatrix} \tilde{\varphi}_{i,j}(1) \\ \mathbf{0}_{L-1} \\ \tilde{\varphi}_{i,j}(2) \\ \mathbf{0}_{L-1} \\ \vdots \\ \tilde{\varphi}_{i,j}(M) \\ \mathbf{0}_{L-1} \end{bmatrix}, \bar{\varphi}_{i,j} = \begin{bmatrix} \mathbf{0}_{L-1} \\ \tilde{\varphi}_{i,j}(1) \\ \mathbf{0}_{L-1} \\ \tilde{\varphi}_{i,j}(2) \\ \vdots \\ \mathbf{0}_{L-1} \\ \tilde{\varphi}_{i,j}(M) \end{bmatrix} \in \mathbb{C}^{ML \times 1}$$

where $\tilde{\varphi}_{i,j} = \text{diag}(\tilde{\mathbf{b}}_i)\tilde{\mathbf{g}}_j \in \mathbb{C}^{M \times 1}, \forall i = 1, \cdots, m,$ and $j = 1, \cdots, N,$ $\tilde{\mathbf{b}}_i$ is the $i$-th column of $\mathbf{B}$, and $\tilde{\mathbf{g}}_j$ is the $j$-th column of $\mathbf{G}$. $\tilde{\varphi}_{i,j}(l)$ represents the $l$-th entry of $\tilde{\varphi}_{i,j}$ and $\mathbf{0}_{L-1}$ denotes a zero vector with $L-1$ dimensions.

So, we can solve the following convex problem

$$\begin{aligned} &\arg\min_{\tilde{\boldsymbol{X}}} \ ||\tilde{\boldsymbol{X}}||_* \\ &\text{subject to } ||\Phi \text{vec}(\tilde{\boldsymbol{X}}) - \text{vec}(\mathbf{Y}^T)||_2 \leq \eta. \end{aligned} \tag{5.33}$$

Note that rank-one matrix $\tilde{\boldsymbol{X}} \in \mathbb{C}^{m \times LN}$ is of bigger size than the case in SMV. The columns of $\tilde{\boldsymbol{X}}$ share the same sparsity. The group sparsity of $\tilde{\boldsymbol{X}}$ is promoted by

$$\begin{aligned} &\arg\min_{\tilde{\boldsymbol{X}}} \ ||\tilde{\boldsymbol{X}}||_* + \lambda||\tilde{\boldsymbol{X}}||_{2,1} \\ &\text{subject to } ||\Phi \text{vec}(\tilde{\boldsymbol{X}}) - \text{vec}(\mathbf{Y}^T)||_2 \leq \eta. \end{aligned}$$

Since minimizing the nuclear norm has higher computational complexity, and $||\tilde{X}||_{2,1} \geq ||\tilde{X}||_1 \geq ||\tilde{X}||_*$ always holds, it suffices to use

$$\begin{aligned} &\arg\min_{\tilde{\boldsymbol{X}}} \ ||\tilde{\boldsymbol{X}}||_{2,1} \\ &\text{subject to } ||\Phi \text{vec}(\tilde{\boldsymbol{X}}) - \text{vec}(\mathbf{Y}^T)||_2 \leq \eta. \end{aligned} \tag{5.34}$$

After the estimate of $\tilde{\boldsymbol{X}}$ is obtained, SVD is used to obtain its eigenvector with the largest eigenvalue, which will be the best estimate of $\mathbf{h}$ and $\mathbf{x}$.

Recalling that the matrix size of $\tilde{\boldsymbol{X}}$ is $m \times LN$. If the number of snapshots $L$ is very large, the computational complexity will be substantial. In order to mitigate this issue, a complexity reduction method is applied in the next subsection.

### 5.3.2 Complexity Reduction

Consider the general case of $L \gg 2$,

$$\mathbf{Y} = \mathbf{DGX} + \mathbf{N}, \quad \mathbf{D} = \text{diag}(\mathbf{Bh}). \tag{5.35}$$

Since the matrix size of $\mathbf{Y} \in \mathbb{C}^{M \times L}$, $\mathbf{X} \in \mathbb{C}^{N \times L}$, and$\tilde{\boldsymbol{X}} \in \mathbb{C}^{m \times NL}$ becomes larger, the singular value decomposition (SVD) can be used to reduce problem size. Take the SVD on $\mathbf{Y}$

$$\mathbf{Y} = \mathbf{U}\Sigma\mathbf{V}^H \tag{5.36}$$

where $\mathbf{U} \in \mathbb{C}^{M \times M}$ is an unitary matrix, $\Sigma \in \mathbb{C}^{M \times L}$ is a rectangular diagonal matrix with nonnegative real numbers on the diagonal, and $\mathbf{V} \in \mathbb{C}^{L \times L}$ is an unitary matrix. Denote $\mathbf{E}_K = [\mathbf{I}_K,\ \mathbf{0}]^T$ where $\mathbf{I}_K$ is a $K \times K$ identity matrix, and $\mathbf{0}$ is a $K \times (L-K)$ zero matrix. Then, a reduced $M \times K$ matrix $\mathbf{Y}_{sv}$ without losing the signal power can be obtained by

$$\mathbf{Y}_{sv} = \mathbf{YVE}_K = \mathbf{DGX}_{sv} + \mathbf{N}_{sv}, \tag{5.37}$$

where $\mathbf{Y}_{sv} \in \mathbb{C}^{M \times K}$, $\mathbf{X}_{sv} = \mathbf{XVD}_K \in \mathbb{C}^{N \times K}$, and $\tilde{\boldsymbol{X}} \in \mathbb{C}^{m \times NK}$. Then, the reduced-sized convex optimization problem is the following

$$\begin{aligned} &\arg\min_{\tilde{\boldsymbol{X}}} \ ||\tilde{\boldsymbol{X}}||_{2,1} \\ &\text{subject to } ||\Phi\text{vec}(\tilde{\boldsymbol{X}}) - \text{vec}(\mathbf{Y}_{sv}^T)||_2 \leq \eta. \end{aligned} \tag{5.38}$$

The problem size $m \times NK$ is much lower than $m \times LK$ such that the computational complexity is reduced significantly. However, this method works well only when there is prior knowledge on the number of the received signals.

## 5.4 Self-Calibration Off-Grid DoA Estimation

When formulating the DoA estimation problem by discretizing the angle space, the off-grid DoAs always occur in the problem formulation, as mentioned in chapter 2. Since the self-calibration DoA estimation problem is a sparse formulation, the off-grid effect cannot be avoided, but this is not considered in [21]. In the following sections, the self-calibration off-grid MMV model and our proposed methods are introduced.

### 5.4.1 Self-Calibration Off-Grid MMV Model

Recall the self-calibration MMV model as

$$\mathbf{Y} = \mathbf{DAS} + \mathbf{N}, \quad \mathbf{D} = \text{diag}(\mathbf{Bh}) \tag{5.39}$$

where $\mathbf{Y} = [\mathbf{y}_1, \cdots, \mathbf{y}_L] \in \mathbb{C}^{M \times L}$ is measurement matrix, $\mathbf{D} \in \mathbb{C}^{M \times M}$ is a diagonal matrix that depends on unknown parameter vector $\mathbf{h} \in \mathbb{C}^{m \times 1}$. The measurement matrix $\mathbf{A} = [\mathbf{a}(\theta_1), \cdots, \mathbf{a}(\theta_K)] \in \mathbb{C}^{M \times K}$ is composed of the steering vectors $\{\mathbf{a}(\theta_i) = [e^{-j(-(M-1)/2)2\pi \frac{d}{\lambda} sin\theta_i}, \ldots, e^{-j((M-1)/2)2\pi \frac{d}{\lambda} sin\theta_i}]^T\}_{i=1}^K$ with wavelength $\lambda$, $\mathbf{S} = [\mathbf{s}_1, \cdots, \mathbf{s}_L] \in \mathbb{C}^{K \times L} (\mathbf{s}_i \in \mathbb{C}^{K \times 1}, \forall i)$ is a signal matrix of interest, and $\mathbf{N} \in \mathbb{C}^{M \times L}$ is additive white Gaussian noise matrix whose entry is with zero-mean and $\sigma^2$-variance, and $\mathbf{B} \in \mathbb{C}^{M \times m} (m < M)$ is composed of the first $m$ columns of the Discrete Fourier Transform (DFT) matrix.

The measurement now follows the sparse array calibration model

$$\mathbf{Y} = \mathbf{D}\bar{\mathbf{A}}\bar{\mathbf{S}} + \mathbf{N}, \quad \mathbf{D} = \text{diag}(\mathbf{Bh}), \tag{5.40}$$

where $\bar{\mathbf{A}} = [\mathbf{a}(\phi_1), \cdots, \mathbf{a}(\phi_N)] \in \mathbb{C}^{M \times N}$, and $\bar{\mathbf{S}} = \bar{[}\mathbf{s}_1, \cdots, \bar{\mathbf{s}}_L] \in \mathbb{C}^{N \times L}$ is a sparse matrix whose each column $\bar{\mathbf{s}}_i \in \mathbb{C}^{K \times 1}$ is sparse.

Using the first order model apprximation to account for off-grid directions, we have:

$$\begin{aligned}\mathbf{Y} &\cong \mathbf{D}(\bar{\mathbf{A}}(\boldsymbol{\phi}) + \bar{\mathbf{B}}\Gamma)\bar{\mathbf{S}} + \mathbf{N} \\ &= \mathbf{D}(\mathbf{A}(\boldsymbol{\phi})\bar{\mathbf{S}} + \bar{\mathbf{B}}\mathbf{P}) + \mathbf{N} \\ &= \mathbf{D}[\mathbf{A}(\boldsymbol{\phi}), \bar{\mathbf{B}}]\mathbf{X} + \mathbf{N} \\ &= \mathbf{DGX} + \mathbf{N},\end{aligned} \tag{5.41}$$

where $\bar{\mathbf{A}} \cong \bar{\mathbf{A}}(\boldsymbol{\phi}) + \bar{\mathbf{B}}\Gamma$, $\bar{\mathbf{B}} = [\frac{\partial \mathbf{a}(\phi_1)}{\partial \phi_1}, \ldots, \frac{\partial \mathbf{a}(\phi_N)}{\partial \phi_N}] \in \mathbb{C}^{M\times N}$, $\boldsymbol{\beta} = [\beta_1, \ldots, \beta_N]^T$, $\Gamma = diag(\boldsymbol{\beta})$, $\mathbf{P} = \Gamma\bar{\mathbf{S}}$, $\mathbf{G} = [\mathbf{A}(\boldsymbol{\phi}), \bar{\mathbf{B}}]$, and $\mathbf{X} = [\bar{\mathbf{S}}^T, \mathbf{P}^T]^T \in \mathbb{C}^{2N\times L}$ whose each column is a sparse vector $\mathbf{x}_i = [\bar{\mathbf{s}}_i^T, \mathbf{p}_i^T]^T \in \mathbb{C}^{2N\times 1}$, and $\mathbf{p}_i = \boldsymbol{\beta}_i \odot \bar{\mathbf{s}}_i$ where $\odot$ denotes the Hadamard product. It's noted that each column $\mathbf{x}_i$ is $2K$-sparse, and $N \gg M > m$.

### 5.4.2 Proposed Methods

By considering the off-grid array calibration model (5.41), one can refer to subsection 5.3.1 and follow the same idea to define (suppose $L = 2$ and noiseless)

- $\mathbf{Y}_{i,:} = [y_{i,1}, y_{i,2}] = \mathbf{b}_i^H[\mathbf{hx}_1^T, \mathbf{hx}_2^T] \begin{bmatrix} \mathbf{g}_i & \mathbf{0} \\ \mathbf{0} & \mathbf{g}_i \end{bmatrix} = \mathbf{b}_i^H \tilde{\boldsymbol{X}} \tilde{\mathbf{G}}_i$
- $\tilde{\boldsymbol{X}} := [\tilde{\boldsymbol{X}}_1, \tilde{\boldsymbol{X}}_2] = \mathbf{h}[\mathbf{x}_1^T, \mathbf{x}_2^T] = \mathbf{h} \begin{bmatrix} \mathbf{x}_1 \\ \mathbf{x}_2 \end{bmatrix}^T \in \mathbb{C}^{m\times 2LN}, \tilde{\mathbf{G}}_i = \begin{bmatrix} \mathbf{g}_i & \mathbf{0} \\ \mathbf{0} & \mathbf{g}_i \end{bmatrix} \in \mathbb{C}^{2LN\times L}$
- Linear operator $\mathcal{A}(\tilde{\boldsymbol{X}}) : \mathbb{C}^{m\times 2LN} \to \mathbb{C}^{M\times L}$ s.t. $\mathcal{A}(\tilde{\boldsymbol{X}}) \overset{\Delta}{=} \{\mathbf{b}_i^H \tilde{\boldsymbol{X}} \tilde{\mathbf{G}}_i\}_{i=1}^M$
- Matrix representation $\Phi : ML \times 2mLN$ of $\mathcal{A}$ such that $\Phi \text{vec}(\tilde{\boldsymbol{X}}) = \text{vec}(\mathcal{A}(\tilde{\boldsymbol{X}})) = \text{vec}(\mathbf{Y}^T)$, and

$$\Phi = [\varphi_1, \cdots, \varphi_i, \cdots, \varphi_M]^H \in \mathbb{C}^{ML\times 2mLN}, \quad \varphi_i = \tilde{\mathbf{G}}_i^* \otimes \mathbf{b}_i \in \mathbb{C}^{2mLN\times L}$$

Thus, a convex optimization problem is proposed as

$$\begin{aligned}&\arg\min_{\tilde{\boldsymbol{X}}} \ ||\tilde{\boldsymbol{X}}||_{2,1} \\ &\text{subject to } ||\Phi \text{vec}(\tilde{\boldsymbol{X}}) - \text{vec}(\mathbf{Y}^T)||_2 \leq \eta.\end{aligned} \tag{5.42}$$

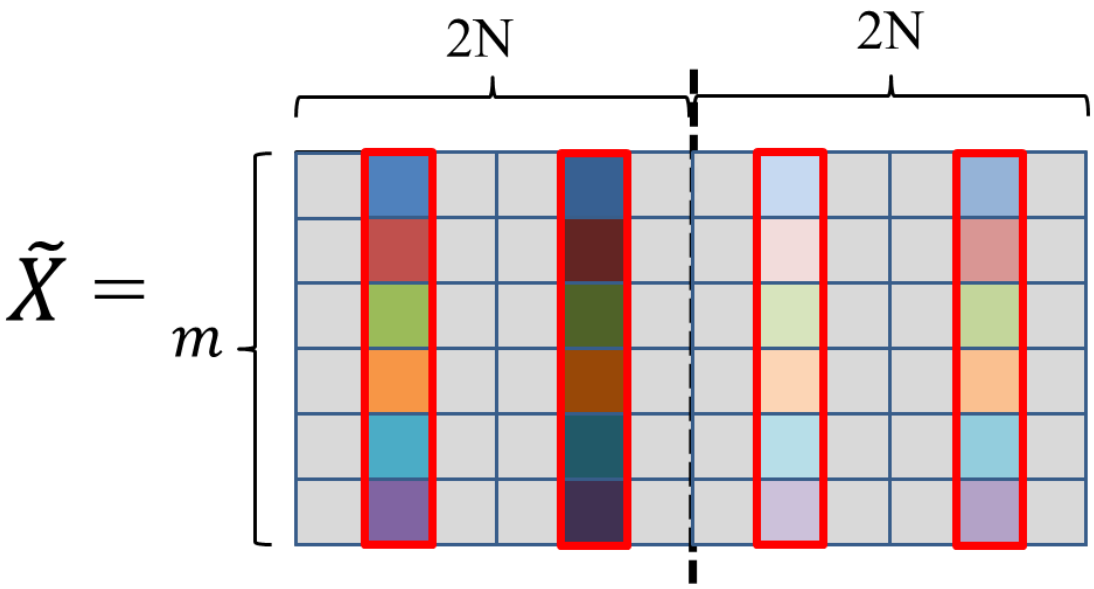


Figure 5.1: Low rank matrix $\tilde{\boldsymbol{X}}$.

Note that SVD still can be applied to reduce computational complexity when the number of snapshots $L \gg 2$ is used for the problem formulation.

Furthermore, we notice that each row of $\tilde{\boldsymbol{X}}$ has joint block sparsity patterns as shown in Figure 5.1. And we have prior information of $\beta_i$, i.e., $0 \leq |\beta_i| \leq r$ and $r = \frac{|\phi_i - \phi_{i+1}|}{2}$ is the half size of the grid interval. Then, we define a new norm for $\tilde{\boldsymbol{X}}$ to take advantage of the properties as

$$\|\tilde{\boldsymbol{X}}\|_{2,2,1} := \|\mathbf{v}\|_{2,1}, \tag{5.43}$$

where $\mathbf{v} := [\|\tilde{\boldsymbol{X}}_{:,1}\|_2, \|\tilde{\boldsymbol{X}}_{:,2}\|_2, \cdots, \|\tilde{\boldsymbol{X}}_{:,2LN}\|_2]^T \in \mathbb{R}_+^{2LN\times 1}$ is a joint-sparse vector variables. So, we can solve a new convex optimization problem as follows

$$\begin{aligned} \arg\min_{\tilde{\boldsymbol{X}},\mathbf{v}} \quad & \|\tilde{\boldsymbol{X}}\|_{2,2,1} \\ \text{subject to } & ||\Phi \text{vec}(\tilde{\boldsymbol{X}}) - \text{vec}(\mathbf{Y}^T)||_2 \leq \eta \\ & \mathbf{v} = [\|\tilde{\boldsymbol{X}}_{:,1}\|_2, \|\tilde{\boldsymbol{X}}_{:,2}\|_2, \cdots, \|\tilde{\boldsymbol{X}}_{:,2LN}\|_2]^T \\ & \mathbf{v} \geq 0 \\ & \mathbf{v}_{N+1:2N} \leq r\mathbf{v}_{1:N} \\ & \mathbf{v}_{3N+1:4N} \leq r\mathbf{v}_{2N+1:3N}. \end{aligned} \tag{5.44}$$

The last new constraints come from the positivity property of the norm, and the prior knowledge of $\mathbf{p}_i = \boldsymbol{\beta}_i \odot \bar{\mathbf{s}}_i$.

After we obtain the estimate of $\tilde{\boldsymbol{X}}$, we take SVD to obtain its eigenvector with the largest eigenvalue, which will be the best estimate of $\mathbf{h}$ and $\mathbf{x}$. However, since $\mathbf{x} = [\bar{\mathbf{s}}^T, \mathbf{p}^T]^T \in \mathbb{C}^{2N\times 1}$ is complex-valued and sparse, we only compute the absolute value of off-grid DoA $|\beta_i| = \frac{|p_i|}{|\bar{s}_i|}$ for non-zero $\bar{s}_i$. In order to recover the sign of off-grid deviation, we should consider all $2^K$ cases of the sign of $|\boldsymbol{\beta}|$, due to the sign of $\{+,-\}$ and prior knowledge on $K$ sources. In order to determine the best estimate of the sign of off-grid DoA $\boldsymbol{\beta}$, one can calculate $||\Phi \text{vec}(\tilde{\boldsymbol{X}}) - \text{vec}(\mathbf{Y}^T)||_2$ of all cases, and choose the best $\boldsymbol{\beta}$ with the minimum value. (Remeber that $\tilde{\boldsymbol{X}}_i = \mathbf{h}\mathbf{x}_i^T$, $\mathbf{x}_i = [\bar{\mathbf{s}}_i^T, \mathbf{p}_i^T]^T$, and $\mathbf{p}_i = \boldsymbol{\beta}_i \odot \bar{\mathbf{s}}_i$.) The drawback is that the number of source signals $K$ has to be known as a priori.

## 5.5 Numerical Results

In this section, numerical simulation is conducted to compare the performance of the proposed methods with CRB, the eigenstructure (ES) method, and Ling's work. A

ULA of $M = 8$ or $M = 64$ sensors with $d/\lambda = 0.5$ is considered. There are two cases of $K = 2$ far-field plane waves from the actual DoAs $\boldsymbol{\theta}$. The first one is the on grid case with $\boldsymbol{\theta} = [-13°, 28°]$; the second one is the off-grid case with $\boldsymbol{\theta} = [13.2220°, 28.6022°]$. The steering vector is given by $\mathbf{a}(\theta_i) = [e^{-j(-(M-1)/2)2\pi\frac{d}{\lambda}sin\theta_i}, \ldots, e^{-j((M-1)/2)2\pi\frac{d}{\lambda}sin\theta_i}]^T$. Narrowband, zero-mean, and uncorrelated sources for the plane waves are assumed, and the noise is AWGN with zero-mean and unit variance. The DoA search space is discretized from $-90°$ to $90°$ with $1°$ separation, so $N = 180$. The number of snapshots is set to $L = 100$. The value of $r$ is set to $0.5°$. Calibration error $\mathbf{d}$ is given by $\mathbf{d} = \mathbf{Bh}$, where $\mathbf{B} \in \mathbb{C}^{\mathbf{M}\times\mathbf{m}}$, whose columns are the first $m = 4$ columns of $M \times M$ DFT matrix. One hundred realizations are performed at each SNR. The root mean square error (RMSE) of DoAs estimation is defined as $(E[\frac{1}{K}\|\hat{\boldsymbol{\theta}} - \boldsymbol{\theta}\|_2^2])^{\frac{1}{2}}$. When solving the optimization problem, the regularization parameters are carefully selected to achieve the best performance.

### 5.5.1 The Case of On Grid

In this subsection, the performance of our proposed method for the on grid case will be verified. In Figure 5.2, the accuracy of estimated DoAs for one realization is shown when $M = 64$ sensor is used at SNR =15 dB. Since a large number of sensors are used, the peak of signal amplitude locates on the true DoAs for our proposed method and Ling's work. In this scenario, the difference of accuracy is not obvious, except that there exists some small peaks abound the true DoAs for the Ling's work. However, when $M = 8$ sensor is used at SNR =25 dB, the accuracy performance of our proposed method is better than the Ling's work as seen in Figure 5.3. The estimated DoAs of our proposed method are on the true locations, while the Ling's work are not. In fact in the latter method one of the true DoAs is missed.

In Figure 5.4, the RMSE of DoA estimation is investigated when $M = 8$ sensors is used. Our proposed method is better than the eigenstructure method and Ling's work. At RMSE=10, the proposed method outperforms Ling's work about 17 dB.

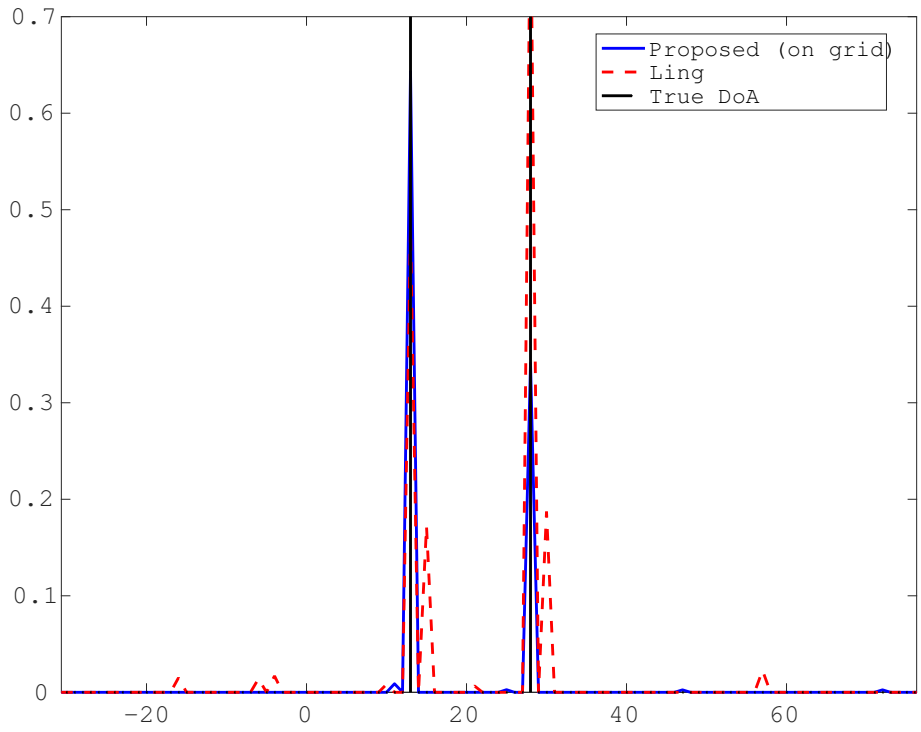


Figure 5.2: Angle space vs signal amplitude at SNR=15 dB, $M = 64$.

This improves a lot, especially when only one hundred snapshots is used. Figure 5.5 shows that the RMSE performance improves with increasing number of snapshots. The most improvement occurs when the number of snapshots is between 1 and 300. In Figure 5.6, by using the complexity-reduction technique, it shows that the computational complexity just increases slightly even when the $L = 1000$ snapshots are used in terms of cpu time consumption for each realization.

### 5.5.2 The Case of Off-Grid

In this subsection, the performance of our proposed method for the off grid case will be verified. In Figure 5.7, the proposed method (off-grid) outperforms the ES, Ling's work at each SNR, and is also better than the proposed method (on grid) which does not consider the off-grid effect. However, the RMSE performance of the proposed method (off-grid) starts to saturate when SNR $\geq$ 20 dB. That means that the estimate of off-grid DoA is not stable at high SNRs. Furthermore, our proposed method is still far away from CRB.

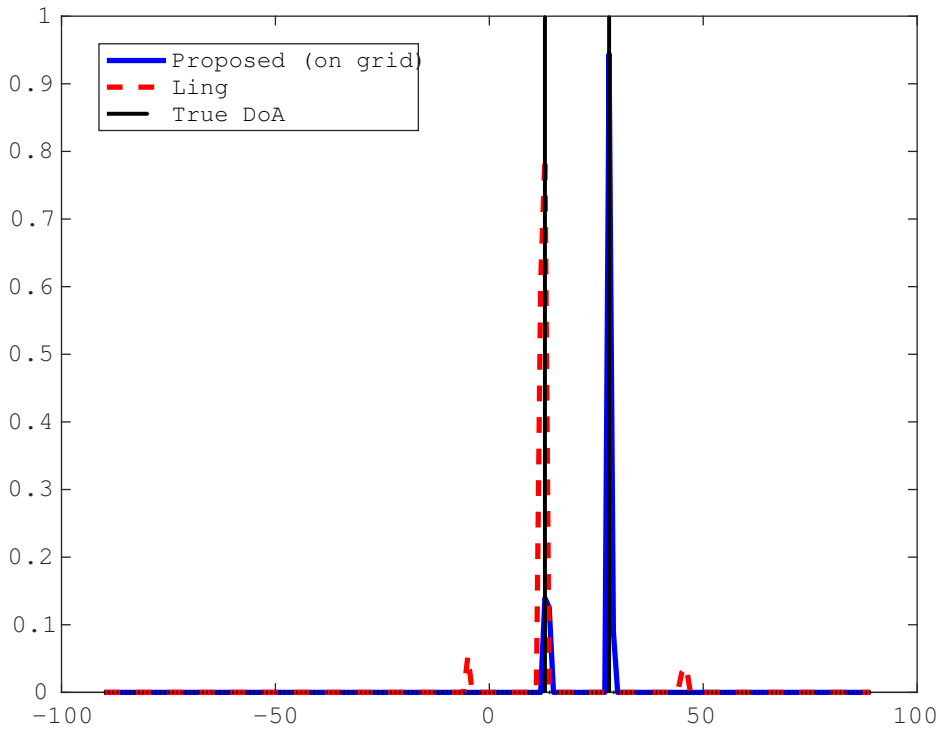


Figure 5.3: Angle space vs signal amplitude at SNR=25 dB, $M = 8$.

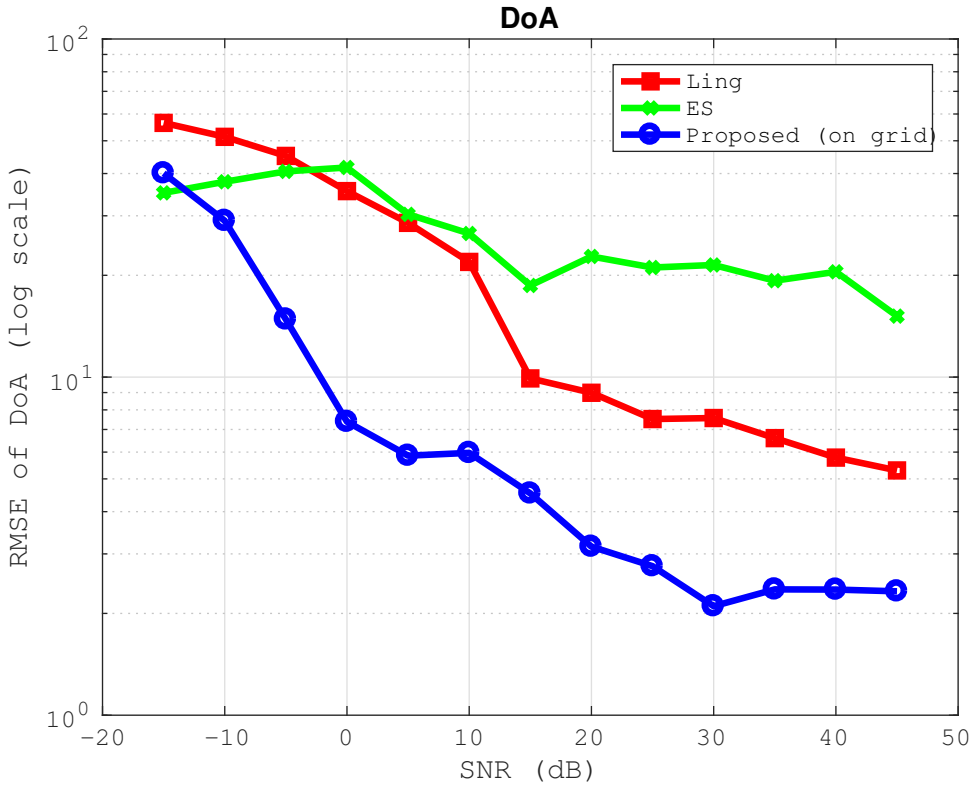


Figure 5.4: RMSE of on-grid DoA estimation versus SNR, $M = 8$.

## 5.6 Summary

In this chapter, the calibrating issue in array processing is introduced. We extended the Ling's work to the MMV system, and proposed a new nuclear norm minimization problem to take advantage of the information brought by multiple measurement vectors. The performance improvement benefits from the use of multiple snapshots is proved by simulaitons. We also apply SVD to reduce the computational complexity of solving our proposed problem. Furthermore, the off-grid effect is also considered in the array self-calibration problem. We come up with a new mixed-norm to formulate a new convex

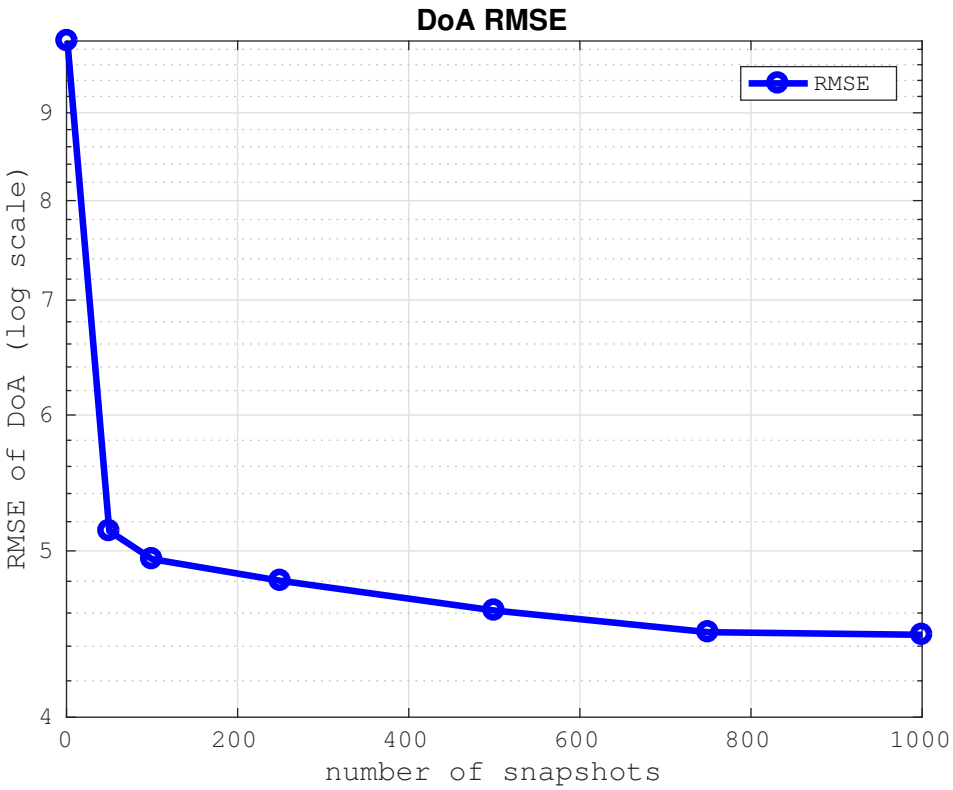


Figure 5.5: RMSE of on-grid DoA estimation versus number of snapshots, SNR=15 dB.

optimization problem with linear inequalities constraints about prior information of off-grid. We verified its performance by numerical results.

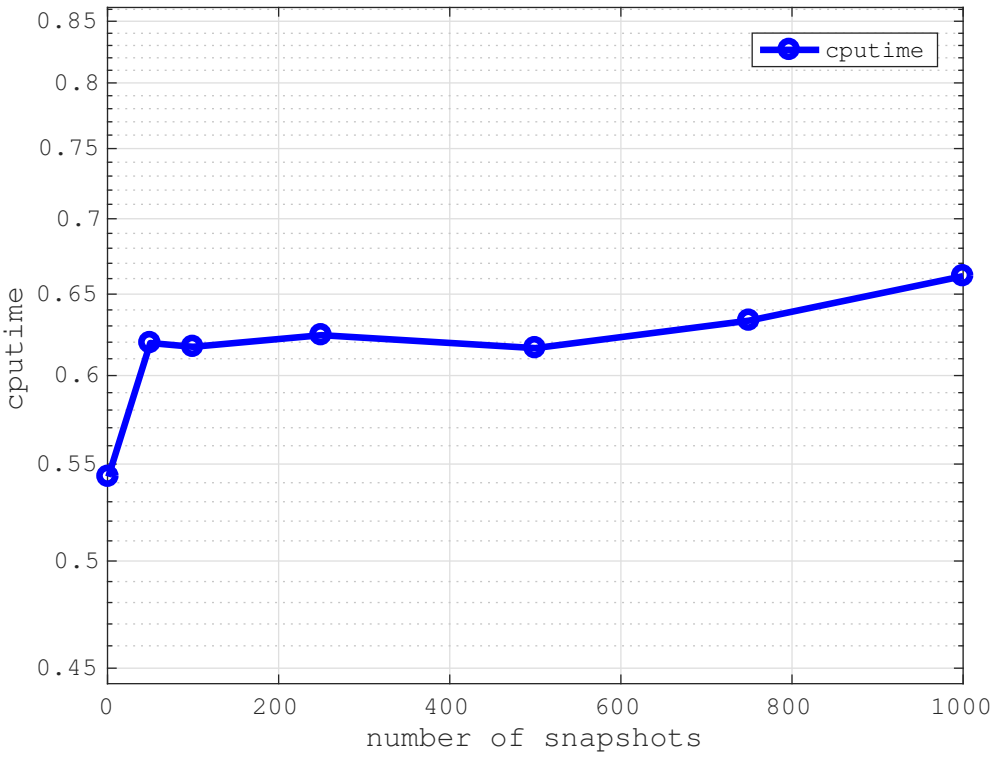


Figure 5.6: CPU time consumption versus number of snapshots, SNR=15 dB.

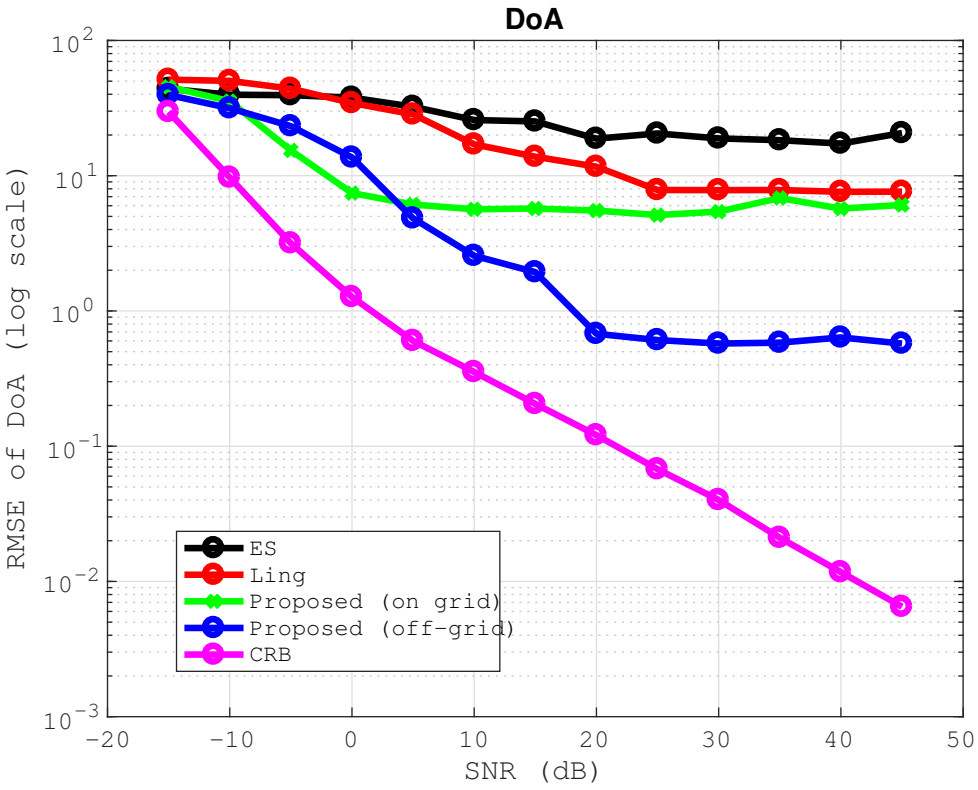


Figure 5.7: RMSE of off-grid DoA estimation versus SNR, $M = 8$.

# Chapter 6

# Conclusion and Discussion

## 6.1 Conclusion

In this dissertation, several topics related to sparse recovery and its applicaitons in array processing were studied.

First, a sparse spatial spectral model was constructed to account in its model source directions that are off the search grid. The alternating Lasso approach achieved the best solution, which alternately estimates the spatial powers and off-grid DoAs at the expense of substantial computational complexity. Then, by taking advantage of group sparsity, group-sparsity estimator and Lasso-based Least Squares were proposed with lower computational complexity. By numerical simulations, we evaluated and verified the performances of the proposed methods from the simulation results. ALasso can achieve the best RMSE performance of DoA. GSE and LLS maintained similar performances as SSFMU at higher SNRs with lower complexity.

In order to efficiently solve the sparse off-grid recovery problem presented in chapter 2, some iterative algorithms were developed to cope with the constrained nonsmooth optimization problem. Our first method was about combining the Nesterov smoothing with the accelerated proximal gradient. We proposed two ASPG methods to estimate

the off-grid DoAs using a sparse observation model. The group-sparsity penalty was reformulated to the max-structure. By choosing a proper smoothing parameter, the reformulated penalty can be smoothed by the Nesterov smoothing technique to become a differentiable function. Then, we can use the accelerated proximal gradient to solve the unconstrained optimization problem with the smoothed objective functions plus only one nonsmooth function. However, the smoothing parameter has to be selected empirically. So, a variant of EGT-based primal-dual mehtod was employed since the smoothing parameter can be chosen systematically. Instead of using BPDN-like solver such as the previous problems we solved, a variant od SDCO method was proposed, and its smoothing parameters can be determined by using the continuation technique. The performance and computational efficiencies of the proposed methods were verified by a numerical example of DoA estimation.

Then, by the super-resolution (SR) theory, the sparse recovery problems can be fitted into the super-resolution framework without discretizing the search space. In order to design a SR-based method and consider the complexity issue, we reformulated the spatial covariance model into an MMV-like system, and exploited the group sparsity in the super-resolution framework. A block total variation norm minimization approach was proposed to formulate a convex optimization problem. The primal variables can be estimated by solving its dual. The dual problem was derived with infinite constraints, but it can be transformed into a SDP. A number of optimal variable candidates was generated via performing root-finding procedure on the trigonometric polynomial of optimized dual variables. Then, the optimal primal solution was obtained by solving the Group Lasso. The robust performance of SR-BTV was demonstrated compared wtih MUSIC and ANM-MMV in cases of uncorrelated and correlated sources by simulation results.

Finally, the calibration issue in array processing was studied. In order to take advantage of multiple measurement vectors, Ling's work was extended to the MMV

system, and a new nuclear norm minimization problem was proposed. The performance improvement of our proposed problem benefits from the information of multiple snapshots. In order to reduce the computational complexity of the proposed approach when a large number of multiple snapshots is used, the SVD was employed to resolve it. Furthermore, the off-grid effect, which occurs in the spare formulation model, was also considered with the array calibration issue. In order to estimate the off-grid value, a new mixed-norm was proposed to formulate a convex optimization problem, and its performance was demonstrated numerically.

## 6.2 Future Work

- **Designing A Regularization Parameter Selector**

  The Stein Unbiased Risk Estimator (SURE) method [85] is a scheme for regularization parameter selection in the case of Gussian noise. Unlike generalized cross validation (GCV), the SURE method requires prior information of noise variance and provides an unbiased assessment of MSE when solving denoising problems. Therefore, when the noise variance is assumed known in our problem setting, we would like to investigate how SURE can be used in the MMV setting.

- **Reducing the Number of Sensors in the Super Resolution Theory**

  In the super-resolution framework, a large number of sensors is used in order to satisfy the smaller minimum distance in accordance with the super-resolution theory [14]. However, large number of sensors usually imply an impractically large array aperture. Our goal is to reduce the number of sensors without performance degradation. Reference [86] shows that recovery of spike trains is possible provided that $\Delta > \frac{1}{f_c}$, but no recovery methods were proposed. In [87], by using short-time Fourier transform (STFT) measurements in the super-resolution theory, spike trains can be recovered if $\Delta > \frac{1}{f_c}$ so that the number of sensors can be reduced to a half of original ones. Extending, their approach to array signal processing

needs to be investigated to reduce the number of sensors in the continuous-domain sparse recovery problems.

- **Designing Efficient Algorithms for Continuous Sparse Recovery Methods**

  The continuous sparse recovery methods can achieve high estimation accuracy if the requirement of numbers of measurement is satisfied. However, we need to solve the semidefinite programming to estimate the dual variables. This can be implemented by the interior point method (CVX tools), but with the cost of high computational complexity. Thus, an efficient algorithm for solving SDP and its convergence analysis will be a very important topic in future.

- **Developing Array Self-Calibration Recovery Methods in the Super-Resolution Framework**

  The accuracy performance of proposed continuous sparse recovery methods is superior under certain assumptions on the number of measurements. In order to avoid the off-grid effect, instead of discretizing the search range on array calibration problems, the super-resolution framework can be applied to construct a gridless convex optimization problem in the SMV scenario, e.g., AtomicLift [88]. The performance guarantee can be analyzed with respect to the super resolution theory. Extending this approach from SMV to MMV will be a challenging task that may worth pursuing.

- **Dectecting the Number of Source Signals**

  Signal subspace methods, such as MUSIC, require knowledge of the number of sources to estimate the signal subspace or its complement, the noise subspace.The performance of DoA estimation is subject to such information. By exploiting eigenvalues from the sample covariance matrix, several well-known criteria are used to estimate the number of signals, such as AIC (Akaike Information Criterion) [89], MDL (Minimum Description Length) [90], the second order statistic of

eigenvalues (SORTE) [91], and the predicted eigen-threshold approach [92]. Unlike the signal subspace methods, the performance of sparsity-promoting methods heavily depends on the selection of regularization parameters. Thus, choosing a good regularization parameter is a critical issue. However, even with the help of good regularization parameters, the information on the number of sources is needed to select the actual signals from the estimated ones because extra candidate sources might appear due to noise. In [93], SORTE is proved to have a better detection accuracy of number of sources. Thus, SORTE can be studied further within the framework of the current approach for DoA estimation.

# References


[1] A Lee Swindlehurst and Thomas Kailath. A performance analysis of subspace-based methods in the presence of model errors. i. the music algorithm. *Signal Processing, IEEE Transactions on*, 40(7):1758–1774, 1992.

[2] Jack Capon. High-resolution frequency-wavenumber spectrum analysis. *Proceedings of the IEEE*, 57(8):1408–1418, 1969.

[3] Feifei Gao and Alex B Gershman. A generalized esprit approach to direction-of-arrival estimation. *Signal Processing Letters, IEEE*, 12(3):254–257, 2005.

[4] Ilan Ziskind and Mati Wax. Maximum likelihood localization of multiple sources by alternating projection. *Acoustics, Speech and Signal Processing, IEEE Transactions on*, 36(10):1553–1560, 1988.

[5] Petre Stoica and Alex B Gershman. Maximum-likelihood doa estimation by data-supported grid search. *Signal Processing Letters, IEEE*, 6(10):273–275, 1999.

[6] S Cotter. Multiple snapshot matching pursuit for direction of arrival (doa) estimation. In *Proceedings of the European Signal Processing Conference*, pages 247–251, 2007.

[7] David L Donoho. Compressed sensing. *Information Theory, IEEE Transactions on*, 52(4):1289–1306, 2006.

[8] Emmanuel J Candès, Justin Romberg, and Terence Tao. Robust uncertainty principles: Exact signal reconstruction from highly incomplete frequency information. *Information Theory, IEEE Transactions on*, 52(2):489–509, 2006.

[9] Marco F Duarte and Yonina C Eldar. Structured compressed sensing: From theory to applications. *IEEE Transactions on Signal Processing*, 59(9):4053–4085, 2011.

[10] Yonina C Eldar and Gitta Kutyniok. *Compressed sensing: theory and applications*. Cambridge University Press, 2012.

[11] Yuejie Chi, Louis L Scharf, Ali Pezeshki, and A Robert Calderbank. Sensitivity to basis mismatch in compressed sensing. *IEEE Transactions on Signal Processing*, 59(5):2182–2195, 2011.

[12] Hao Zhu, Geert Leus, and Georgios B Giannakis. Sparsity-cognizant total least-squares for perturbed compressive sampling. *Signal Processing, IEEE Transactions on*, 59(5):2002–2016, 2011.

[13] Zai Yang, Cishen Zhang, and Lihua Xie. Robustly stable signal recovery in compressed sensing with structured matrix perturbation. *IEEE Transactions on Signal Processing*, 60(9):4658–4671, 2012.

[14] Emmanuel J Candès and Carlos Fernandez-Granda. Towards a mathematical theory of super-resolution. *Communications on Pure and Applied Mathematics*, 67(6):906–956, 2014.

[15] Ming Yuan and Yi Lin. Model selection and estimation in regression with grouped variables. *Journal of the Royal Statistical Society: Series B (Statistical Methodology)*, 68(1):49–67, 2006.

[16] Scott Shaobing Chen, David L Donoho, and Michael A Saunders. Atomic decomposition by basis pursuit. *SIAM review*, 43(1):129–159, 2001.

[17] Emmanuel Candes and Terence Tao. The dantzig selector: Statistical estimation when p is much larger than n. *The Annals of Statistics*, pages 2313–2351, 2007.

[18] Gongguo Tang and Arye Nehorai. Performance analysis for sparse support recovery. *IEEE transactions on information theory*, 56(3):1383–1399, 2010.

[19] Gongguo Tang and Arye Nehorai. Computable performance bounds on sparse recovery. *IEEE Transactions on Signal Processing*, 63(1):132–141, 2015.

[20] Emmanuel J Candès and Carlos Fernandez-Granda. Super-resolution from noisy data. *Journal of Fourier Analysis and Applications*, 19(6):1229–1254, 2013.

[21] Shuyang Ling and Thomas Strohmer. Self-calibration and biconvex compressive sensing. *Inverse Problems*, 31(11):115002, 2015.

[22] Benjamin Friedlander. Array self-calibration with large initial errors. In *Signals, Systems and Computers, 2014 48th Asilomar Conference on*, pages 1169–1173. IEEE, 2014.

[23] Anthony J Weiss and Benjamin Friedlander. Eigenstructure methods for direction finding with sensor gain and phase uncertainties. *Circuits, Systems and Signal Processing*, 9(3):271–300, 1990.

[24] Dmitry Malioutov, Müjdat Çetin, and Alan S Willsky. A sparse signal reconstruction perspective for source localization with sensor arrays. *Signal Processing, IEEE Transactions on*, 53(8):3010–3022, 2005.

[25] J Zheng, M Kaveh, and H Tsuji. Sparse spectral fitting for direction of arrival and power estimation. In *Proc. IEEE/SP 15th Workshop on Statistical Signal Processing*, 2009.

[26] Joseph S Picard and Anthony J Weiss. Direction finding of multiple emitters by spatial sparsity and linear programming. In *Proc. Communications and Information Technology, ISCIT 2009. 9th International Symposium on*, pages 1258–1262, 2009.

[27] Jimeng Zheng and Mostafa Kaveh. Directions-of-arrival estimation using a sparse spatial spectrum model with uncertainty. In *Proc. IEEE International Conference on Acoustics, Speech and Signal Processing (ICASSP)*, 2011.

[28] Gongguo Tang, Badri Narayan Bhaskar, Parikshit Shah, and Benjamin Recht. Compressive sensing off the grid. In *Communication, Control, and Computing (Allerton), 2012 50th Annual Allerton Conference on*, pages 778–785. IEEE, 2012.

[29] Zhao Tan, Peng Yang, and Arye Nehorai. Joint-sparse recovery in compressed sensing with dictionary mismatch. In *Computational Advances in Multi-Sensor Adaptive Processing, IEEE 5th International Workshop on*, 2013.

[30] Aris Gretsistas and Mark D Plumbley. An alternating descent algorithm for the off-grid doa estimation problem with sparsity constraints. In *Signal Processing Conference (EUSIPCO), 2012 Proceedings of the 20th European*, pages 874–878, 2012.

[31] Jimeng Zheng and Mostafa Kaveh. Sparse spatial spectral estimation: a covariance fitting algorithm, performance and regularization. *IEEE Transactions on Signal Processing*, 61(11):2767–2777, 2013.

[32] Zhao Tan, Peng Yang, and Arye Nehorai. Joint sparse recovery method for compressed sensing with structured dictionary mismatches. *Signal Processing, IEEE Transactions on*, 62(19):4997–5008, 2014.

[33] Gongguo Tang, Badri Narayan Bhaskar, Parikshit Shah, and Benjamin Recht. Compressed sensing off the grid. *IEEE Transactions on Information Theory*, 59(11):7465–7490, 2013.

[34] Rakshith Jagannath and KVS Hari. Block sparse estimator for grid matching in single snapshot doa estimation. *IEEE Signal Processing Letters*, 20(11):1040–1043, 2013.

[35] Bo Lin, Jiying Liu, Meihua Xie, and Jubo Zhu. Super-resolution doa estimation using single snapshot via compressed sensing off the grid. In *Signal Processing, Communications and Computing (ICSPCC), 2014 IEEE International Conference on*, pages 825–829. IEEE, 2014.

[36] Ralph O Schmidt. Multiple emitter location and signal parameter estimation. *Antennas and Propagation, IEEE Transactions on*, 34(3):276–280, 1986.

[37] Ron Rubinstein, Michael Zibulevsky, and Michael Elad. Double sparsity: Learning sparse dictionaries for sparse signal approximation. *Signal Processing, IEEE Transactions on*, 58(3):1553–1564, 2010.

[38] Paul Tseng. Convergence of a block coordinate descent method for nondifferentiable minimization. *Journal of optimization theory and applications*, 109(3):475–494, 2001.

[39] Stephen Boyd, Neal Parikh, Eric Chu, Borja Peleato, and Jonathan Eckstein. Distributed optimization and statistical learning via the alternating direction method of multipliers. *Foundations and Trends® in Machine Learning*, 3(1):1–122, 2011.

[40] A Ben-Tal and M Teboulle. A smoothing technique for nondifferentiable optimization problems. In *Optimization*, pages 1–11. Springer, 1989.

[41] Yurii Nesterov. Smooth minimization of non-smooth functions. *Mathematical programming*, 103(1):127–152, 2005.

[42] Dimitri P Bertsekas. Nondifferentiable optimization via approximation. In *Non-differentiable optimization*, pages 1–25. Springer, 1975.

[43] Jean-Jacques Moreau. Proximité et dualité dans un espace hilbertien. *Bulletin de la Société mathématique de France*, 93:273–299, 1965.

[44] Yurii Nesterov. Excessive gap technique in nonsmooth convex minimization. *SIAM Journal on Optimization*, 16(1):235–249, 2005.

[45] Xi Chen, Qihang Lin, Seyoung Kim, Jaime G Carbonell, Eric P Xing, et al. Smoothing proximal gradient method for general structured sparse regression. *The Annals of Applied Statistics*, 6(2):719–752, 2012.

[46] Amir Beck and Marc Teboulle. Smoothing and first order methods: A unified framework. *SIAM Journal on Optimization*, 22(2):557–580, 2012.

[47] Quoc Tran-Dinh. Adaptive smoothing algorithms for nonsmooth composite convex minimization. *arXiv preprint arXiv:1509.00106*, 2015.

[48] Nikos Komodakis and Jean-Christophe Pesquet. Playing with duality: An overview of recent primal? dual approaches for solving large-scale optimization problems. *Signal Processing Magazine, IEEE*, 32(6):31–54, 2015.

[49] Naum Zuselevich Shor. *Minimization methods for non-differentiable functions*, volume 3. Springer Science & Business Media, 2012.

[50] Yurii Nesterov. *Introductory lectures on convex optimization: A basic course*, volume 87. Springer Science & Business Media, 2013.

[51] Francesco Orabona, Andreas Argyriou, and Nathan Srebro. Prisma: Proximal iterative smoothing algorithm. *arXiv preprint arXiv:1206.2372*, 2012.

[52] Neal Parikh and Stephen P Boyd. Proximal algorithms. *Foundations and Trends in optimization*, 1(3):127–239, 2014.

[53] Stephen R Becker, Emmanuel J Candès, and Michael C Grant. Templates for convex cone problems with applications to sparse signal recovery. *Mathematical programming computation*, 3(3):165–218, 2011.

[54] Stephen Becker, Jérôme Bobin, and Emmanuel J Candès. Nesta: A fast and accurate first-order method for sparse recovery. *SIAM Journal on Imaging Sciences*, 4(1):1–39, 2011.

[55] Cheng-Yu Hung, Jimeng Zheng, and Mostafa Kaveh. Directions of arrival estimation by learning sparse dictionaries for sparse spatial spectra. In *Sensor Array and Multichannel Signal Processing Workshop (SAM), 2014 IEEE 8th*, pages 377–380. IEEE, 2014.

[56] Guanghui Lan, Zhaosong Lu, and Renato DC Monteiro. Primal-dual first-order methods with iteration-complexity for cone programming. *Mathematical Programming*, 126(1):1–29, 2011.

[57] Amir Beck and Marc Teboulle. A fast iterative shrinkage-thresholding algorithm for linear inverse problems. *SIAM journal on imaging sciences*, 2(1):183–202, 2009.

[58] Arkadii Nemirovskii, David Borisovich Yudin, and Edgar Ronald Dawson. Problem complexity and method efficiency in optimization. 1983.

[59] Yurii Nesterov. A method for unconstrained convex minimization problem with the rate of convergence o (1/k2). In *Doklady an SSSR*, volume 269, pages 543–547, 1983.

[60] Yurii Nesterov. On an approach to the construction of optimal methods of minimization of smooth convex functions. *Ekonomika i Mateaticheskie Metody*, 24(3):509–517, 1988.

[61] Yurii Nesterov et al. Gradient methods for minimizing composite objective function, 2007.

[62] Paul Tseng. On accelerated proximal gradient methods for convex-concave optimization cite. 2008.

[63] Alfred Auslender and Marc Teboulle. Interior gradient and proximal methods for convex and conic optimization. *SIAM Journal on Optimization*, 16(3):697–725, 2006.

[64] Leonid I Rudin, Stanley Osher, and Emad Fatemi. Nonlinear total variation based noise removal algorithms. *Physica D: Nonlinear Phenomena*, 60(1-4):259–268, 1992.

[65] Zai Yang and Lihua Xie. Exact joint sparse frequency recovery via optimization methods. *arXiv preprint arXiv:1405.6585*, 2014.

[66] Cheng-Yu Hung and Mostafa Kaveh. Direction-finding based on the theory of super-resolution in sparse recovery algorithms. In *Proc. IEEE International Conference on Acoustics, Speech and Signal Processing (ICASSP)*, 2015.

[67] Petros Boufounos, Volkan Cevher, Anna C Gilbert, Yi Li, and Martin J Strauss. Whats the frequency, kenneth?: Sublinear fourier sampling off the grid. In *Approximation, Randomization, and Combinatorial Optimization. Algorithms and Techniques*, pages 61–72. Springer, 2012.

[68] Alan T Moffet. Minimum-redundancy linear arrays. *Antennas and Propagation, IEEE Transactions on*, 16(2):172–175, 1968.

[69] Palghat P Vaidyanathan and Piya Pal. Sparse sensing with co-prime samplers and arrays. *Signal Processing, IEEE Transactions on*, 59(2):573–586, 2011.

[70] Walter Rudin. *Real and complex analysis*. Tata McGraw-Hill Education, 1987.

[71] Zhao Tan, Yonina C Eldar, and Arye Nehorai. Direction of arrival estimation using co-prime arrays: A super resolution viewpoint. *Signal Processing, IEEE Transactions on*, 62(21):5565–5576, 2014.

[72] Stephen Boyd and Lieven Vandenberghe. *Convex optimization*. Cambridge university press, 2009.

[73] CMS See. Sensor array calibration in the presence of mutual coupling and unknown sensor gains and phases. *Electronics Letters*, 30:373–374, 1994.

[74] Aifei Liu, Guisheng Liao, Cao Zeng, Zhiwei Yang, and Qing Xu. An eigenstructure method for estimating doa and sensor gain-phase errors. *IEEE Transactions on signal processing*, 59(12):5944–5956, 2011.

[75] Laura Balzano and Robert Nowak. Blind calibration of sensor networks. In *Proceedings of the 6th international conference on Information processing in sensor networks*, pages 79–88. ACM, 2007.

[76] Rémi Gribonval, Gilles Chardon, and Laurent Daudet. Blind calibration for compressed sensing by convex optimization. In *2012 IEEE International Conference on Acoustics, Speech and Signal Processing (ICASSP)*, pages 2713–2716. IEEE, 2012.

[77] Christophe Schulke, Francesco Caltagirone, Florent Krzakala, and Lenka Zdeborová. Blind calibration in compressed sensing using message passing algorithms. In *Advances in Neural Information Processing Systems*, pages 566–574, 2013.

[78] Çağdaş Bilen, Gilles Puy, Rémi Gribonval, and Laurent Daudet. Convex optimization approaches for blind sensor calibration using sparsity. *IEEE Transactions on Signal Processing*, 62(18):4847–4856, 2014.

[79] Xiaodong Li and Vladislav Voroninski. Sparse signal recovery from quadratic measurements via convex programming. *SIAM Journal on Mathematical Analysis*, 45(5):3019–3033, 2013.

[80] Emmanuel J Candes, Thomas Strohmer, and Vladislav Voroninski. Phaselift: Exact and stable signal recovery from magnitude measurements via convex programming. *Communications on Pure and Applied Mathematics*, 66(8):1241–1274, 2013.

[81] Emmanuel J Candes, Yonina C Eldar, Thomas Strohmer, and Vladislav Voroninski. Phase retrieval via matrix completion. *SIAM review*, 57(2):225–251, 2015.

[82] Anat Levin, Yair Weiss, Fredo Durand, and William T Freeman. Understanding blind deconvolution algorithms. *IEEE transactions on pattern analysis and machine intelligence*, 33(12):2354–2367, 2011.

[83] Ali Ahmed, Benjamin Recht, and Justin Romberg. Blind deconvolution using convex programming. *IEEE Transactions on Information Theory*, 60(3):1711–1732, 2014.

[84] Samet Oymak, Amin Jalali, Maryam Fazel, Yonina C Eldar, and Babak Hassibi. Simultaneously structured models with application to sparse and low-rank matrices. *IEEE Transactions on Information Theory*, 61(5):2886–2908, 2015.

[85] Charles M Stein. Estimation of the mean of a multivariate normal distribution. *The annals of Statistics*, pages 1135–1151, 1981.

[86] David L Donoho. Superresolution via sparsity constraints. *SIAM Journal on Mathematical Analysis*, 23(5):1309–1331, 1992.

[87] Céline Aubel, David Stotz, and Helmut Bölcskei. Super-resolution from short-time fourier transform measurements. *arXiv preprint arXiv:1403.2239*, 2014.

[88] Yuejie Chi. Guaranteed blind sparse spikes deconvolution via lifting and convex optimization. *IEEE Journal of Selected Topics in Signal Processing*, 10(4):782–794, 2016.

[89] Hirotugu Akaike. A new look at the statistical model identification. *Automatic Control, IEEE Transactions on*, 19(6):716–723, 1974.

[90] Jorma Rissanen. Modeling by shortest data description. *Automatica*, 14(5):465–471, 1978.

[91] Zhaoshui He, Andrzej Cichocki, Shengli Xie, and Kyuwan Choi. Detecting the number of clusters in n-way probabilistic clustering. *Pattern Analysis and Machine Intelligence, IEEE Transactions on*, 32(11):2006–2021, 2010.

[92] Weiguo Chen, Kon Max Wong, and James P Reilly. Detection of the number of signals: A predicted eigen-threshold approach. *Signal Processing, IEEE Transactions on*, 39(5):1088–1098, 1991.

[93] Keyong Han and Arye Nehorai. Improved source number detection and direction estimation with nested arrays and ulas using jackknifing. *Signal Processing, IEEE Transactions on*, 61(23):6118–6128, 2013.

[94] Stephen Boyd and Lieven Vandenberghe. *Convex optimization*. Cambridge university press, 2004.

[95] Bogdan Alexandru Dumitrescu. *Positive trigonometric polynomials and signal processing applications*. Springer Science & Business Media, 2007.

# Appendix A

# Derivation of the dual problem (4.19)

*Proof.* First, we know $\mathbf{S} = [\mathbf{s}_1, \ldots, \mathbf{s}_M]$ as the data matrix where $\mathbf{s}_t = [b_{1t}, \ldots, b_{Kt}]^T$, and $\|s\|_{TV,1} = \|\mathbf{S}\|_{1,1} = \sum_{i,j} |\mathbf{S}_{j,i}| = \sum_j \|\mathbf{S}_{j,:}\|_1 = \sum_i \|\mathbf{S}_{:,i}\|_1$, where $\mathbf{S}_{j,i}$ is the entry of data matrix $\mathbf{S}$ located on the $j$-th row, $i$-th column. $\mathbf{S}_{j,:}$ is the $j$-th row of data matrix $\mathbf{S}$, and $\mathbf{S}_{:,i}$ is the $i$-th column of data matrix $\mathbf{S}$.

We reformulate the optimization problem (4.17) by employing auxiliary variables $\mathbf{z}_i, \forall i = 1, \cdots, M$. Then, the reformulated problem is as follows:

$$\begin{aligned} \min_{s,\mathbf{z}_i} \ & \|s\|_{TV,1} \\ \text{s.t.} \ & \sum_{i=0}^{M-1} \|\mathbf{z}_i\|_2 \leq \epsilon \\ & \mathbf{r}_i - \mathcal{F}_i s(\tau; i) + \mathbf{z}_i = 0, \forall i. \end{aligned} \tag{A.1}$$

The Lagragian function can be expressed as

$$L(s, \mathbf{z}_i, \mathbf{u}_i, v_i) = \|s\|_{TV,1} + \sum_i v_i(\|\mathbf{z}_i\|_2 - \frac{\epsilon}{M}) + \mathrm{Re}\{\sum_i \mathbf{u}_i^*(\mathbf{r}_i - \mathcal{F}_i s(\tau; i) + \mathbf{z}_i)\} \quad \text{(A.2)}$$

$$= \|s\|_{TV,1} - \mathrm{Re}\{\sum_i \mathbf{u}_i^* \mathcal{F}_i s(\tau; i)\} + \sum_i v_i \|\mathbf{z}_i\|_2 + \mathrm{Re}\{\sum_i \mathbf{u}_i^* \mathbf{z}_i\} \quad \text{(A.3)}$$

$$+ \mathrm{Re}\{\sum_i \mathbf{u}_i^* \mathbf{r}_i\} - \sum_i v_i \frac{\epsilon}{M},$$

where $\mathbf{u}_i \in \mathbb{C}^{M\times 1}$, and $v_i \in \mathbb{R} \geq 0$ are the Lagrangian multipliers for all $i$.

So, the dual function is

$$g(\mathbf{u}_i, v_i) = \mathrm{Re}\{\sum_i \mathbf{u}_i^* \mathbf{r}_i\} - \sum_i v_i \frac{\epsilon}{M} + \inf_{s,\mathbf{z}_i} \|s\|_{TV,1} - \mathrm{Re}\{\sum_i \mathbf{u}_i^* \mathcal{F}_i s(\tau; i)\} \quad \text{(A.4)}$$

$$+ \sum_i v_i \|\mathbf{z}_i\|_2 + \mathrm{Re}\{\sum_i \mathbf{u}_i^* \mathbf{z}_i\}.$$

By using the conjugate function [94], we have

$$\inf_s \|s\|_{TV,1} - \mathrm{Re}\{\sum_i \mathbf{u}_i^* \mathcal{F}_i s(\tau; i)\} = -\sup \sum_i (\mathrm{Re}\{\mathbf{u}_i^* \mathcal{F}_i s(\tau; i)\} - \|\mathbf{s}_i\|_1) \quad \text{(A.5)}$$

$$= \begin{cases} 0, & \|\mathcal{F}_i^* \mathbf{u}_i\|_\infty \leq 1, \forall i \\ -\infty, & o.w. \end{cases},$$

and

$$\inf_{\mathbf{z}_i} \sum_i v_i \|\mathbf{z}_i\|_2 + \mathrm{Re}\{\sum_i \mathbf{u}_i^* \mathbf{z}_i\} = -\sup \sum_i (-\mathrm{Re}\{\sum_i \mathbf{u}_i^* \mathbf{z}_i\} - v_i \|\mathbf{z}_i\|_2) \quad \text{(A.6)}$$

$$= \begin{cases} 0, & \|-\mathbf{u}_i\|_2 \leq v_i, \forall i \\ -\infty, & o.w. \end{cases}.$$

Note that we can choose $\mathbf{u}_i = v_i \frac{\mathbf{z}_i}{\|\mathbf{z}_i\|_2}$ so that $\|\mathbf{u}_i\|_2 = v_i$, which satisfies the constraint in the solution of (A.6).

Thus, we have the dual problem

$$\max_{\mathbf{u}_i} \ \mathrm{Re}\{\sum_i \mathbf{u}_i^* \mathbf{r}_i\} - \frac{\epsilon}{M} \sum_i \|\mathbf{u}_i\|_2 \quad \text{(A.7)}$$

$$\text{s.t. } \|\mathcal{F}_i^* \mathbf{u}_i(\tau)\|_\infty \leq 1, \forall i = 0, \ldots, M-1.$$

By stacking each column $\mathbf{u}_i$ and $\mathbf{r}_i$ into matrix $\mathbf{U}$ and $\mathbf{R}$, the above optimization problem is equivalent to (4.18). Then, theorem 4.24 in [95] is applied to recast problem (4.18) with infinite constraints into a semidefinite programming problem (4.19). □